THESIS

DEVELOPMENT OF NOVEL REMINERALISING ANTIMICROBIAL BRUSHITE CEMENTS

Thesis submitted by

Nor Azlina Ismail
BDS (Malaysia)

In partial fulfilment of the requirements for the Degree of

CLINICAL DOCTORATE IN DENTISTRY (PAEDIATRIC DENTISTRY)

UNIVERSITY COLLEGE LONDON

2014

DECLARATION OF ORIGINALITY

I hereby certify that the work embodied in this thesis is the result of my own investigations, except where otherwise stated. Information derived from the published and unpublished work of others had been acknowledged in the text and the relevant references are included in this thesis.

Nor Azlina Ismail

Eastman Dental Institute, University College London

September 2014

ACKNOWLEDGMENT

I wish to express my extreme appreciation firstly to Dr Anne Young. Her guidance and unending quest to understand had profound impact on my skills, my drive and my philosophy. I thank her for giving me the opportunity and the pleasure of working with her during this research.

My deepest gratitude also goes to my supervisor Dr Paul Ashley. His excellent guidance and invaluable assistance enable me to complete my thesis successfully.

I would also like to thank, Dr Wendy Xia, Dr Graham Palmer and Dr George Georgiou for their help in my experimental works, for which I am much obliged.

The author acknowledges the scholarship and study leave by Ministry of Higher Education Malaysia and Islamic Science University of Malaysia (USIM).

Dedication

This work is lovingly dedicated to my husband and both of my sons; for their support, encouragement, and constant love which have sustained me throughout my life.

Finally, my parents for their unconditional love.

ABSTRACT

Brushite cements have potential as drug carriers and bone filling materials. They can also act as a reservoir for calcium and phosphate ions in remineralisation of hard tissues.

Aim and objectives: To optimize brushite cement properties and assess the effect of incorporation of a novel antimicrobial ε-polylysine (PLS) into brushite.

Materials and Methods: Powders were mixed with aqueous solutions at a powder to liquid ratio of 3.3:1 or 4:1 to produce cement pastes and start the setting reaction. The powder consisted of 1g of monocalcium phosphate monohydrate (MCPM) and 1.23 g of β -tricalcium phosphate (β-TCP). Two different types of MCPM and different β-TCP particle size range from 4 micron to 34 micron were used. The liquid phase was prepared by dissolving PLS powder in aqueous citric acid 800 mM in incrementally percentages. In control formulations, only citric acid 800 without the PLS was employed. Biaxial flexural strength and modulus were determined using a ball on ring jig. Setting kinetics and chemistry were examined using Fourier transforms infrared spectroscopy (FTIR). Microstructure of brushite cements were examined with scanning electron microscopy (SEM).

Results: The largest particle size of β-TCP (34 micron) produced the highest flexural strength of 30 MPa. The handling of brushite cements was better with MCPM 2 (Sigma). This was observed to have much larger flat crystals rather than the more powdered MCPM 1 from Himed. Powder to liquid ratio 4:1 overall increased the strength 5 MPa – 7 MPa compared to powder to liquid ratio 3.3:1. High levels of PLS could be added with only a minor reduction in the strength. Setting time however was delayed and an alternative anhydrous dicalcium phosphate complex formed rather than all brushite which is hydrated dicalcium phosphate.

Conclusion: The findings of this research demonstrated that very high levels of PLS could be introduced into brushite cements without serious detrimental effects on mechanical properties. PLS however, did delay the setting time and altered the final chemistry and microstructure of the dicalcium phosphate product.

.

Table of Contents

LIST OF TABLES

LIST OF EQUATION

LIST OF FIGURES

ABBREVIATIONS

σ	stress
Ω	Poisson's ratio
ϵ	strain
µm	micrometre
$\Delta P/\Delta W$	change in force versus change in displacement gradient of the force displacement curve.
Δm (%)	percentage mass change
a	radius of support ring
BFS	Biaxial flexural strength
BFM	Biaxial flexural modulus
β-TCP	β-Tricalcium phosphate
CA	citric acid
CHX	chlorhexidine diacetate
CI	confidence interval
CPC	calcium phosphate cements
E	Young's modulus
FTIR	Fourier transforms infrared spectroscopy
g	gram
GPa	Giga Pascals
HA	hydroxyapatite
kN	kilo Newton
L	litre
m_0	mass at initial
m_t	mass at the *t*
MCPM	monocalcium phosphate monohydrate

MCPA	monocalcium phosphate anhydrate
mg	milligrams
mM	millimolar
mm	millimetre
ml	millilitre
MPa	megapascals
MTA	mineral trioxide aggregate
n	number of samples
P	maximum load
PLR	powder to liquid ratio
PLS	ε-polylysine
PMMA	polymethylmethacrylate
ppm	part per million
SD	standard deviation
Sr	Strontium
SEM	scanning electron microscopy
UK	United Kingdom
wt %	weight percentage

CHAPTER 1
INTRODUCTION

1 INTRODUCTION

1.1 Statement of the problem

In children, premature tooth loss as a result of traumatic dental injuries or caries can be a challenge to clinicians. Early extraction of teeth will result in alveolar bone loss which subsequently complicates the treatment outcome. Alveolar bone resorption as a sequel to premature tooth loss can be very rapid and result in loss of bone height and volume. Post extraction alveolar bone remodelling often results in aesthetic compromise in the area of tooth extraction site. It is also leads to inadequate bone for ideal implant positioning or placement.

Currently, dental implants are considered the best solution for management of tooth loss but in children they have to be delayed until the child has reached full maturity. This will potentially lead to a long time period between the loss of the tooth and the placement of implant. If no measure is taken to preserve or generate the alveolar bone after tooth loss, future implants will be a problem since bone volume will be insufficient (Day et al., 2008).

Brushite cements have great potential as a bone substitute. Brushite cements have an ability to act as a reservoir of calcium and phosphate ions for remineralisation of hard tissue. Due to the excellent bioresorbability of brushite cement, newly forming immature / woven bone might substitute the cements after implantation (Dorozhkin, 2008). In clinical applications, the brushite cements can be used in the form of blocks or as a self–setting paste.

In children, immediate bone filling of extraction sockets with brushite cements is a potential therapy to minimise bone loss if the properties of these cements can be improved for alveolar bone regenerative therapy. The following study therefore focuses on optimizing brushite cements to achieve this aim. Injectable brushite cements would ideally be placed in the socket immediately after tooth extraction with the aim to maintain the alveolar bone height, width and contour in children.

However there are several issues which must be addressed in order to optimize the possible benefits of brushite cements in preserving alveolar bone. These issues include:

i) Injectability

ii) Low mechanical strength:

Compressive cement strengths must be at least as high as trabecular bone, which is close to 10 MPa. Since brushite cements originated from ceramic, they are also brittle, have both a low impact resistance and particularly low flexural strength.

iii) Cement microstructure and porosity

Brushite cements can be highly porous materials. Adequate porosity is often sought to enhance the material's resorbability and makes these materials a good carrier for controlled drug delivery systems. Unfortunately, the mechanical properties of brushite cements are found to decrease exponentially with the porosity increase (Dorozhkin, 2008). Porosity can therefore limit the use of this material to only low load-bearing applications.

iv) Incorporation of antibacterial agent:

Various factors influence any drug delivery device. These include the microstructure (porosity, permeability and surface area), the drug solubility, the potential degradation of the materials and the interaction between drug and the material matrix. Drug release from brushite cements often tends to have fast initial release due to porosity.

CHAPTER 2

BACKGROUND

2 BACKGROUND

2.1 Tooth loss in children

Tooth loss can occur for a variety of reasons including trauma and caries. Extraction of a tooth is followed by three-dimensional bone resorption that delays dental restoration procedures. The resorption is lifelong, irreversible, chronic and cumulative (Bodic et al., 2005). Alveolar ridge resorption following tooth extraction is a frequently observed phenomenon that may decrease the possibility of placing dental implants or impair the aesthetic result after prosthodontics treatment.

2.1.1 Caries

Although dental caries is a preventable disease it is a persistent public health problem. Once a child contracts the disease it has a significant impact on their quality of life. Dental caries can progress to the extent that teeth are beyond the ability to be restored to function. Decay can also lead to significant infection in the bone around the ends of the roots requiring tooth extraction to prevent further infectious complications. The DMFT (decay, missing and filling teeth) for 14 year olds is 1.48 with missing component 0.10 (Pitts et al., 2004).

2.1.2 Trauma

Traumatic injury to the oro-dental region may involve both soft and hard tissues (Roberts and Longhurst, 1996). Trauma can cause loss of teeth in a variety of ways. Andreasen's classification contains 19 groups and includes injuries to the teeth, supporting structures, gingiva and oral mucosa (Andresen et al., 2007). A national study in the United Kingdom in 1993 found a prevalence of 17.0% at age 14 years (O'Brien, 1994). Accidents within and around the home have been reported as the major source of injury to the primary dentition.

For the permanent dentition, accidents at home and school are the major factor of trauma (Galea, 1984, Forsberg and Tedestam, 1990). Accidents as a result of sports, violence and road traffic accidents were also a common cause of dental trauma. Uncomplicated crown fracture without pulp exposure was the common injury to the permanent dentition (Kania et al., 1996, Caliskan and Turkun, 1995).

Subluxations and complete luxation were the most frequently occurring injuries in the primary dentition (Galea, 1984, Martin et al., 1990). The maxillary central incisors were the most frequent injured teeth in all studies for both the primary and secondary dentitions.

Removal of a permanent maxillary incisor is not a common occurrence. Indeed every effort is usually made to avoid such extractions. However, there are some clinical situations where incisor loss is inevitable. These mainly include trauma-related sequel such as persistent uncontrollable periapical infection and vertical root fractures. Epidemiological data have shown that 19% of 12 year olds suffer some trauma to their maxillary incisor and three in every 1000 incisors will be lost as result of trauma (O'Brien, 1994).

2.2 Alveolar bone and alveolar ridge resorption

Alveolar bone is the part of the maxilla and mandible which supports the teeth and serves as a fibrous attachment for the periodontal ligament fibres, and thus alveolar bone is part of the periodontium (Bath and Fehrenbach, 2006). Essentially the alveolar process consists of two parallel plates of cortical bone, buccal and palatal (maxilla) or lingual (mandible) plates. The alveolar process which separates each tooth socket is known as interalveolar or interdental septa. In multirooted teeth the sockets are divided by interradicular septa. The cancellous bone occupies most of the interdental septa but only a relatively small portion of buccal and palatal bone plates (Lindhe et al., 2008).

2.1.2 Function of Alveolar Bone

1. Supporting tissue
2. To distribute and resorb forces generated by mastication and other tooth contacts (Lindhe et al., 2008)
3. Giving attachment to muscles
4. Providing a framework for bone marrow
5. Acting as a reservoir for ions especially calcium

2.3 Consequences of alveolar bone loss

Alveolar bone resorption is an inevitable and undesirable consequence of tooth loss. Local factors known to exacerbate the resorptive process include persistence infection, bony fracture of the thin buccal plate during tooth removal and subsequent loading of the alveolar ridge from the removable prosthesis (Jeffcoat, 1993).

Following permanent maxillary incisor loss in a young population, clinical experience suggests that a variable degree of alveolar resorption does ensue. The sequence of events that lead to alveolar healing after tooth extraction has been documented as follows (Amler, 1969, Schroeder, 1986):

1. Immediately after removal of the tooth, a blood clot with a tight fibrin network fills the alveolus. Polymorph nuclear cells and fibroblast invade the clot.
2. Granulation tissue starts to develop after 2-3 days.
3. On the fourth day, epithelial tissue grows out from the edge of the alveolus. Osteoclasts resorb the alveolar ridge.
4. On the seventh day, connective tissue containing a few areas of osteoid tissue develops.
5. Re-epithelialisation is complete by day 20. When mineralization starts, it produces woven bone that subsequently undergoes remodelling.
6. Forty days after tooth extraction, the ridge height is decrease by about one third.

The resorption of the alveolar process after tooth extraction in the maxilla or mandible is significantly larger at the buccal aspect than at the lingual aspect (Pietrokovski and Massler, 1967). Extraction of anterior maxillary teeth is associated with a progressive loss of bone mainly from the labial side (Cawood and Howell, 1988). A 25% decrease in volume of the anterior maxilla during the first year post extraction has been reported (Carlsson and Persson, 1967, Pietrokovski and Massler, 1967). Other investigators have reported a 10% loss of ridge volume determined at 2 months and 18% at 12 months (Adam LP and RJC, 1985).

A study has been done in a young patient to investigate changes in the alveolar ridge width following removal of ankylosed second primary molars. The changes were measured on dental study casts. Alveolar ridge width was found to decrease 25% within 3 years after the extraction (Ostler and Kokich, 1994).

Post extraction bone resorption has also been quantified by examining radiographs. One study estimated an annual 0.5 mm reduction in alveolar height in adults following tooth removal (Atwood, 1973). Over 25 years, the alveolar ridge may lose up to 10 mm in height at the mandible. Height loss is usually about four times smaller at the maxilla than at the mandible. This may be ascribable to the fact that loads are distributed over a smaller surface at the mandible than at the maxilla.

2.4 Current methods of alveolar bone preservation

Reduction in alveolar bone mass will have a considerable impact on future treatment options. Implant, resin bonded bridges and dentures all require adequate bone mass for the successful and aesthetic replacement of missing anterior teeth. Therefore, it would be an advantage to avoid this loss of tissue (Levin et al., 2008). Approaches to maintain alveolar bone are listed below.

2.4.1 Immediate placement of dental implant

Implant placement in children is not indicated as they are still growing and the implant will become infra-occluded.

2.4.2 Decoronation

Ankylosis and replacement resorption are frequent sequelae of severe tooth injuries (Filippi et al., 2001) in the growing child. This usually will lead to predictable loss of the teeth and localized interference of jaw development (Andreasen et al., 2007). In children, when ankylosed or heavily resorbed teeth are present, these teeth could be indicated for decoronation (Malmgren, 2000). The procedure involves removing of the tooth crown and root filling, leaving the root in situ to be resorbed by the process of replacement resorption. The retained root is then covered with a mucoperiosteal flap.

Any roots intentionally retained must be monitored clinically and radiographically and endodontically treated or removed if infection arises (Day et al., 2008). Decoronation of a tooth undergoing replacement resorption may help to maintain bone width (buccopalatally) for future implant placement (Filippi et al., 2001).

2.4.3 Immediate bone filling of extraction socket

Immediate bone filling with bone substitutes offer an alternative to managing alveolar bone loss following an extraction. Immediate bone filling offers a non–surgical approach in preserving the alveolar bone after tooth loss in children. In attempts to maintain alveolar bone width and height for future implant placement in children, ideally the bone substitute should have the following properties:-

1. Biocompatible
2. Bioresorbable
3. Promotes bone regeneration
4. Injectable into socket (to avoid surgical approach).

To be injected *in vivo*, the material must have two features which are injectability and cohesion (Bohner et al., 2000b). Injectability refers to the ability of the material to be extruded through a small and long needle without demixing (liquid being expelled without the particle). Material with appropriate cohesion (forces which causing various particle to unite) will set in a fluid without disintegrating.

The following section will focus on different materials that are currently used for bone repair and the properties of the ideal material.

2.5 Bone graft material

There are various types of bone filling materials that have been extensively studied. There are two main approaches which have been studied:

1. biologic approaches – bone graft material

i) Autograft

ii) Allograft

iii) xenografts

2. Synthetic bone graft approaches - alloplasts (synthetic hydroxyapatite, bioactive glass, tricalcium phosphate ceramics and osteoactive polymers) which act as foreign scaffold material (Meyer et al., 2009).

They operate by promoting osteointegration, osteogenesis, osteoinduction or osteoconduction. Osteointegration is the ability to chemically bond to the surface of bone without an intervening layer of fibrous tissue (Costantino and Friedman, 1994). Osteogenesis is the formation of new bone by osteoblastic cells present within the graft material (Cypher and Grossman, 1996). It occurs when viable osteoblasts and precursor osteoblasts are transplanted with the grafting material into the defects, where they may establish centres of bone formation. Autogenous iliac bone and marrow grafts are examples of transplants with osteogenic properties (Lindhe et al., 2008).

Osteoinduction is the ability to induce differentiation of pluripotential stem cells from surrounding tissue to an osteoblastic phenotype (Cypher and Grossman, 1996). It involves new bone formation by the differentiation of local uncommitted connective tissue cells into bone–forming cells under the influence of one or more inducing agents (Lindhe et al., 2008).

Osteoconduction is the ability to support the growth of bone over its surface (Constantino and Friedman, 1994). It occurs when non–vital implant material serves as a scaffold for the ingrowth of precursor osteoblasts into the defect. This process is usually followed by a gradual resorption of the implant material. Autogenous cortical bone or banked bone allografts may be examples of grafting of grafting materials with osteoconductive properties However degradation and substitution by viable bone is often poor. If the implanted material is not resorbable, the incorporation is restricted to bone apposition to the material surface, but no substitution occurs during the remodelling phase (Lindhe et al., 2008). Collagen is also known to have the osteoconductive properties due to its structure which promotes mineral deposition. Collagen also binds matrix proteins that initiate and control mineralization (Meyer et al., 2009).

2.6 Biological bone graft material

The biological approaches operate on the principle that the bone graft material should mimic as closely as possible the positive attributes of bone (Meyer et al., 2009). Bone substitutes should also have the osteotransductive property, i.e., the bone grafts are replaced by a new bone tissue after implantation (Dorozhkin, 2008).

2.6.1 Autograft

Autografts are grafts transferred from one position to another within the same individual. They is harvested either from intraoral or extraoral donor sites. This type of graft comprises:

- Cortical bone
- Cancellous bone and marrow

Autografts of bone are advocated by some clinicians to augment the alveolar bone. Autologous iliac crest bone is currently the gold standard in bone graft material (Meyer et al., 2009). The rationale of advocating autogenous grafts in regenerative therapy is that they may retain viable cells to promote bone healing through osteogenesis or osteoconduction. They are gradually resorbed and replaced by new viable bone. Issues of histocompatibility and disease transmission are eliminated with autogenous grafts (Lindhe et al., 2008).

The disadvantages of this approach include increased operative time and associated morbidity related to chronic pain, blood loss, wound complication and local sensory loss (Moore et al., 2001). This is due to the need for a second surgical site and requirement of surgical intervention to harvest the bone from the donor site. Furthermore, often the amount of graft materials is inadequate (Lu et al., 1999).

2.6.2 Allograft

Allograft refers to a graft which is transferred between genetically dissimilar members of the same species. Allograft can be frozen, freeze–dried or demineralised freeze – dried. A calcified freeze–dried allogeneic bone graft (FDBA) is a mineralized/calcified bone graft.

FDBA loses its viability through the manufacturing process and it is supposed to promote bone regeneration through osteoconduction / osteoinduction (Lindhe et al., 2008). On the other hand, a decalcified freeze–dried allogenic bone graft (DFDBA) has been suggested to enhance osteogenic potential by exposing bone morphogenic proteins which have the ability to induce host cells to differentiate into osteoblasts (Lindhe et al., 2008). Both FDBA and DFDBA have been studied in attempts for alveolar bone preservation and regeneration.

The advantage of allograft include availability and avoidance of morbidity associated with harvesting autogenous graft. Allografts are of particular importance when there are large bone defects which require structural support or when inadequate autogenous graft is available. However, the use of allogeneic grafts carries a certain risk regarding antigenicity even though the grafts are usually pre-treated by freezing radiation or chemicals in order to suppress foreign body reactions (Lindhe et al., 2008). Other complications include fracture, non-union and infection.

2.6.3 Xenogenic graft

Xenogeneic grafts are taken from a donor of another species. Xenogeneic grafts have been used in managing ridge defects (Norton et al., 2003) and in alveolar ridge preservation (Carmagnola et al., 2003). Example of the xenogeneic graft is a deproteinized bovine bone mineral (DBBM, market name is Bio-Oss). The DBBM is a biocompatible bone derivative (Artzi et al., 2000) and has been shown to be osteoconductive (Camelo et al., 1998). However, it was concluded that Bio-Oss® merely acts as a scaffold for tissue formation during healing rather than enhancing bone formation (Araujo and Lindhe, 2009) and complete alveolar bone preservation with DBBM is not possible (Fickl et al., 2008). Furthermore, with xenograft materials, there is a potential for cross contamination.

2.7 Alloplasts

Alloplastic materials are synthetic or inorganic implant materials which are used as substitute for bone grafts. Ideally synthetic bone grafts should be biocompatible, have minimal fibrotic reaction and undergo remodelling and encourage new bone formation.

Synthetic bone grafts should have a similar strength to the cortical / cancellous bone that is being replaced. This also needs be of similar modulus of elasticity to prevent stress as well as maintaining adequate toughness to prevent fatigue fracture under cycle loading. Synthetic materials that demonstrate some of these properties are often calcium, silicon, aluminium or polymer-based. Examples of commonly used alloplastic materials include:

1. Silicon based: bioactive glass or glass ionomer cements
2. Aluminium oxide
3. Polymethylmethacrylate (PMMA)
4. Synthetic hydroxyapatite, beta tricalcium phosphate, and calcium phosphate cements

2.7.1 Bioactive glass and Glass ionomer cements

Silicon based compounds have the ability to bond directly to bone. These are the bioactive glasses and the glass ionomers. Bioactive glasses are hard, solid and non-porous materials. These materials possess both osteointegrative and osteoconductive properties. A mechanically strong bond between bioactive glass and bone forms as a result of a silica-rich gel layer that forms on the surface of the bioactive glasses when exposed to physiological aqueous solutions (Gross et al., 1988).

Bioactive glasses have been successfully used as a bone graft expander and alone in maxillofacial surgery (Kinnunen et al., 2000). However, bioactive glasses have low fracture toughness in relation to cortical bone. Bioactive glass blocks resist drilling and shaping. They are relatively brittle and prone to fracture with cyclic loading. This makes it difficult to fix in the skeleton (Peltola et al., 2000). Despite the increase in strength and toughness, materials also showed a higher modulus of elasticity compared to cortical bone. Glass ionomer cements (GIC) were first introduced in 1971 for dental use. Their primary use is for tooth restoration but they have also been used in bone. Ionomer cements consist of calcium / aluminium / fluorosilicate glass powder which is mixed with polycarboxylic acid.

The paste sets hard approximately after 5 minutes but prior to this, it must be protected from wound fluid which will dissolve it. After 24 hours it has a compressive strength (180-220MPa) and modulus of elasticity comparable to cortical bone (Bresciani et al., 2004). It is also biocompatible and can be osteointegrated as well as bioactive glasses. Increasing its porous structure aids osteoconduction and subsequent bone ingrowth. The drawback of glass ionomers cements, however, is non-resorbable properties and therefore it is not replaced by bone.

2.7.2 Aluminium oxide

Alumina is a component of several bioactive materials but can also act as a bone graft substitute on its own. Alumina ceramics are very hard, rigid and have greater resistance to flexural fracture as compared to ceramic HA. They have been used as a bone graft expander, orbital implants and prosthetic joint lining (Constantino and Friedman, 1994). However, their application has been limited by their inability to become osteointegrated.

2.7.3 Polymethylmethacrylate

Polymethylmethacrylate (PMMA) bone cements are the material of choice in vertebroplasty for the treatment of metastatic, cystic lesion and osteoporotic spine fracture (Turner et al., 2008). The drawback of this material is their significant exothermic setting reaction during polymerization that carries the risk of localized thermal tissue necrosis (Belkoff and Molloy, 2003).

The high compressive strength and stiffness of PMMA causes a biomechanical mismatch between treated and untreated vertebral levels that leads to vertebral collapse (Berlemann et al., 2002). Furthermore, PMMA is non-resorbable and allergy to PMMA bone cements or its components has also been reported. PMMA may also have antibiotics and high molecular weight proteins added to them for slow release properties (Thomas et al., 2008). However, glass ionomers have the ability to release protein more efficiently than PMMA and are less likely to damage heat-labile proteins (Moore et al., 2001).

2.7.4 Beta tricalcium Phosphate

Beta tricalcium phosphate (β-TCP) was one of the earliest calcium phosphate compounds to be used as a bone graft substitute. Porous β-TCP has compressive and tensile strength similar to cancellous bone. β-TCP undergoes reabsorption via dissolution and fragmentation. Unfortunately, β-TCP has been found to be brittle and weak under tension and shear but it is resistant to compressive loads (Houmard et al., 2013).

2.7.5 Synthetic hydroxyapatite

Hydroxyapatite (HA) forms the principal mineral component of bone. It comes in ceramic or non-ceramic forms as porous or solid and blocks or granules. Ceramic refers to HA crystals that have been heated at between 700 and 1300°C to form a highly crystalline structure. Ceramic HA are resistant to reabsorption *in vivo* compared to non-ceramic HA that is more readily reabsorbed. Synthetic HA have good compressive strength but a week in tension and shear. They are brittle and are fracture prone on shock loading areas. Synthetic HA in solid block forms are difficult to shape, do not permit fibro-osseous ingrowth and have a higher modulus of elasticity than bone (Habibovic et al., 2008).

2.7.6 Calcium phosphate Cements

Calcium phosphate cements (CPC) have been extensively studied and have great potential as bone substitutes. These cements are self – setting, bioactive and biodegradable grafting materials in the form of a powder and a liquid.

These cements also possess an excellent osteoconductivity, moulding capabilities and are easy to manipulate. In contrast to PMMA based cement, the setting reaction of these cements occur with minimal exothermal at physiological pH value without the release of monomer. Nearly perfect adaptation of the tissue surface in bone defects and gradual bioresorption followed by new bone formation are additional advantage of these cements. These properties of the calcium orthophosphate cements contribute to their usage as a potential regenerative material (Tamimi et al., 2012).

The cements are obtained by mixing one or several reactive calcium phosphate powders with an aqueous solution to form a paste that hardens within a period of time, thus differentiating calcium orthophosphate cements from traditional bone substitute preparations (Bohner et al., 2005). Due to the potential of these materials for repair, augmentation and regeneration of bones, sometimes they are also known as calcium phosphate bone cements (Dorozhkin, 2008). The implanted CPC might be resorbed by two possible mechanisms:-

- Active resorption – mediated by the cellular activity of macrophages, osteoclasts by phagocytosis (Grossardt et al., 2010).

- Passive resorption due to either chemical dissolution (Dorozhkin, 2008) or chemical hydrolysis. Chemical hydrolysis only applies to brushite cements (Grover et al., 2003).

Apart from the potential regenerative property, CPC also can be used for controlled drug delivery. In principle, drugs might be incorporated into both liquid and a powder phase of the cements. After setting, the drugs are slowly released through the cements pores. This cement has been used as a carrier to deliver:

- Antibiotics
- Anti – inflammatory drugs
- Growth factors
- Bone morphogenetic proteins

Over the years, many different forms and composition of CPC have been formulated and commercialized. Based on the final end product of the formulation reactions, CPC are classified into two categories:

- Hydroxyapatite
- Brushite Cement

2.8. Hydroxyapatite

One of the most extensively studied bioactive ceramics is hydroxyapatite. Bone, enamel, dentine and cementum all contain biological apatite, which comprise the mineral phases of calcified tissues.

The biological apatite is similar to synthetic hydroxyapatite (HA) but they are differing in terms of composition, stoichiometry, physical and mechanical properties. The synthetic hydroxyapatite shows biocompatibility with not only hard tissues, but also soft tissues such as skin and muscle. Another advantage of HA is it is bioactive and promotes osseointegration when directly implanted into bone. The setting reaction of HA does not increase the local pH and it has favourable mechanical properties (Ambard and Mueninghoff, 2006, Ginebra et al., 2010).

Unfortunately the inability of hydroxyapatite to degrade for full replacement of surrounding tissues poses a major problem in the regenerative therapy of alveolar bone. The commonly used conventional bioactive material HA is extremely weak in its porous form which limits its application to none or low-load bearing areas and cannot be used as structural bone. Furthermore, the properties cannot be easily, structurally and synthetically adjusted for bone implantation.

Hydroxyapatite forming cements have a long setting time, thus during preparation of this material, the mixing liquid is reduced to a minimum (Bohner et al., 2000b). By altering the ratio of mixing liquid the product becomes more viscous, easily mouldable, but tends to be difficult to inject. As previously mentioned, injectability of material is one important criteria for novel bone substitute in children. HA also have limited solubility which leads to a growing interest in highly soluble brushite cements.

2.9 Brushite Cements

In 1987, Mirtchi and Lemaître reported the formation of brushite cements from the reaction of β-tricalcium phosphate (β-TCP) and monocalcium phosphate monohydrate (MCPM)(Mirtchi et al., 1989). Brushite cements also known as dicalcium phosphate dihydrate (DCPD). It generally forms at a pH of less than 4.2. The main components include:

1. Alkaline calcium source

Different sources of calcium have been use for example, calcium oxide (Nurit et al., 2002), calcium hydroxide (Desai and Chandler, 2009), tetracalcium phosphate (TTCP) (Lilley et al., 2005), tricalcium phosphate (TCP) and hydroxyapatite (HA) (Matsunaga et al., 2010). TTCP is an ideal choice because it has calcium to phosphate ratio of 2 but its preparation is highly energy demanding (Lilley et al., 2005)).

TCP with calcium to phosphate ratio 1:5 has two crystallographic forms known as β-TCP and α-TCP and both have been used to prepare DCP cements. β-TCP has lower energy requirement for its production making it the more suitable choice (Bohner et al., 2000a, Pina et al., 2010).

2. Acidic phosphate source

The simplest choice is phosphoric acid (PA) because it is inexpensive and has been used in many cement formulations (Bohner et al., 2000b, Lilley et al., 2005, Bohner et al., 2000a). However, monocalcium phosphate monohydrate (MCPM) is often used as it provides superior cement handling properties (Marino et al., 2007, Nurit et al., 2002).

3. Water

4. Additives

To improve DCP properties, additives have been included. The most significant of these are:

1. Pyrophosphates, for example calcium pyrophosphates (Mirtchi et al., 1989) and pyrophosphoric acid (Grover et al., 2006). These have been added to regulate the setting reaction.

2. Sulphates have also been found to modify the setting reaction of brushite cements by substituting for phosphate ions and interacting with calcium phosphates (Bohner et al., 2000a).

3. Carboxylate and carboxylic acids are used as a setting retardant in brushite cements for example as sodium citrate and citric acids (Barralet et al., 2004).

4. Polymers are added to improve injectibility, cohesion and mechanical properties. To improve injectability and cohesion, hydrophilic polymers such as xanthan gum (Flautre et al., 2003) and polyacrylic acid (Bohner et al., 1997b) are used.

5. Ionic substitutions can have an important effect on the reaction and final properties of the materials. Metallic ions such as strontium (Alkhraisat et al., 2008b) and magnesium (Boaninia et al., 2009) can be added to the cements simply by mixing the cements powder phase with a salt containing the ion that is needed. Alternatively, metal ion salts instead of pure calcium and phosphate precursors can be used (Huan and Chang, 2009, Pina et al., 2010).

Brushite cements setting reaction consists of:

1. Dissolution of the cement powder in a solvent
2. Super-saturated gel formation.
3. Nucleation within the gel
4. Formation of a solid interlocked crystal by crystal growth.

2.9.1 Setting time

Brushite cements setting reaction begins by the dissolution of MCPM which causes a rapid decrease in pH (Bohner and Gbureck, 2008, Bohner et al., 1997a). Cements with excess MCPM will have a pH that remains low even after the setting reaction is complete. Conversely, cements that have excess β-TCP have their pH settle at ~5.

Upon exposure to water, MCPM tends to hydrolyse into diphosphate and calcium ions, via an endothermic reaction (Bohner and Gbureck, 2008). As a result of acid exposure, simultaneous exothermic dissolution of β-TCP occurs. The cements experience a second pH jump as a result of the exothermic precipitation of brushite crystals after the initial dissolution of the reagents (Hofmann et al., 2006b).

Adding any additive to brushite cement can affect the dissolution of the reagent, precipitation of the brushite crystal or both thereby altering the setting reaction time. For example citrate ions can interact with β-TCP particles and affect the dissolution (Alkhraisat et al., 2008a). Alternatively, sulphate, pyrophosphate and citric acid can inhibit brushite precipitation (Bohner and Gbureck, 2008) resulting in prolongation of the cements initial low pH (Bohner et al., 2000a).

The effects of sulphate ions will vary dependent on the concentration used. Adding a low concentration will delay the cement reaction whereas a high concentration will lead to the formation of calcium sulphate dihydrate crystals that can act as nuclei for the crystallization of brushite thus accelerating the setting reaction (Mirtchi et al., 1989, Bohner et al., 1997a, Van Landuyt et al., 1999).

Organic acids have the ability to bind with calcium ions and interact with brushite cements crystals, leading to inhibition of setting times. α- Hydroxyl carboxylic acids (e.g. tartaric, glycolic and especially citric acids) have an inhibitory effect on brushite cements setting reaction (Marino et al., 2007, Barralet et al., 2004, Lilley et al., 2005) whereas carboxylic acids with no hydroxyl groups have been shown to have no inhibitory effect on brushite crystal growth and may shorten the cement setting time (Marino et al., 2007, Giocondi et al., 2010).

Protein also can interact with brushite crystals and alter the setting reaction. The effect of protein varies depending on the ability of the protein to absorb onto the calcium phosphate surface. (Metz et al., 2006). Another important factor regulating the setting time is the amount of water present in the cement paste. Limiting the water available for the setting reaction will favour a faster precipitation of brushite crystals hence accelerating the setting time. This is usually seen when cement with low powder to liquid ratio is used (Mirtchi et al., 1989, Alkhraisat et al., 2010, Tamimi-Marino et al., 2007).

Another way to control the setting reaction of brushite cements is by premixing it with a non-aqueous liquid, for example glycerol, in order to form a premixed calcium phosphate cement that can only set when in contact with water (Aberg et al., 2010, Han et al., 2009). The cements can also freeze once they are mixed to stop the setting reaction, stored for a long time and thawed when needed. The resulting cements have a similar porosity and composition compared to the unfrozen cements (Grover et al., 2008).

2.9.2 Mechanical properties

Ideally, any cements and bioceramics for bone generation should have mechanical properties similar to bone. According to the current standards for testing bone cements of the American Society for Testing and Materials (ISO 5833, 2002) (ASfTa, 1999), cements are allowed to set for at least 24 hours prior to testing (Tamimi-Marino et al., 2007, Tamimi et al., 2010, Barralet et al., 2004, Hofmann et al., 2009).

Cements can be cured either in dry condition (room temperature and humidity) (Tamimi-Marino et al., 2007) or in physiological condition (37^{o}C and 100% humidity) (Hofmann et al., 2009) which are more preferred as it is more relevant to clinical application. Two mechanical assessments that are usually performed are compressive strength and tensile strength. Mechanical properties of this cement can be modified by several factors such as:

1. Porosity
2. Powder to liquid ratio
3. Particle sizes
4. Degree of cements setting
5. Delayed cements setting
6. Ultrastructural organization
7. Presence of additive
8. Addition of free ions or certain proteins

The strength of brushite cements are inversely correlated to the porosity which means mechanical performance will be higher when porosity of the cements is lower (Flautre et al., 2003). Cements with a low powder to liquid ratio will have excess water in the setting reaction that results in increased porosity and poorer mechanical properties. On the other hand, if a high powder to liquid ratio is used, it will result in cements that are difficult to handle and cannot be properly mixed.

The mechanical properties of brushite cement can be improved by modifying particle sizes of the cements reactants. For example, adjusting particle size of reagents in MCPM/β-TCP- based cements has been shown to increase its mechanical properties (Hofmann et al., 2009). Some cement additives have also been proven to increase the cements mechanical properties. Adding pyrophosphate salt and α-hydroxyl carboxylic acids such as citric, glycolic and tartaric acids help to increase cement powder to liquid ratio. This will result in easier mixing of cements and resulting in improved mechanical properties (Marino FT et al., 2007, Alkhraisat MH et al., 2008b, Bohner M et al., 2000a, Van Landuyt P et al., 1997, Barralet JE et al, 2004).

Nevertheless, any additive used usually has an optimal concentration, too much or too little can adversely affect other properties. For example, a high concentration of citric acid will weaken the brushite cements (Hofmann et al., 2006b). In contrast, with optimised cement particle size, powder to liquid ratio and cement retardant concentration (800 mM citric acid in the cement liquid phase) cements have been shown to have the highest reported wet compressive strength 52 MPa (Hofmann et al., 2009). Addition of free ions to the cements system will also affect the mechanical properties of the cements. Adding metallic ions such as strontium chloride was shown to have no valuable effect on the mechanical properties (Alkhralsat MH et al., 2008b).

Furthermore, brushite cements with magnesium substitute in either α-TCP or β-TCP result in increased compressive strength up to 40 MPa (Klammert, 2010, Pina S, 2009). Addition of certain protein such as albumin will interfere with crystal-crystal interaction within the cements ultrastructure that leads to negative effect on mechanical properties of brushite cements (Metz et al., 2006). Nevertheless, adding collagen type I to TTCP/MCPM cements system has been shown to slightly increase the cements compressive strength (Guo and Li, 2009).

Increasing the ultrastructural organization of the brushite cements is also one of the methods that have been found to increase mechanical properties of the cements. This can be achieved by adding additives such as gentamicin sulphate and calcium sulphate hemi-hydrates to the brushite cements that will act as crystallization nuclei and therefore will enhance the mechanical properties (Perez et al., 2012, Cai et al., 2011). Other methods such as freezing the cements during the mixing process will lead to formation of ice crystals that will help to arrange growing brushite crystals upon precipitation that result in increasing cements compressive strength (Grover et al., 2008).

2.9.3. Shelf-life

Long term stability of the cements is important and will be affected by temperature, humidity and mixing. Additives may help to preserve the cement properties for longer periods of time (Gbureck et al., 2005). When cements containing pyrophosphate are stored for long periods of time, it will result in spontaneous hydrolysis of pyrophosphate into orthophosphate. This reaction can affect the cements mechanical properties and shorten the setting time. On the other hand, adding citric acids to the cements powder and keeping in an inert cold atmosphere has been proven to prolong the cement storage life and stability (Van Landuyt P et al., 1999, Gbureck et al., 2005).

2.9.4 Injectability

It is important to have good cement injectability particularly for minimal invasive surgical procedures that require injection of the cements into the bone defect (Baroud et al., 2005). During the injection process, the liquid to powder ratios should not change in order to be capable for injectability but many brushite cements were found to suffer from phase separation during injection. These make it hard for them to be injected. There are a few changes that can be made in the cements composition that will help to enhance the cement injectability such as:

1. Decreasing the powder to liquid ratio (Habib et al., 2008).
2. Increasing the viscosity of the mixing liquid by adding gelling agent for example as xanthan gum (Habib et al., 2008).

3. Lowering the particle-particle interaction by using additive such as carboxylic acids (Habib et al., 2008).
4. Decreasing the particle size of the powder by extensive milling of the cement powder (Habib et al., 2008).
5. Increasing the extrusion velocity (Habib et al., 2008).
6. Using a small syringe with a short cannula (Habib et al., 2008).
7. Dissolving citric acids or sodium citrate in the cements liquid phase (Barralet et al., 2004).

Nevertheless, caution should be taken when any modification is done because it may affect other important properties of the brushite cements. For example, lowering the powder to liquid ratio will increase the injectability but it also will result in reduction in the cements mechanical properties. Some studies have shown that the most convincing method to increase injectable properties of cements is by reducing particle size and adding hydrogels to the cements liquid phase (Alkhraisat et al., 2009, Habib et al., 2008).

2.9.5 Degradation

Brushite cements are resorbed *in vivo* to a much greater extent compared to hydroxyl apatite cements. During the first weeks following implantation, brushite appears to be rapidly resorbed by simple dissolution and cellular activity (Theiss et al., 2005, Frayssinet et al., 2000) . In vivo observations have shown that early resorption of brushite cements is regulated by macrophages rather than osteoclasts (Kuemmerle et al., 2005). Initial resorption of brushite is affected by the inherent cement properties such as cement porosity, the rate of fluid exchange and the properties of the surrounding medium (Grover et al., 2003). Under physiological conditions brushite cements exhibit an increase in porosity, a decrease in mass, deterioration and a reduction in the cement mechanical properties (Grover et al., 2006, Ikenaga et al., 1998). This initial drop in mechanical properties is an important clinical issue when cement is used to repair load-bearing bone defects. Therefore further research is needed to address this problem. Nevertheless, after a few weeks implantation the mechanical properties of the cement may improve due to bone in-growth into the biomaterial (Ikenaga et al., 1998).

After the initial fast degradation of the cement the remaining brushite is converted into less soluble apatite. It has been observed that after 24 weeks of *in vivo* implantation in sheep, brushite cements completely convert to poorly crystalline carbonated apatite. At this point there is almost no dissolution of the cement and resorption is carried out solely by osteoclast activity, rather than macrophage phagocytosis (Grossardt et al., 2010, Constantz et al., 1998).

2.9.6 Adhesion

Proper adhesion between bone and cements is very important to allow better transmission of force at the cement-bone interface. Brushite cements have poor adhesion quality. Nevertheless it can be improved by adding pyrophosphoric acids in the liquid phase that are shown to have an increased adherence to bone. However more research needs to be done (Grover et al., 2006).

2.9.7 Cohesion

Cohesion of bone cements is very important for clinical applications because if cement particles are released into the bloodstream, it could result in pulmonary embolism and other potentially life threatening consequences (Bohner et al., 2006). Cements cohesion is evaluated by measuring the amount of solid particles released from the cements proceeding to its final setting (Bohner et al., 2006, Alkhraisat et al., 2008a). Cohesion of the cements can be influenced by:

1. Particle size (Bohner et al., 2006).
2. Presence of additives such as citric acids and $SrCl_2$ which reduce the particle-particle interaction in the cements and cause the particles to release from the cement and reduce the cohesion (Alkhraisat et al., 2008b).
3. Hydrogel that increase the viscosity of the cement liquid phase and improve cements cohesion by several folds for examples as collagen type I and silica gel (Alkhraisat et al., 2008b, 2009, 2010, Tamimi et al., 2008).

2.9.8 Bone formation

Brushite cements have been prepared and used for bone regeneration in different physical forms. These range from injectable paste, pre-set casted blocks, 3-D printed blocks and granules. Brushite cements are generally well tolerated by bone and soft tissues and do not cause inflammations in the long term (Theiss et al., 2005).

Following implantation, brushite cements are first enclosed in loose connective tissue (Frayssinet P et al., 1998) or surrounded by fibrous connective tissue if the cement composition is too acidic (Tamimi et al., 2009). The surfaces of brushite stimulate osteoblast activity *in vitro* (Klammert et al., 2009). This is followed by centripetal trabecular in-growth towards the material, leading to remodelling of the bone. During the later stages the brushite resorption rate slows down due to conversion to hydroxyl apatite. New bone is formed in direct contact with the cement margins resulting in osteointegration of the cement and its later remodelling (Frayssinet et al., 1998, Lu et al., 1999).

Brushite cement has been successfully tested in the regeneration of bone at various surgical sites in animal models such as in tibial condyle (Lu et al., 1999) and calvaria (Kuemmerle et al., 2005). However the amount of bone formation is highly dependent on the site of the implantation and the vascular supply, as an adequate blood supply can increase the speed of cement resorption and replacement by new woven bone (Constantz et al., 1998).

2.9.9 Macroporosity

It is important to allow cellular infiltration and proliferation inside the biomaterial and this can be achieved by altering the macroporosity of bone bioceramics. Cements should have a balanced incorporation of macropores within the cements structure without increasing the overall cement porosity due to the fact that increasing the cements porosity will have direct effect in reducing mechanical properties of brushite cements. Adding porogens such as mannitol will widen the pores in brushite cements to 250-500 µm without reducing the initial compressive strength of the cements (Cama et al., 2009) while adding gelatine powder as template will open pores about 100-200 µm (Yin et al., 2003).

The other way of creating macroporosity is by using computer aided design of 3-D printed brushite cements that allow specific pore design but this technique was limited by rapid prototyping technique pore resolution that currently only set at 0.5mm (Habibovic et al., 2008).

2.9.10 Application

Brushite cements have been tested *in vitro*, *in vivo* and clinically for various applications for example as drug delivery devices, in orthopaedics, craniofacial surgery, cancer therapy and amperometric biosensors.

1. Drug delivery:

   Different bioactive molecules have been added to brushite cements to improve the biological properties. These bioactive molecules can be added to the cements either as solid particles, by dissolving in the cement liquid phase or by soaking the set cement in a solution containing the drug (Tamimi et al., 2008, Alkhraisat et al., 2010).

   Drugs incorporated into brushite cements need to be stable in acidic environments due to the initial low pH of the cements, withstand the temperature changes during the setting reaction and have appropriate adsorption to the cement. The antibiotics and antiseptics that have been used for drug release from brushite cements include vancomycin, doxycycline, tetracycline, gentamycin, ciprofloxacin and chlorhexidine. Vancomycin is used in prevention of Staphylococcus aureus or osteomyelitis and upon release from the brushite cements matrix able to effectively eliminate the bacteria in the local environment (Jiang et al., 2009).

   Brushite cements loaded with doxycycline have antibacterial activity against periodontal pathogens, rendering it an interesting material for bone regeneration in periodontal bone defects (Tamimi et al., 2008). Brushite cements also have been used to release growth factors to stimulate angiogenesis and bone regeneration (De la Riva et al., 2009).

2. Orthopaedics

I. Restoration of metaphyseal defects:

A few studies have been done in both animal and humans for restoration of metaphyseal defects using injectable brushite cements. These cements have shown significant potential in the treatment of fractures in the tibial plateau done in animal studies (Theiss et al., 2005, Ryf, 2009). It also shows 89% success rate for reconstruction of tibial plateau fracture and 76% success in distal radial metaphysic fracture in clinical studies (Ryf et al., 2009).

The failure of brushite cements for these clinical studies were reported due to lack of stable fixation, poor bone quality between cements or joint and leakage of the cements into the adjacent tissue but it was then resorbed without any complication (Ryf C et al., 2009).

II. Ligament anchor:

Recent studies have shown that brushite cements have the potential to anchor ligaments to bone and create proper mechanical interface *in vitro*. The cements composition and shape of the anchor system had to be determined carefully in order to achieve this effect (Paxton et al., 2010). These studies have investigated the use of a 3-D printing technique of brushite and monetite bracket for bone-ligament-bone replacement compared to hand made bracket to optimize the cements ligament sinews. It resulted in similar strength (Ma et al., 2012).

III. Reinforcement of ostesynthesis screws:

Brushite cements have been shown to increase the pull- out forces needed to remove an osteosynthesis screw from artificial polyurethane bone *in vitro* by 3-fold (Van Landuyt et al., 1999). It is very important to stabilize the ostesynthesis screws in order to achieve positive results in patients with complicated bone fractures. This is a more critical issue when dealing with patients suffering from osteoporosis.

3. Vertebroplasty

Injectable brushite cements have been used as a filling material in repairing damage in osteoporotic vertebrae with results showing 20-50% increasing of bone mineral density of osteoporotic vertebrae and 120% increase in vertebral stiffness in vertebrae. Nevertheless, the 12% cases of cements extrusion to the spinal canal had been reported and the finding also concluded that brushite cements had no significant effect on healthy vertebra (Heini et al., 2001).

4. Craniofacial surgery

Brushite cements have been tested for cranioplasty treatment and in oral and maxillofacial bone regeneration. Some have been used for craniotomy defects in several animal models. For example one study used brushite cements to treat 23mm wide cranial defects in sheep. The results showed some resorption with moderate bone formation and formations of fibrous tissue on the treated areas (Kuemmerle et al., 2005). Another recent study used brushite cements clinically to prevent temporal depression in parietal craniotomies. The cement use enabled precise and easy contouring of the defect and produced a superior aesthetic outcome for simple repair by preventing depression of the temporal bone after craniotomy procedures.

However, a long period of time for full resorption of the material and replacement of the new bone was needed (Ji and Ahn, 2004). Brushite cements have been tested for bone regeneration in oral and maxillofacial surgery as injectable cements and pre-set cement granules. Both techniques have been used for vertical bone augmentation and bone defect healing (Tamimi et al., 2009, Marinno et al., 2007).

Injectable brushite cements have been used for minimal invasive craniofacial vertical bone augmentation in an animal study. In one study, the brushite cements were injected under the periosteum of the treated area and was allowed to set on the bone surface. The results showed that brushite cements help to promote vertical bone growth (Tamimi et al., 2009).

Several studies also showed that injectable brushite cements were capable of regenerating oral and maxillofacial bone in atrophic areas, buccal dehiscence and maxillary sinuses (Tamimi et al., 2010). Nevertheless, the development of complete bioresorbable cements is needed to allow more clinical applications in the future. Pre-set brushite cements granules have been tested in animal studies and result in promoting craniofacial vertical bone augmentation (Marinno et al., 2007).

Some *in vivo* study have also been done comparing them to commercial bovine materials for bone regeneration. It was shown that brushite cements showed a higher amount of vertical bone growth suggesting good potential application of these cements in the future (Tamimi et al., 2006).

5. Cancer therapy

Filling bone defect created by pathological tumours. This has been done in animal models. First bone defects were created in the animal at the distal femoral condyle and the defects were than filled with brushite cements and collagen gels or PMMA cements by percutaneous injection into the trabecular defect. The result showed that bone formation gaining with brushite cements was superior compared to the PMMA cements (Pasquier et al., 1998).

As a biomaterial to target and destroy cancer cells, this can be done by co-precipitated brushite cements with ferrous chloride to form a magnetic nanoparticle for the hyperthermic treatment of cancer. In vitro studies showed that these nanoparticles have the ability to kill the cancer cells without damaging the normal cells (Hou et al., 2009)

6. Amperometric biosensors

Amperometric biosensors are electronic devices based on monitoring enzymatic reaction on highly sensitive electrodes that are able to detect small amount of specific molecules in either gases or solution. Traditional biosensor systems are based on polymeric or clay matrices. Brushite cements as a new biosensor have been shown to result in more faster signalling and higher sensitivity compared to traditional biosensor system detection.

Two recent studies on brushite-based biosensors reported detection of glucose using the enzyme glucose oxidase (Lopez et al., 2006) and phenol by combining the brushite cements with enzyme tyrosinase (Sanchez-Paniagua Lopez et al., 2009). Brushite cements have two properties that are important for such devices:

I. Ability to conduct electricity through a mechanism known as proton conduction.

II. Ability to adsorb proteins.

2.10 Brushite cements with antibacterial properties

Bacterial infection is one of the main complications after surgery and may lead to permanent damage of tissue and bone (Fialkov et al., 2001). PMMA antibiotic loaded bone cements have been used in orthopaedic surgery (van de Belt et al., 2001). PMMA bone cements are however not bioresorbable. Calcium phosphate cements (CPC) have excellent bioactivity, bioresorbability and biocompatibility properties compared to PMMA.

CPC also can easily be moulded and injected to defects and it sets *in situ* (Ginebra et al., 2006b). Large numbers of studies have investigated the release of antibiotic using HA bone cements. However, HA cements were not able to degrade for full replacement by the surrounding tissue (Bohner et al., 2000a, Bohner et al., 2005). For this reason, degradable brushite cements have been evaluated as potential drug carriers. Different antibacterial agents, such as chlorhexidine, Nisin F, doxycycline and ε-polylysine, have been introduced in both commercial and experimental brushite cements. Recent studies have shown the feasibility of drug release from brushite cements for periodontal applications (Tamimi et al., 2008). For the treatment of common infections in the oral cavity and jaw bone, use of antibiotics was extensive. The frequent use of antibiotic-loaded bone cement may increase the chances of developing antibiotic resistance (Thomes et al., 2002). Chlorhexidine (CHX) and polylysine may offer an alternative to conventional antibiotics.

2.10.1 Chlorhexidine

Chlorhexidine (CHX) is a highly effective non-antibiotic with antibacterial properties. CHX has been used extensively in dentistry mostly for the treatment of periodontal infection (Heasman et al., 2001) and as an anti-plaque mouthwash (e.g. Corsodyl ^{TM}). CHX has a broad spectrum of activity against both gram-positive and negative bacteria, yeast, dermatophytes and some viruses (Hassan et al., 2008). However, the presence of CHX might interfere with the hydrolysis reaction of any brushite cements systems (Hofmann et al., 2006b, Bohner et al., 2006). Furthermore, CHX release was found to be rapid due to porosity of brushite cements thus limiting the desired antimicrobial effectiveness (Young et al., 2008). This has led us to consider a new natural biomaterial by its physico-chemical properties, controlled release capability as well for its antimicrobial activity. This agent is polylysine.

2.10.2 ε-Polylysine

ε-Polylysine is pale yellow powder and has a slightly bitter taste. Epsilon (ε) refers to the linkage of the lysine molecules. ε-Polylysine belongs to the group of cationic polymers. The systematic name of ε-polylysine is (S)-poly (amino (2-amino-1-oxo-1, 6-hexanediyl). ε-Polylysine is a basic polyamide that consist of 25-30 residues of L-lysine, one of essential amino acids. It is linked by peptide bond formed with α-carboxyl of L-lysine and ε-azyl from another L-lysine. It has strong hygroscopicity and easily soluble in water and hydrochloric acid but not in organic solvents such as alcohol or ether. The chemical formula of ε-polylysine is:

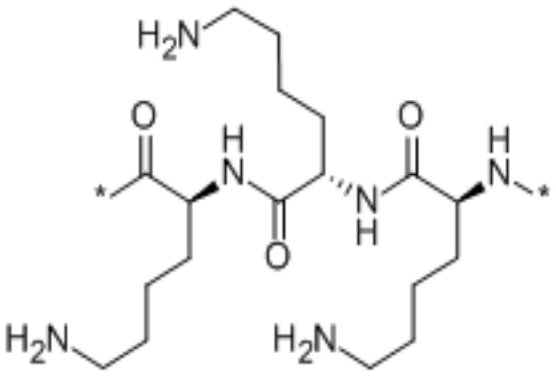

Figure 2-1: The chemical structure of ε-polylysine

In water, ε-polylysine contains a positively charged hydrophilic amino group. ε-Polylysine has a molecular formula for the typical homopolymer molecule of $C_{180}H_{362}N_{60}O_{31}$ and a molecular weight of approximately 4700 (Hiraki et al., 2003). ε-Polylysine is commercially produced by Streptomyces albulus ssp under aerobic conditions. The Gram-positive bacterium S.albulus ssp.lysinopolymerus strain 346 was first isolated from Japanese soil (Shima et al., 1984). A mutant of strains 346 which produced four times higher amount of ε-polylysine was later isolated (Kahar et al., 2001, Hamano et al., 2007).

No degradation is observed even when the ε-polylysine solution is boiled at 100 °C for 30 min or autoclaved at 120 °C for 2 min (Kawai et al., 2003). ε-Polylysine has good water solubility, nature, odourless and do not affect food flavour. ε-Polylysine has hydrophobic methylene groups on the inside and amino groups on the outside of the molecule in polar solution. ε-Polylysine molecules are cationic and surface active due to the positively charged amino groups in water. Cationic surface active compounds generally inhibit the proliferation of microorganism.

2.10.2.1 Application of ε-polylysine

Naturally occurring ε-polylysine is water soluble, biodegradable, edible and nontoxic toward human and environment. Therefore, ε-polylysine and its derivatives have been of interest in food, medicine and electronics industries.

1. ε-Polylysine as preservative

   ε-Polylysine is an approved antimicrobial preservative for food use in Japan. ε-Polylysine are used as preservatives in multiple foods including fish sushi, boiled rice, soup stocks, sukiyaki, noodles and cooked vegetables. The levels of ε-polylysine used in the foods range from 10ppm to 5000ppm. Studies have shown that feeding of ε-polylysine to rats using relatively high maximum concentrations in the diet of 20,000ppm and 50,000ppm had produced no toxicologically significant adverse effect in the animals. ε-Polylysine was practically non-toxic in an acute oral toxicity study in rats with no mortality up to 5g/kg and was not mutagenic in bacterial reversion assays (Fukutome et al., 1995).

Absorption, distribution, metabolism and excretion (ADME) studies of ε-polylysine revealed low absorption from the gastrointestinal tract and approximately 94% ε-polylysine passes unabsorbed through the gastrointestinal tract in the faeces. Whole body autoradiography did not show concentration of absorbed ε-polylysine in any organ or tissue (Hiraki et al., 2003, (Fukutome et al., 1995). The probable reasons for ε-polylysine's lack of toxicity are its poor absorption from the gastrointestinal tract and the absence of any chemical moiety of likely hazard in the ε-polylysine polymer (Hamano, 2011).

2. ε-Polylysine as antimicrobial agent

ε-Polylysine has been shown to be an effective antimicrobial by growth inhibition studies with yeast, fungi, gram positive and gram negative bacterial species, indicating broad-spectrum antimicrobial activity and is stable in a broad range of pH (Kito et al., 2002, Yoshida and Nagasawa, 2003). ε-Polylysine is believed to exert antimicrobial activity by adsorbing electrostatically onto the cellular membrane. The process followed by stripping off the membrane and abnormal distribution of the cytoplasm (Shima et al., 1984). ε-Polylysine was found significantly potent against streptococcus mutans and total aerobic oral microflora with the rate of reduction of microbial counts was proportional to the amount of ε-polylysine used (Najjar et al., 2009). Recently, ε-polylysine has been immobilized on polyethylene terephthalate fabrics. The immobilized fabric showed antimicrobial activity against both Gram positive and Gram negative bacteria (Lin et al., 2011).

3. ε-Polylysine as a drug carrier

ε-Polylysine is available in a large variety of molecular weights. As a polypeptide, ε-polylysine can be degraded by cells effortlessly. Therefore, it has been used as a delivery vehicle for small drugs (Shen and Ryser, 1981). It can also be used as a carrier in the membrane transport of protein and drugs as it was found to be easily taken up by cultured cells. The conjugation of drugs to ε-polylysine markedly increase its cellular uptake and offer a new way to overcome drug resistance related to deficient transport (Ryser and Shen, 1980, Shen and Ryser, 1981).

4. ε-Polylysine as nanoparticles

Nowadays, ε-polylysine is also being used for gene delivery and controlled drug delivery. The epsilon amino group of lysine is positively charged at physiological pH. Thus the polycationic polylysine ionically interacts with polyanion, such as DNA. In addition, the epsilon amino group is a good nucleophile above pH 8.0 and easily reacts with a variety of reagents to form a stable bond and covalently attached ligands to the molecule. Nanoparticle construct of polylysine has been reported by several studies such as polylysine-graft imidazole acetic acid-DNA (Locher et al., 2003). Recently, antimicrobial activities of multiwalled carbon nanotubes (MWNT) were found to increase by coupling it with ε-polylysine using hexamethylene diisocyanate as a coupling agent. The new Nano composite showed enhance antimicrobial activity as compared to MWNT and killed about 97.6% of E. coli, 91.5% of Pseudomonas aeruginosa and 88.5% Staphylococcus aureus. The new MWNT- ε-polylysine was found to facilitate its use as antimicrobial material in food and pharmaceutical industries (Yu et al., 2011).

5. ε-Polylysine as liposomes

Liposomes are widely used as carrier for a variety of drug and also for gene delivery (Ma and Wei, 1996, Waelti and Gluck, 1998). Liposomes offer a protective biocompatible and biodegradable delivery system that can enhance cellular uptake (Thierry et al., 1993). Biodegradability and low permeability to small hydrophilic molecules make liposomes excellent reservoirs for drug loading or release. However, liposomes are quite unstable and can release an active entrapped compound into the biological fluids. ε-Polylysine coating of liposomes stabilizes them against disruption upon adsorption (Michel et al., 2005, Michel et al., 2004).

6. ε-Polylysine as coating material

ε-Polylysine had been used as the coated tissue for animal cell culture (Ahn et al., 2004). ε-Polylysine is also used to improve cell attachment to plastic and glass surfaces. Tissue culture flasks with a net negative charge are produced by treatment of polystyrene.

The negatively charged polystyrene becomes positively charged on its surface by coating with ε-polylysine. It was also seen that when a serum-free or reduced-serum media was used, the cultivation efficiency of individual cell lines was improved by coating the culture surface with ε-polylysine. Many cell types adhere better to this surface and are less dependent on the presence of serum proteins.

7. ε-Polylysine as lipase inhibitor

ε-Polylysine and taurocholate forms a surface-active complex that binds to emulsion particles, thereby retarding lipase adsorption and triacylglycerol hydrolysis in both *in vivo* and *in vitro*. It was concluded that the ε-polylysine acts as an anti-obesity agent and it was found that inhibition increases with the degree of ε-polylysine polymerization (Tsujita et al., 2006, Tsujita et al., 2007).

2.11 Citric acid as setting retardant

As mention earlier, brushite cements have short setting times and are too weak to be used in load – bearing areas. Many studies have been done to improve the mechanical properties of the set cements. Incorporating setting retardants into the brushite cements will help to increase the cements setting time. It will also lead to precipitation of smaller crystals and thus an improvement of the mechanical properties of the cements (Grases et al., 2000, Bohner M et al., 1996).

Examples of setting retardants used are sodium pyrophosphate, citrate ions and sulphates. Pyrophosphate inhibit the crystallization of brushite by binding to the crystalline nuclei preventing the incorporation of ions into the crystal lattice, thus inhibited the crystal growth.

The addition of citric acid to the liquid phase improves the setting time, injectability and mechanical properties (Barralet et al., 2004). It was reported that all these acids prolong the setting reaction with different effects on the mechanical properties. For example, citric acid solution produced stronger cements when compared to cement produced by lactic acids. However, there is an upper limit to the use of citric acids as a setting retardant.

When citric acid is used in the cement reaction at concentrations higher than 800 mM, citrate ions slowly diffuse out of the cement, allowing greater conversion of dicalcium phosphate anhydrate (DCPA) into dicalcium phosphate dehydrate (DCPD) leading to more heterogeneous and therefore weaker structure (Hofmann et al., 2006a).

Citric acid anhydrous appears as an odourless white crystalline granule with a strong acidic taste. It is very soluble in water, freely soluble in alcohol and slightly soluble in ether. The pH of a 0.1 M solution of citric acid is 2.1.Citric acid has three carboxyl or - COOH groups. The systematic name for citric acid is 2-hydroxypropane-1, 2, 3-tricarboxylic acid. Citric acid molecule molecular formula is $C_6H_8O_7$. Its chemical structure is below:

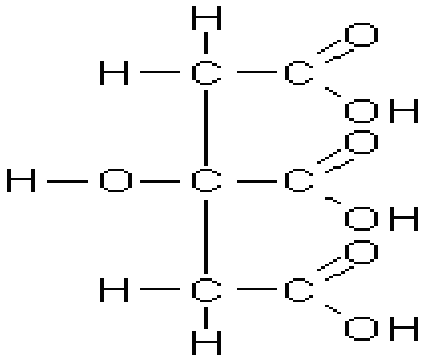

Figure 2-2: The chemical structure of citric acid

Citric acid as an organic acid has the most ability to bind calcium ions enabling them to interact with growing brushite cement crystals and inhibit their setting more than many other carboxylic acids. (Lilley et al., 2005).

Although adding setting retardant has been shown to improve the mechanical performance of brushite cements, there is an upper optimal concentration beyond which strength reduction can occur (Hoffmann et al., 2009). Hoffmann also reported that at a combination of small particles, reactant and citric acid at concentrations of 800 mM, the powder to liquid ratio could be raised and provides low porosity cements with compressive strength of 52 MPa.

Citric acid is a constituent of fruit soft drinks and other food products. One of the most common citric acid uses is for preserving foods. It is also added to provide a sour and acidic taste to food and drinks. It can easily mix with water thereby, making it acidic. Other uses include flavour enhancement, bacterial inhibitor, pH adjustment, and as an anti-oxidant.

2.12 Summary

Early tooth loss will result in alveolar bone loss and subsequently complicate treatment outcomes. Alveolar bone resorption as a sequel to premature tooth loss results in loss of bone height and volume. This results in aesthetic and functional issues in the area of tooth extraction site. It is also leads to inadequate bone for ideal implant positioning or placement. As such, an ideal outcome in the young patient with missing teeth either due to trauma or caries or with poor prognosis teeth is to preserve bone and soft tissue as long as possible. This will help to improve restorative options that can be offered in adulthood after growth has ceased (Day et al., 2008).

These have led to various materials and protocols to preserve or regenerate alveolar bone. Thus, the development of brushite cements as a potential bone substitute may offer clinicians the opportunity of preserving alveolar bone. The combination of self – setting nature, moldability, injectability, biocompatibility, remineralising antibacterial effect and also other properties suggests a great potential of brushite cements in regenerative therapy.

An important benefit is their ability to act as a reservoir of calcium and phosphate ions for remineralisation of hard tissue. Brushite cement is biocompatible, bioresorbable and has the osteoconductive properties (Bohner et al., 2000a). Due to its excellent bioresorbality, woven bone might substitute the cement after the implantation (Bohner et al., 2000a, Dorozhkin, 2008).

Brushite cements are also easy to manipulate and have excellent moldability. It can adapt to shape of bone defect and rapidly integrated into the bone structure. It will then transform into the new bone by cellular action of the bone cells that is responsible for bone remodelling. However, several issues may limit their application. Firstly, brushite has a rapid setting reaction which results in:

- High porosity – this makes brushite cement relatively weak and gives rapid drug release properties

- Weak mechanical strength limiting clinical application. Mechanical properties can be improved by using small particle size reactant and by adding additives or free ions.

Brushite cements have very short setting time. The original composition of brushite cements set within 30 seconds of mixing (Mirtchi et al., 1989). Setting time of brushite cements can be increased to a workable length through:

- Using low powder to liquid ratio, or

- Adding additives or setting retardants

The drawback of low powder to liquid ratio is that the end product will have a higher porosity and therefore lower strength. In contrast to ratio manipulation, the effect of setting retardant led to precipitation of smaller crystal and thus results in an increased setting time, an improvement of mechanical strength and injectability of the brushite cement. Examples of setting retardant used are sulphuric acid, sodium pyrophosphate and sodium citrate solution (Bohner M et al., 1996).

Material degradation is good for bone repair as it enables full bone remodelling but with brushite cements this property can be difficult to control. The drug release from brushite cements has been shown to be very rapid. This problem can be addressed by modifying the porosity of the cements and by in-cooperating polymer into the composition (Bohner et al., 2006). Brushite cement adhesion to the bone also may be limited.

CHAPTER 3

AIM AND OBJECTIVES

3 AIM AND OBJECTIVE

3.1 Aim:

The aim of this study to produce high strength brushite cements with release of a novel antimicrobial ε-polylysine.

3.2 Null Hypothesis

The null hypothesis was that the addition of citric acid (CA) and / or ε-polylysine (PLS) would not improve the mechanical properties, handling and setting characteristics

3.3 Objectives:

The objectives of these studies are:

1) To optimize the size of the reactant particles with regards to the handling properties and strength.
2) To optimize the powder to liquid ratio
3) Assess the effect of varying concentrations of PLS.

This research involves monitoring of the following parameters:

i) Strength and modulus
ii) Reaction kinetics
iii) Cements degradation
iv) Polylysine release profile
v) Microstructure

CHAPTER 4

MATERIAL AND METHODS

4 MATERIAL AND METHODS

4.1 Materials

Table 4-1: Summary of materials used in experimental brushite cements

Name	Abbreviation	Formula	Particle sizes (µm)
Monocalcium phosphate monohydrate (HIMED)	MCPM 1	$Ca(H_2PO_4)_2.H_2O$	50 micron
Monocalcium phosphate monohydrate (SIGMA)	MCPM 2	$Ca(H_2PO_4)_2.H_2O$	-
β-Tricalcium phosphate	β-TCP 4	$Ca_3(PO_4)_2$	4 micron
β-Tricalcium phosphate	β-TCP 6	$Ca_3(PO_4)_2$	6 micron
β-Tricalcium phosphate	β-TCP 8	$Ca_3(PO_4)_2$	8 micron
β-Tricalcium phosphate	β-TCP 12	$Ca_3(PO_4)_2$	12 micron
β-Tricalcium phosphate	β-TCP 34	$Ca_3(PO_4)_2$	34 micron
ε-Polylysine	PLS	$C_{18}H_{36}N_6O_3X_2$	-
Citric acid	CA	$C_6H_8O_7$	-
Distilled water	-	H_2O	-

4.1.1 Powder

4.1.1.1 Monocalcium phosphate monohydrate

Initial brushite cements were prepared by mixing water with a powder consisting of an acidic calcium phosphate and a basic calcium phosphate. The brushite cements has calcium to phosphate ratio of 1. Therefore, the source of acidic phosphate ions should have a calcium to phosphate ratio lower than 1. The only calcium phosphates with this property are monocalcium phosphate monohydrate (MCPM) and monocalcium phosphate anhydrous (MCPA). However, the presence of a water molecule in MCPM facilitates the setting reaction. These results in cements with better properties that are easier to handle compared to cement with MCPA.

In this study, MCPM (MW=252 g/mol) was obtained from 2 different manufacturers, Himed Medical, US and Sigma-Aldrich, UK. MCPM Himed has particle size 53 micron as quoted by the supplier. There was no information with regards to particle size of MCPM Sigma provided by the supplier.

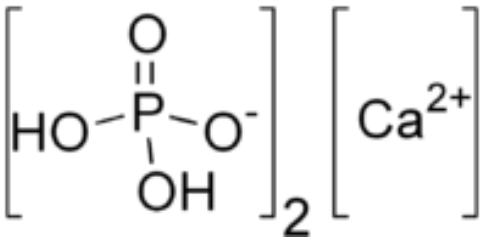

$Ca(H_2PO_4)_2 \cdot H_2O$

Figure 4-1: The chemical structure of MCPM

4.1.1.2 β – tricalcium phosphate

The alkaline calcium source has a calcium to phosphate ratio of 1, therefore a compound with a ratio higher than 1 can be used as the alkaline source. The most common basic calcium source in brushite cements is tricalcium phosphate (TCP) which has a calcium to phosphate ratio of 1.5. It has two crystallographic forms; either β – tricalcium phosphate (β-TCP) or α –TCP. β-TCP was the one used in the original cement formula presented by Mirtchi (1989).

β-TCP (MW=310 g/mol) with a particle size ranging from 4 micron to 34 micron was obtained from Plasma Biotal LTD, UK. The particle sizes were as quoted from the supplier as shown in table 4.2.

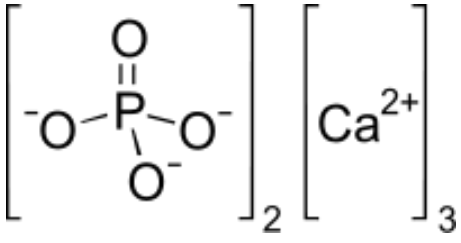

$Ca_3(PO_4)_2$

Figure 4-2: The chemical structure of β - TCP

Table 4-2: The chemical structure of β-TCP particle characterisations (quoted from suppliers)

β-TCP	Size d_{10} µm	Size d_{50} µm	Size d_{90} µm	Surface area m^2/g	Solubility at 25°C -logKs
β-TCP 1	2.1	4.32	8.8	1.65	28.9
β-TCP 2	3.0	5.78	12.5	1.28	28.9
β-TCP 3	3.4	7.76	18.0	1.49	28.9
β-TCP 4	2.82	12.03	27.73	---	28.9
β-TCP 5	7.89	33.8	53.6	0.3533	28.9

4.1.1.3 ε-polylysine

ε-polylysine powder was used in the formulation for its antimicrobial. ε-polylysine was purchase from Handary, Spain. ε-polylysine or Epolyly ® P is pharmaceutical grade. Epsilon – polysine is a small polypeptide of the essential amino acid L – lysine. It is produced by bacterial fermentation from Streptomyces strains growing in Lunia – Bertani bacterial culture media, fully renewable and non – GMO (genetic modified).

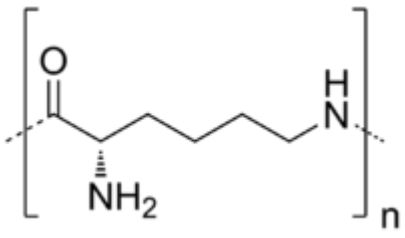

$(C_6H_{12}N_2O)_n$

Figure 4-3: The chemical structure of ε-polylysine

4.1.2 Liquid

4.1.2.1 Citric acid

Citric acid crystals were purchased from Fisher, Longborough, UK. These were mixed with distilled water to produce a concentration of 800 mM.

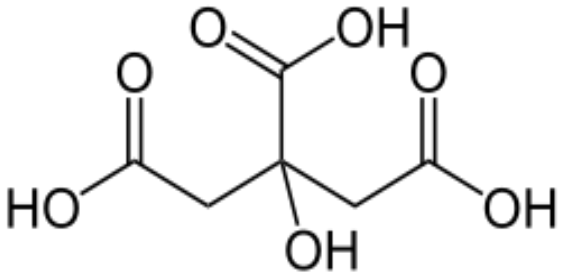

$C_6H_8O_7$

Figure 4-4: The chemical structure of ε-polylysine

4.2 Methods

4.2.1 Cement and disc preparation

The cement powder consisted of 1.00 g of MCPM and 1.23 g of β-TCP. For all experimental formulations, powder phase and liquid phase were weighed using a four-figure balance. Powders were hand mixed with aqueous solutions on a glass plate to produce the cement paste and start the setting reaction. Both powders were mixed for about 10 seconds before adding the liquid phase until a homogenous consistency was established. Metal washer rings of 10 mm internal diameter and 1 mm depth were used as the moulds to prepare the cement discs.

Excess cement was removed with the spatula before sealing top and bottom cement with acetate sheet. After mixing, cements were left to set at room temperature for 24 hours. The samples were then removed from the moulds and excess material removed to get smooth edges. The samples were then placed in a plastic bottle before testing as dry samples.

For wet samples, the cements were then immersed in 10 ml of distilled water in sterilin tubes and left for another 24 hours at 37°C. The cements were then blotted dry before testing. The set cement discs were used in mechanical, microstructure, degradation and drug release studies. Six samples of each formula were prepared for mechanical testing. Five samples for each individual formula were used for testing pH, degradation and ε-polylysine release.

4.2.2 First series

The first series of experimental cements were prepared by using powder consisting of 1.23 g TCP (4 to 34 microns) and 1.00 g MCPM from Himed (MCPM 1) or Sigma (MCPM 2). The liquid phase consisted of aqueous citric acid (CA) 800 mM with powder to liquid ratio (PLR) of 3.3:1 (i.e. 0.68 g of liquid).

4.2.3 Second series

For the second series, cements were prepared with PLR of 3.3:1 and 4:1 using MCPM 2 (1.00 g) and TCP (1.23 g) particle size of 34 micron as powder phase. The liquid phase (0.68 or 0.56 g) was prepared by diluting increasing percentages (10, 20, 30, 40 and 50 wt %) of ε-polylysine powder in the CA 800 mM solution.

Solutions were stirred until all the powder dissolved and a homogenous liquid was produced (see Table 4.2 and table 4.3). In the control formulation, only CA 800 mM was used as a liquid phase without adding the ε-polylysine powder in 3.3:1 and 4:1 weight ratio.

Table 4-3: Formulation of cements at second series with PLR 3.3:1

Formulation Code	MCPM Sigma powder (g)	TCP 34micron powder (g)	800mM citric acid solution (g)	ε-polylysine powder (g)
PLS 0%	1.00	1.23	0.68	0
PLS 10%	1.00	1.23	0.61	0.07
PLS 20%	1.00	1.23	0.54	0.14
PLS 30%	1.00	1.23	0.48	0.20
PLS 40%	1.00	1.23	0.41	0.27
PLS 50%	1.00	1.23	0.34	0.34

Table 4-4: Formulation of cements at second series with PLR 4:1

Formulation Code	MCPM Sigma powder (g)	TCP 34micron powder (g)	800mM citric acid solution (g)	ε-polylysine powder (g)
PLS 0%	1.00	1.23	0.56	0
PLS 10%	1.00	1.23	0.50	0.06
PLS 20%	1.00	1.23	0.44	0.12
PLS 30%	1.00	1.23	0.39	0.17
PLS 40%	1.00	1.23	0.34	0.22
PLS 50%	1.00	1.23	0.28	0.28

Figure 4-5: Image showing mixed set cement and its ring mould

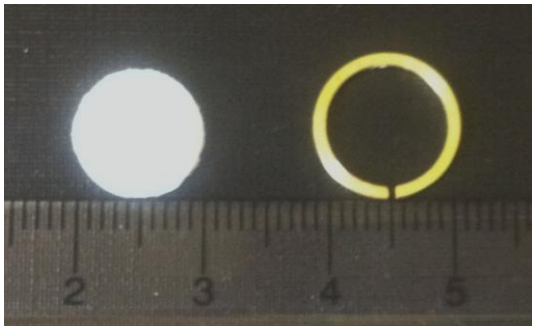

Figure 4-6: Flowchart of experimental design

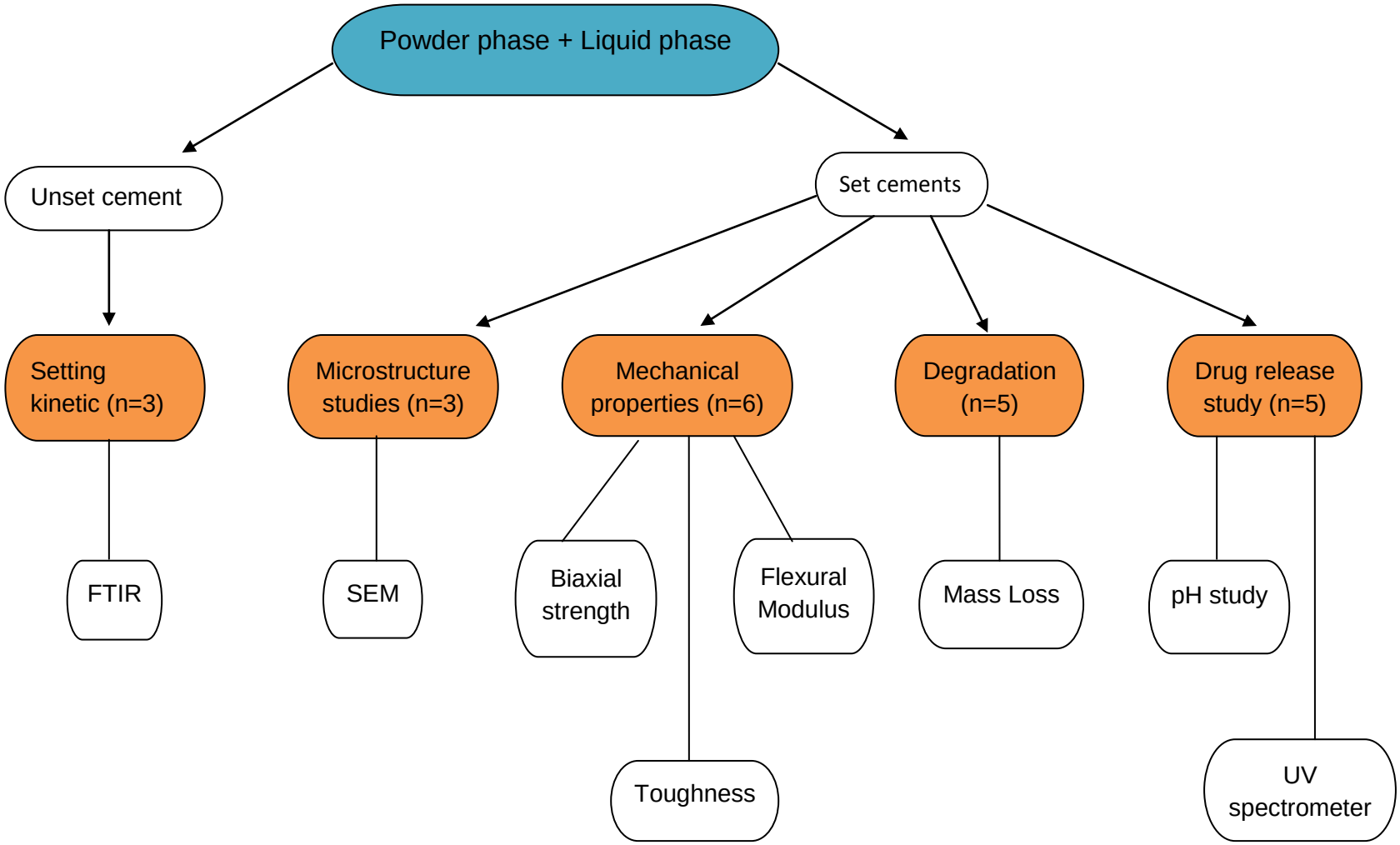

4.2.4 Mechanical Property Studies

4.2.4.1 Biaxial flexural strength

Biaxial flexural strength (BFS) and flexural modulus of the cements were measured by using an Instron mechanical testing frame. BFS is the maximum stress experienced in the material at its moment of rupture when subjected to bending load. A number of standard tests such as compressive and diametral tensile have been used for testing mechanical properties of brushite cements. In this study, the BFS test was selected over the compressive test. A recent study had showed that brushite cement can produce high compressive strength (as discussed earlier); however they are brittle and unable to withstand high tensile stresses. Therefore tensile strength is an important factor that may influence the clinical success (Zhang et al., 2004). This is due to possible application of this cement as dental material which can be subjected to flexural stress during mastication.

Standard test methods for determining the flexural strength are either uniaxial or biaxial flexural strength (BFS). BFS tests have several advantages over uniaxial test. In this test the disc of the cement prepared is supported near its periphery by a continuous ring shaped structure and later loaded by a coaxially located ball. In addition the disc shape is circularly symmetrical; the stress field is equibiaxial in the central region in which it is at a maximum. Therefore, this method will minimise the effect of the test specimen edge preparation because the generated stresses are lowest at the test specimen edges as shown in figure 4.7 and figure 4.8 (Chung et al., 2004)

In BFS test, a thin disc is supported by a ring near its periphery and loaded through a smaller coaxial ring, a piston or a ball in its central region. The disc is subjected to biaxial movement in its central region and the stress is the biaxial in this region. BFS is also relatively simple and accurate procedure for preparing the specimens. This will help to reduce the operator-induced variability and improves the standard for assessing mechanical properties of the cements.

4.2.4.2 Biaxial flexural modulus

Young's modulus is a measurement of stiffness or elasticity of a material. It indicates how much a material will stretch when put under a given stress and resists elastic deformation. This can be experimentally determined from the slope of a stress-strain curve created during tensile tests conducted on a sample of the material. The Instron machine produces data in pound (lbs.) and inches, so the data needed to be converted to Newton (N) and millimetres (mm). From the load -displacement data, a graph was plotted for each sample (load against displacement) to determine the slope required for the calculation of modulus based on the following equation showed below:

$$E = \left(\frac{\Delta P}{\Delta W} \right) \left(\frac{\beta c a^2}{t^3} \right)$$

Equation 1

Where:

$\Delta P/\Delta W$ change in force/change in displacement
gradient of the force displacement curve.

E elastic modulus of the disc (from BFS test).

βc central deflection function. For a ball on ring geometry βc is 0.502 (Higgs et al., 2001)

4.2.5.3 Toughness

Toughness was determined by measuring the area underneath the stress-strain curve. Toughness indicates how much energy a material can absorb before rupturing.

$$\frac{\text{Energy}}{\text{Volume}} = \int_0^{\epsilon f} \sigma d\epsilon$$

Equation 2

Where:

ϵ strain

ϵ_f strain upon failure

σ stress

4.2.4.4 Test method

The strength and modulus was determined by biaxial flexural strength testing method using the Instron Model 4505 Universal Testing Machine. Each composition was replicated into 6 discs of 10 cm diameter and approximately 1mm thickness. For dry samples, cements were left to set at room temperature for 24 hours before testing.

For wet samples, the cements were then placed in plastic bottle containing 10ml distilled water and left in the incubator for another 24 hours at 37°C. This was to act as a simulator of the clinical environment. All the wet samples were blotted dry before testing was undertaken. For each sample thickness, t was measured (mm) accurately to 0.001 mm at three different points and the average thickness recorded.

The hydrated disc / dry sample then were loaded using a spherical tip in an Instron mechanical testing jig and the maximum load at break recorded. The specimen disc was placed on the knife edge ring support (radius a = 4mm) and then loaded by the spherical tip. The instrument crosshead speed was set at 1mm / min.

The maximum load (kN) at fracture, P and load versus central displacement gradient, dP/dw were determined. The strength for each sample was calculated by using the average thickness of the cements obtained and the maximum load recorded by the computer. This was calculated using the following formula by Timoshenko (Timonshenko and K.S, 1964):

$$\sigma = \frac{P}{t^2}\left[(1+\Omega)\left(0.485\ln\left(\frac{a}{t}\right)+0.52\right)+0.48\right]$$

Equation 3

Where:

σ is biaxial flexural strength.

P is maximum load.

a is support radius.

t is average thickness of specimen.

Ω is Poisson's ratio= 0.3 (Charriére et al, 2001)

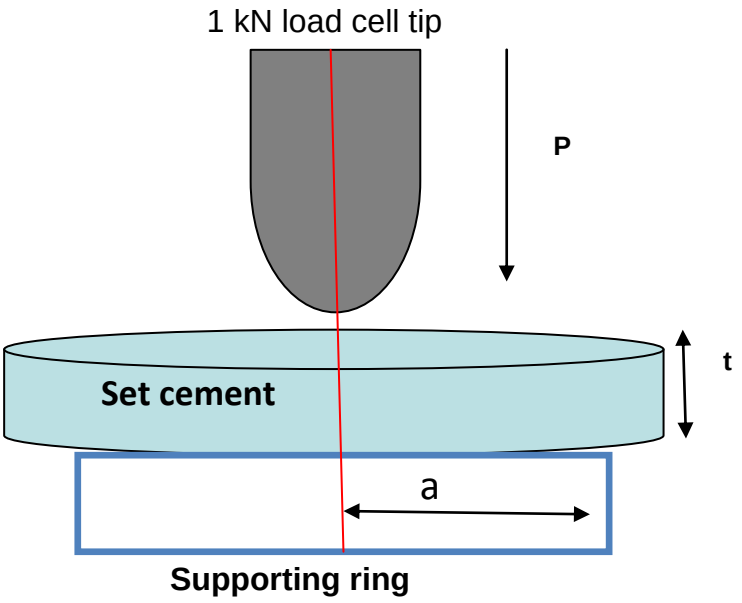

Figure 4-7: Schematic diagram of biaxial flexural strength test.

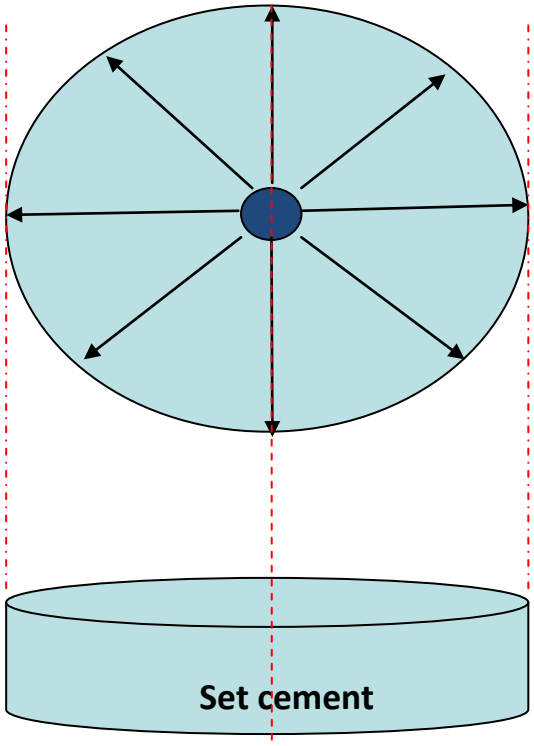

Figure 4-8: Blue area demonstrated the maximum stress region. The stresses are equally distributed along its radial direction in which the stresses generated at the edge of the specimen are the lowest.

4.2.5 Study on setting kinetics

4.2.5.1 FTIR spectroscopy

Fourier Transform Infrared (FTIR) spectroscopy uses infrared radiation to assess molecule movement vibration. It can help identify relative levels of different chemicals in mixtures. With this spectroscopy, infrared radiation is passed through a sample. Some of the infrared radiation is absorbed by the sample and some of it is passed through or transmitted. Different chemical bonds absorb different frequencies of infrared radiation. The resulting spectra have peaks characteristic of different chemical groups at high wavenumbers and fingerprint region unique to each chemical at lower wavenumbers.

4.2.5.2 Test method

Setting reaction and kinetics of the cements was assessed using a Perkin Elmer Series 2000 Fourier Transform Infra Red (FTIR) spectrometer (Beaconsfield, UK). The background of the instrument was scanned first using an ATR diamond attachment without any sample. This was done to ensure that the ratio of light intensity through the instrument either with or without the sample could be calculated by the computer. Scan number was set at 4 with wavenumbers range 500 to 4000 cm^{-1} and resolution of 8 cm^{-1}.

For experiments with powder to liquid ratio 3.3:1, approximately 0.43g of each formulation paste was used. With powder to liquid ratio 4:1, each formulation was prepared by mixing 0.40g powder phase with 0.1g liquid phase. Spectra were obtained from within the 60 second from the start of cements mixing using Time-based software (Perkin Elmer).

The FTIR time base program is set to start once both of the MCPM and β-TCP powders were mixed together. The powder phases of reactants were hand-mixed for 10 second before the addition of the liquid phase. The unset cements were loaded immediately into the metal ring which is put over the centre of an ATR-FTIR diamond at 37°C within 60 second of mixing the powder and liquid. A layer of acetate sheet was placed on top of the cement loaded into the ring.

Excess cement was expressed from the side of the metal ring using finger pressure over the acetate sheet to ensure contact of the specimen with the diamond piece and to standardize the thickness of specimen to about 1 mm. Each experiment was set to last for 60 minutes. The setting reactions however were not completed after 60 minute for experiment containing 30, 40 and 50 wt % of ε-polylysine. Therefore, the scan time was extended up to 120 minutes. Spectra were obtained every 6.4s within 60 seconds from initial cement mixing. Three individual specimens for each of the six formulations of brushite cement were scanned.

4.2.6 Scanning electron microscopy (SEM)

Scanning electron microscopy (SEM) was used to investigate the effect of adding citric acid and ε-polylysine on the microstructure of brushite cements. SEM is an instrument that produces a magnified image by using electrons instead of light. It uses a focused beam of high-energy electrons to generate a variety of signals at the surface of solid specimens. A beam of electrons is produced at the top of the microscope by an electron gun. The beam travels through electromagnetic fields and lenses, which focus the beam down toward the sample. A series of electromagnetic coils pull the beam back and forth, scanning it slowly and systematically across the specimen's surface.

The electrons that are reflected off the specimen, known as secondary electrons are collected and converted into a signal directed at a screen, similar to a television screen. This produces the final image. The signals that derive from electron-sample interactions reveal information about the sample including external morphology (texture), chemical composition, and crystalline structure and orientation of materials making up the sample. All non-metals samples need to be made conductive by covering the sample with a thin layer of conductive material. All water also must be removed from the samples because the water would vaporize in the vacuum.

4.2.6.1 Test method for microstructure

Scanning electron microscopy (Phillip XL-30, Eindhoven, The Netherland) was used to examine the morphology of each MCPM, β-TCP and ε-polylysine powder at primary beam energy of 5kV and approximately 200 pA.

The set brushite cements surface and cross-sectional fracture was also determined by using the same method. The prepared cements were snapped in order to obtain cross-sectional fracture image. Firstly, cements were coated by placing it on aluminium stubs and sputtered by gold-palladium under vacuum (Polaron E5000, Quorum Technology, UK) for 90 seconds at 20 mA.

For dry samples, the cements were left to set for 24 hours after mixing before test was done. For wet samples, the set cements were place in the sterilin tube containing 10ml water for another 24 hours at 37°C. Afterward, the cements were blotted dry and left again for 24 hours at room temperature before being vacuum and ready to be used with SEM. High resolution images of the cement were taken at different magnification (x500, x1500, x2500, x3500 and x5000).

4.2.7 Degradation study

4.2.7.1 Test method for degradation study

For each formulation, a set of 5 discs (n=5) were prepared and weighed before being immersed in 10ml of distilled water in sterilin tubes and kept at 37°C. Each of the cements were then removed, blotted dry, weighed again and then replaced in fresh distilled water at time points of 1, 2, 4, 6, 24, 72, 168, 336 and 672 hours. All the solutions were kept aside for pH analysis and polylysine release. Mass change was calculated as:

$$\Delta m\ (\%) = \frac{(m_0 - m_t)\ x100}{m_0}$$

Equation 4

Where

m_0 is sample mass initially

m_t is sample mass at time

Δm mass change

4.2.8 pH studies

4.2.8.1 Test method for pH study

The solutions from the degradation study at different time points were all kept in the fridge at 4°C. The solutions were then examined with Jenway 3340 pH/Ion Meters (BDH, Poole, Dorset, UK) at room temperature. Before beginning the test, the machine was calibrated at pH 3, 7 and 10. The Ion Meter was washed with distilled water every time before putting in different solutions to eliminate impurity. From the definition of pH

$$[H^+] = 10^{-pH}$$

Equation 5

[H+] is the acid concentration in moles/l. This can be converted to acid release (in moles) in 10 ml of storage solution by dividing by 100. Cumulative release is then obtained by summing all acid release up to each given time point.

4.2.9 Drug release study

4.2.9.1 Test method for ε-polylysine (PLS) release profile

For ε-polylysine (PLS) release, the absorbance of different storage solutions from mass loss studies was obtained using the Unicam Ultraviolet-visible (UV) 500 spectrometer (Thermo Spectrotonic, UK) for a period of up to 4 weeks. Several methods were attempted to detect the PLS release. In the following however, Trypan blue assay (TB assay) method was used.

There were a few steps needed to be done to produce the TB solution (also known as working reagent solution). First of all, 8000 ppm of TB solution was prepared by dissolving 0.080 g of TB in 10 ml distilled water. The solution then was diluted further by mixing 1 ml of 8000 ppm solution with 99 ml of distilled water to produce 80 ppm of TB solution which can be used up for 6 month.

For determination of a calibration curve, standard PLS solutions were prepared in distilled water. PLS solutions of 2, 4, 8, 10, 14, 18 and 20 ppm were made using the following dilutions:

i) 10,000 ppm solution: 0.10000 g of PLS mixed with 10 ml distilled water

ii) 100 ppm solution: 1 ml of 10,000 ppm mixed with 99 ml distilled water

iii) 20 ppm solution: 10 ml of 100 ppm mixed with 40 ml of distilled water

iv) 18 ppm solution: 18 ml of 20 ppm mixed with 2 ml of distilled water

v) 14 ppm solution: 14 ml of 20 ppm mixed with 6 ml of distilled water

vi) 10 ppm solution: 1 ml of 100 ppm mixed with 9 ml of distilled water

vii) 8 ppm solution: 8 ml of 10 ppm mixed with 2 ml of distilled water

viii) 4 ppm solution: 4 ml of 10 ppm mixed with 6 ml of distilled water

ix) 2 ppm solution: 2 ml of 10 ppm mixed with 8 ml of distilled water

The same amount of prepared TB solution and the above PLS solutions were mixed to produce PLS standard solutions of 1, 2, 4, 5, 7, 9 and 10 ppm. The mixture was left in the incubator for 1 hour at 37^{o}C and then cooled at room temperature for about 4 hours. All the mixture solutions were then centrifuged at 13,000 rpm for 20 minutes to remove any TB dye that has reacted with PLS. The supernatant solution was taken and dispensed in 1.5 ml disposable cuvettes. The absorption spectrum was recorded against distilled water as reference buffer between 200 nm – 800 nm with the maximum absorbance of the TB dye being observed at 580 nm. A standard graph was then determined by plotting the different concentrations of PLS against the absorbance (Grotzky, Manaka et al, 2010).

In order to determine the amount of antimicrobial release, the solutions from degradation study (n=5) at different time points were kept in the fridge at 4°C until analysis. For analysis the same amount of TB solution and storage solution was mixed, reacted and tested as mention above. Finally, the amount of release was calculated using the following equation:

$$\% \text{ of PLS} = \frac{\left(C \times 10^{-6} \right) \times 2V}{M} \times 100$$

Equation 6

Where:

C cumulative concentration of PLS (ppm)

V volume of storage solution (10 ml)

M total mass PLS in sample

The factor 2 accounts for dilution of the storage solution by the dye. M is equal to:

(Initial mass of specimen) X (% of mass PLS in CA) X
(Weight fraction of liquid in the specimen) (0.2g)

Equation 7

4.2.4 Data analysis

In order to assess mechanical behaviour, PLS release and mass changes at each formula, data were analysed by comparing the mean and standard deviation. The effect of the different MCPM, PLR and wt % level of PLS on development brushite cement was analysed using univariate analysis of variance for all variables and simple t test where appropriate using SPSS 22. In addition, for line fitting the function linest in excel was used. This gives gradients and intercepts in addition to their standard errors. 95% confidence intervals were estimated assuming they were equal to 2 times standard error.

4.2.4.1Simple T test

This test is used for comparing the means of two samples. The t-test compares the actual difference between two means in relation to the variation in the data (expressed as the standard deviation of the difference between the means). In this study, the T test where used with mechanical study result.

4.2.4.2 Univariate Analysis of Variance

Univariate analysis is the simplest form of quantitative (statistical) analysis. It explores each variable in a data set, separately. It looks at the range of values, as well as the central tendency of the values. It describes the pattern of response to the variable as it's describes each variable on its own. In this study, six samples were made for each formula for testing the effect and changes of different MCPM, PLR and wt % level of PLS on the mechanical behaviour on the new development brushite cement to investigate any evidence of differences between them at the significance level 0.05.

4.2.4.3 Error bar analysis

Throughout this study, 95 % confidence interval (CI) of the mean was calculated using:

$$CI = \frac{1.96 \times SD}{\sqrt{n}}$$

Equation 8

SD standard deviation

n number of samples

Samples prepared were six for mechanical study and five for acid release, degradation study and PLS release). Results were considered significantly different when the CI error bars did not overlap.

CHAPTER 5
RESULTS

5 RESULTS

5.1 Mechanical properties

5.1.1 Biaxial flexural strength (BFS)

5.1.1.1 Biaxial flexural strength with different MCPM and β-TCP particle sizes

The mean and 95% confidence intervals of biaxial flexural strength (BFS) using different MCPM and TCP with CA 800 mM are presented in Table 5.1. Varying MCPM source had no significant effect ($p > 0.05$) on the flexural strength. Increase in particle size however, significantly ($p < 0.05$) increased the strength as seen by the gradients being larger than the error on the gradient. This was additionally confirmed using T – test and Univariant test (appendix 1). The highest result was 30.0 MPa with MCPM 2 and β-TCP particle size of 34 micron.

Table 5-1: Biaxial flexural strength / MPa for different MCPM and β-TCP (n=6).

	Biaxial flexural strength / MPa (95% CI)	
Different MCPM / Different TCP	MCPM Himed (1)	MCPM Sigma-Aldrich (2)
TCP 4 micron	22.2 (2.4)	22.3 (1.7)
TCP 6 micron	22.5 (2.7)	22.7 (2.7)
TCP 8 micron	23.0 (2.2)	24.0 (2.4)
TCP 12 micron	26.4 (2.7)	27.5 (2.8)
TCP 34 micron	28.5 (1.8)	30.0 (1.1)
Gradient (95% CI)	0.2 (0.1)	0.3 (0.1)
Intercept (95% CI)	21.9 (1.8)	22.1 (2.2)

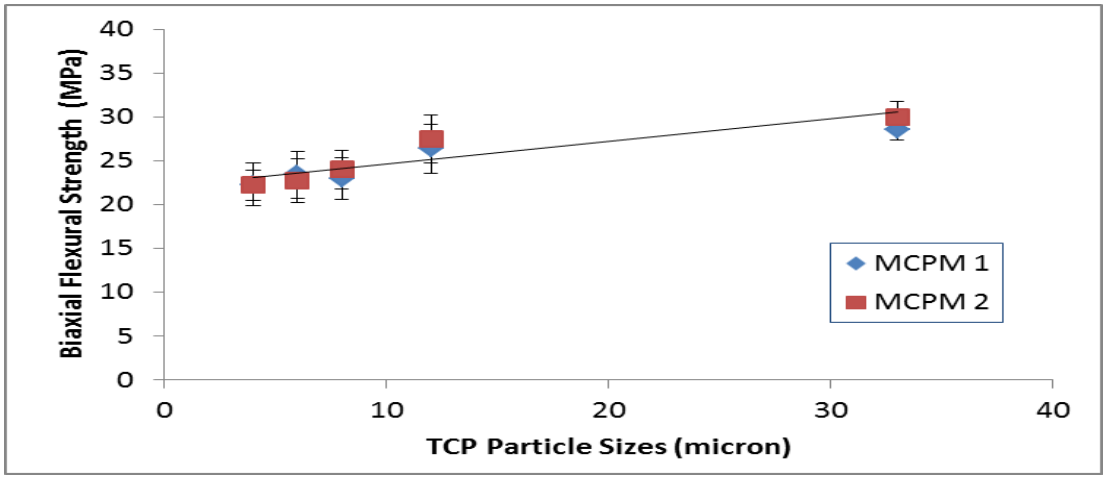

Figure 5-1: Biaxial flexural strength (error bars are 95% CI with n=6) for different β-TCP and MCPM particle sizes with CA 800mM at PLR 3.3:1.

5.1.1.2 Biaxial flexural strength with different powder to liquid ratios (PLR)

The mean and 95% confidence intervals of biaxial flexural strength (BFS) for dry samples with increasing percentage of ε-polylysine (PLS) and different PLR 3.3:1 and 4:1 are presented in Table 5.2. Cements were prepared using MCPM 2, β-TCP of 34 micron and CA 800mM with increase wt % of PLS showed increase in dry flexural strength upon raising PLR from 3.3 to 4. This is seen as a significant change in the intercepts ($p < 0.05$). The gradients show a reduction in strength with increasing wt % of PLS (appendix 2).

Table 5-2: Biaxial flexural strength / MPa for dry samples with different PLR 3.3:1 and 4:1 (n=6) with increase wt % PLS. *indicates results in two columns are significantly different.

	Biaxial flexural strength / MPa (95% CI)	
Cement code (PLS %)	PLR 3.3:1	PLR 4:1
PLS 0%	30.0 (1.1)	32.5 (1.7)
PLS 10%	27.9 (1.5)	34.6 (1.8) *
PLS 20%	25.8 (2.6)	32.4 (2.9) *
PLS 30%	24.3 (1.4)	30.7 (1.7) *
PLS 40%	23.7 (2.7)	30.0 (2.2) *
PLS 50%	23.0 (2.7)	26.5 (2.5)
Gradient (95% CI)	-14.0 (3.4)	-13.0 (7.2)
Intercept (95% CI)	29.3 (1.0)	34.4 (2.2) *

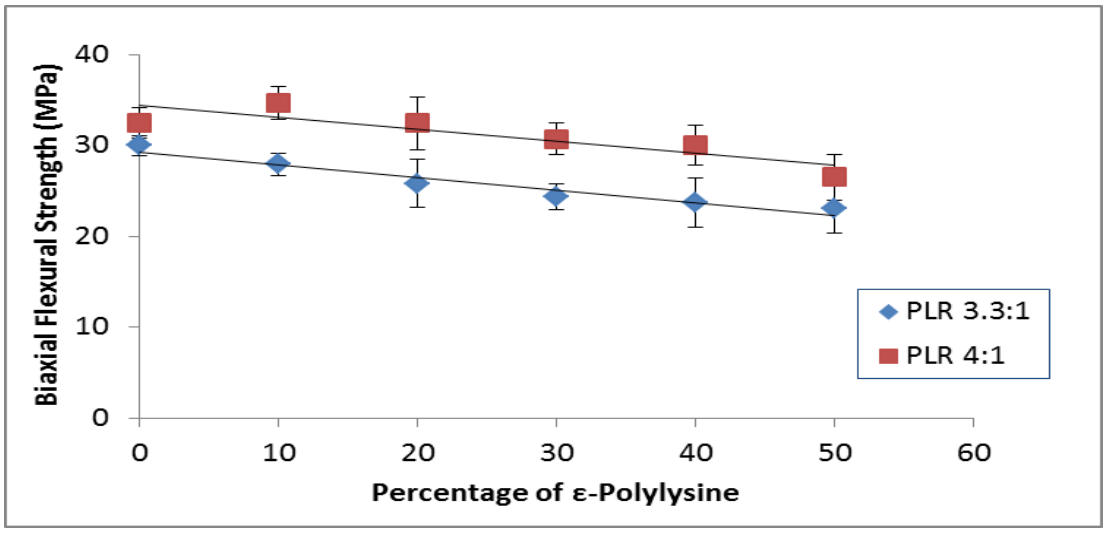

Figure 5-2: Biaxial flexural strength (error bars are 95% CI with n=6) for different PLR with increase wt % PLS.

5.1.1.3 Biaxial flexural strength of wet and dry samples

The mean and 95% confidence intervals of biaxial flexural strength (BFS) for wet and dry samples with ε-polylysine (PLS) are compared in Table 5.3 and Figure 5.3 Cements were prepared using MCPM 2, β-TCP of 34 micron and CA 800mM with increase wt % of PLS at PLR 4:1. Flexural strength decreased after 24 hours water immersion. Significant difference ($p < 0.05$) can be observed between wet and dry samples as seen in appendix 3. Wet samples strength however, barely changed on raising the level of PLS.

Table 5-3: Biaxial flexural strength / MPa for dry samples and wet samples with PLR 4:1 (n=6) with increase wt % PLS. *indicates results in two columns are significantly different.

	Biaxial flexural strength / MPa (95% CI)	
Cement code (PLS %)	Dry samples	Wet samples
PLS 0%	32.5 (1.7)	18.3 (3.1) *
PLS 10%	34.6 (1.8)	20.4 (2.0) *
PLS 20%	32.4 (2.9)	19.9 (1.5) *
PLS 30%	30.7 (1.7)	17.9 (1.5) *
PLS 40%	30.0 (2.2)	17.7 (1.3) *
PLS 50%	26.5 (2.5)	13.7 (1.2) *
Gradient (95% CI)	-13.0 (7.2)	-9.5 (8.4)
Intercept (95% CI)	34.4 (2.2)	20.3 (2.6) *

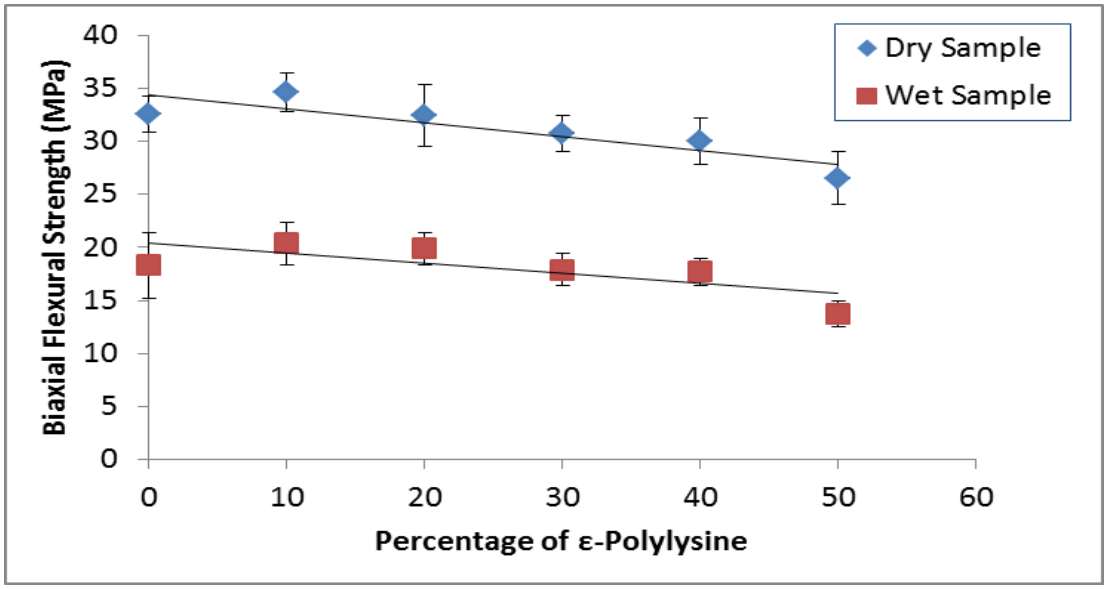

Figure 5-3: Biaxial Flexural Strength (error bars are 95% CI with n=6) for dry and wet samples with increase wt % PLS.

5.1.2 Biaxial flexural modulus (Young's modulus)

5.1.2.1 Biaxial flexural modulus of different MCPM and β-TCP particle sizes

Figure and Tables 5.4 show the Young's modulus for each sample. The error bars show the 95% confidence interval. For formulation with different MCPM and TCP particle sizes, only MCPM 2 showed a small but experimentally significant ($p < 0.05$) increased modulus with increase TCP particle size as seen in appendix 1.

Table 5-4: Biaxial flexural Modulus / GPa for different MCPM and β-TCP (n=6).

	Young's Modulus / GPa (95% CI)	
Different MCPM / Different TCP	MCPM Himed (1)	MCPM Sigma-Aldrich (2)
TCP 4 micron	2.6 (0.4)	1.8 (0.5)
TCP 6 micron	1.9 (0.7)	2.1 (0.4)
TCP 8 micron	2.6 (0.7)	2.4 (0.9)
TCP 12 micron	2.9 (0.6)	2.7 (0.9)
TCP 34 micron	2.4 (0.5)	3.5 (1.1)
Gradient (95% CI)	0.0 (0.0)	0.1 (0.0)
Intercept (95% CI)	2.5 (0.6)	1.9 (0.4)

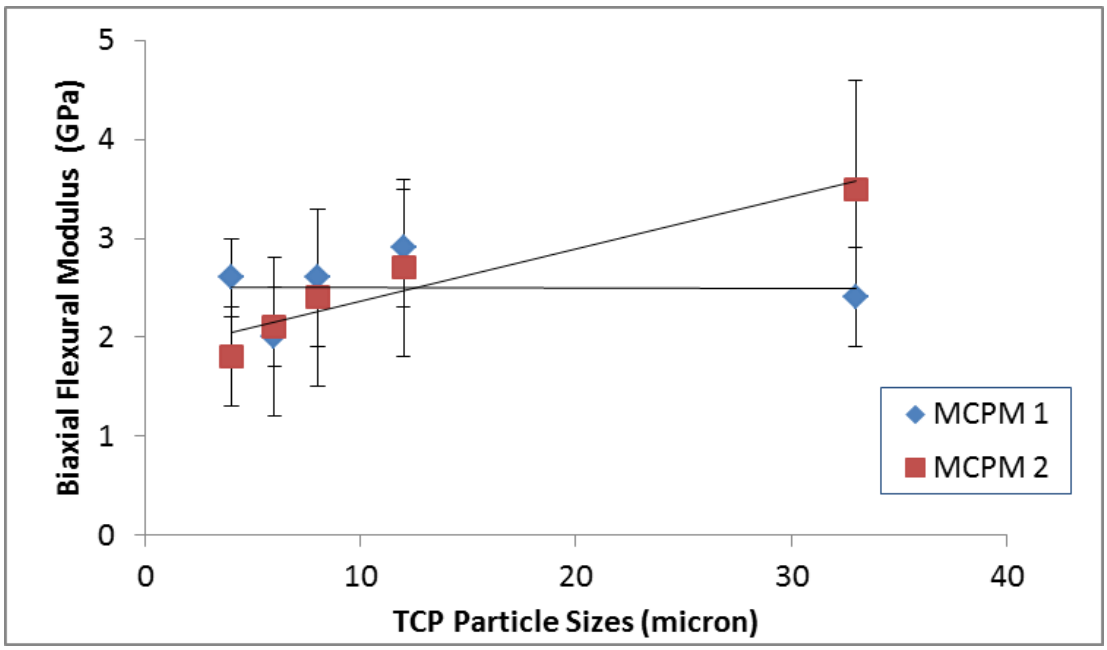

Figure 5-4: Biaxial Flexural Modulus (error bars are 95% CI with n=6) for different β-TCP and MCPM particle sizes (n=6).

5.1.2.2 Biaxial flexural modulus of different powder to liquid ratio (PLR)

The mean and 95% confidence intervals of biaxial flexural modulus (Young's modulus) for dry samples with increase wt % of ε-polylysine (PLS) at different PLR 3.3:1 and 4:1 are presented in Table and Figure 5.5. This formulation was prepared by using MCPM 2, β-TCP 34 micron and CA 800 mM with increase wt % PLS. On average there was a slight increase of modulus upon increasing the PLR from 3.3:1 to 4:1. The effect of increasing PLS was not experimentally significant ($p > 0.05$) except with 20 wt % PLS as seen in appendix 2 with 95% confidence.

Table 5-5: Biaxial flexural modulus / GPa for dry samples with different PLR 3.3:1 and 4:1 (n=6) with increase wt % ε-polylysine. *indicates results in two columns are significantly different.

	Young's Modulus / GPa (95% CI)	
Cement code (PLS %)	PLR 3.3:1	PLR 4:1
PLS 0%	3.3 (0.6)	3.3 (0.8)
PLS 10%	2.7 (0.4)	3.4 (0.8)
PLS 20%	2.2 (0.2)	3.7 (0.9) *
PLS 30%	2.8 (0.5)	3.4 (0.7)
PLS 40%	2.7 (0.4)	3.2 (0.6)
PLS 50%	2.2 (0.6)	2.7 (0.5)
Gradient (95% CI)	-1.4 (1.8)	-1.1 (1.4)
Intercept (95% CI)	3.0 (0.6)	3.6 (0.4)

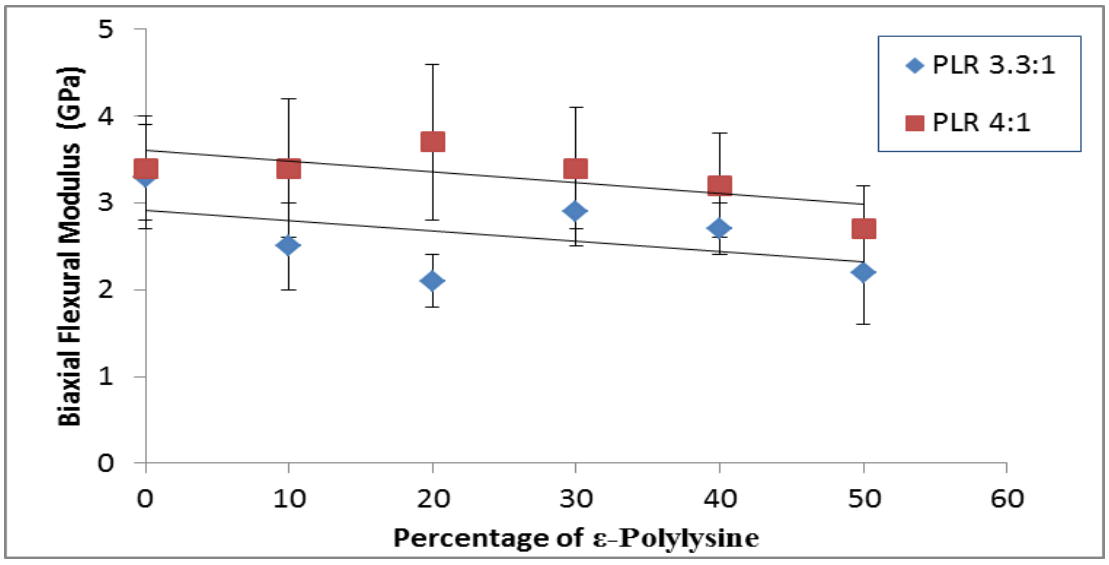

Figure 5-5: Biaxial Flexural Modulus (error bars are 95% CI with n=6) for different PLR with increase percentage of wt % PLS.

5.1.2.3 Biaxial flexural modulus of wet and dry samples

The mean and 95% confidence intervals of biaxial flexural modulus (Young's modulus) for wet and dry samples with ε-polylysine (PLS) are presented in Figure and Table 5.6. This formulation was prepared by using MCPM 2, β-TCP 34 micron and CA 800 mM with increase wt % PLS at PLR 4:1. The tread line showed that on average the dry sample had higher modulus than the wet samples as expected from previous data from flexural strength. However both wet and dry samples modulus did not depend significantly ($p > 0.05$) as seen in appendix 3 on the level of PLS.

Table 5-6: Biaxial flexural modulus / GPa for dry samples and wet samples with PLR 4:1 (n=6) with increase percentage of PLS.

	Young's Modulus / GPa (95% CI)	
Cement code (PLS %)	Dry samples	Wet samples
PLS 0%	3.3 (0.8)	2.0 (0.6)
PLS 10%	3.4 (0.8)	3.1 (0.3)
PLS 20%	3.7 (0.9)	2.8 (0.8)
PLS 30%	3.4 (0.7)	2.8 (0.7)
PLS 40%	3.2 (0.6)	2.4 (0.5)
PLS 50%	2.7 (0.5)	1.7 (0.6)
Gradient (95% CI)	-1.1 (1.4)	-1.0 (2.6)
Intercept (95% CI)	3.6 (0.4)	2.7 (0.8)

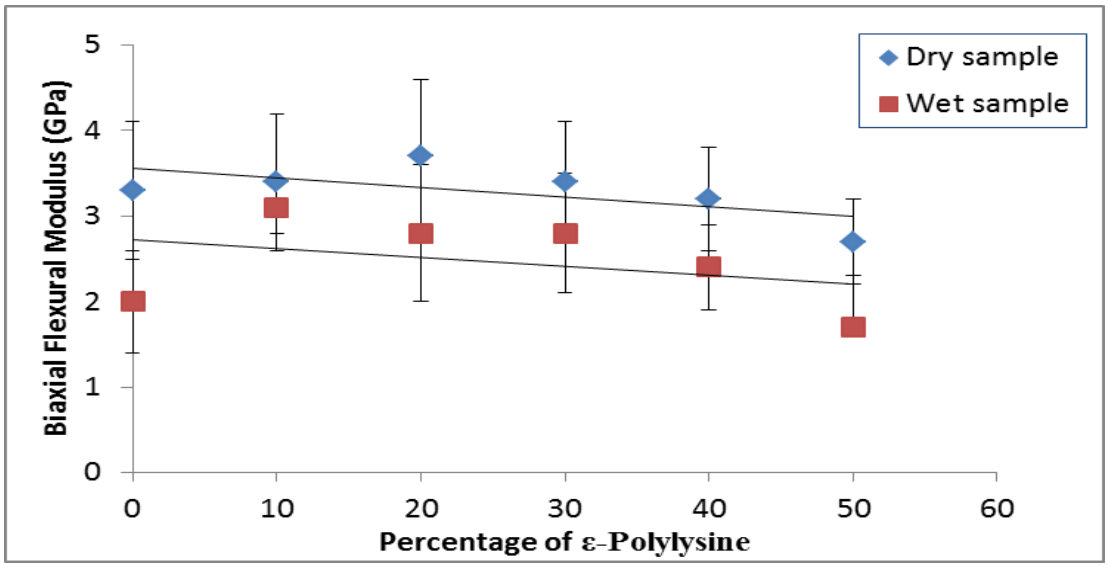

Figure 5-6: Biaxial Flexural Modulus (error bars are 95% CI with n=6) for dry and wet samples with increase wt % PLS.

5.1.3 Toughness

5.1.3.1 Toughness of different MCPM and β-TCP particle sizes

Table and Figure 5.7 show the toughness for each sample. The error bars show the 95% confidence interval. For all formulations with either different MCPM or TCP particle sizes, there was no significant difference ($p > 0.05$) or trend as seen appendix 1.

Table 5-7: Toughness for different MCPM and β-TCP (n=6).

	Toughness (95% CI)	
Different MCPM / Different TCP	MCPM Himed (1)	MCPM Sigma-Aldrich (2)
TCP 4 micron	0.8 (0.3)	1.2 (0.6)
TCP 6 micron	0.8 (0.3)	0.7 (0.4)
TCP 8 micron	0.6 (0.2)	1.1 (0.5)
TCP 12 micron	0.9 (0.2)	0.8 (0.3)
TCP 34 micron	0.7 (0.1)	0.8 (0.3)
Gradient (95% CI)	- 0.0 (0.0)	- 0.0 (0.0)
Intercept (95% CI)	0.8 (0.2)	1.0 (0.4)

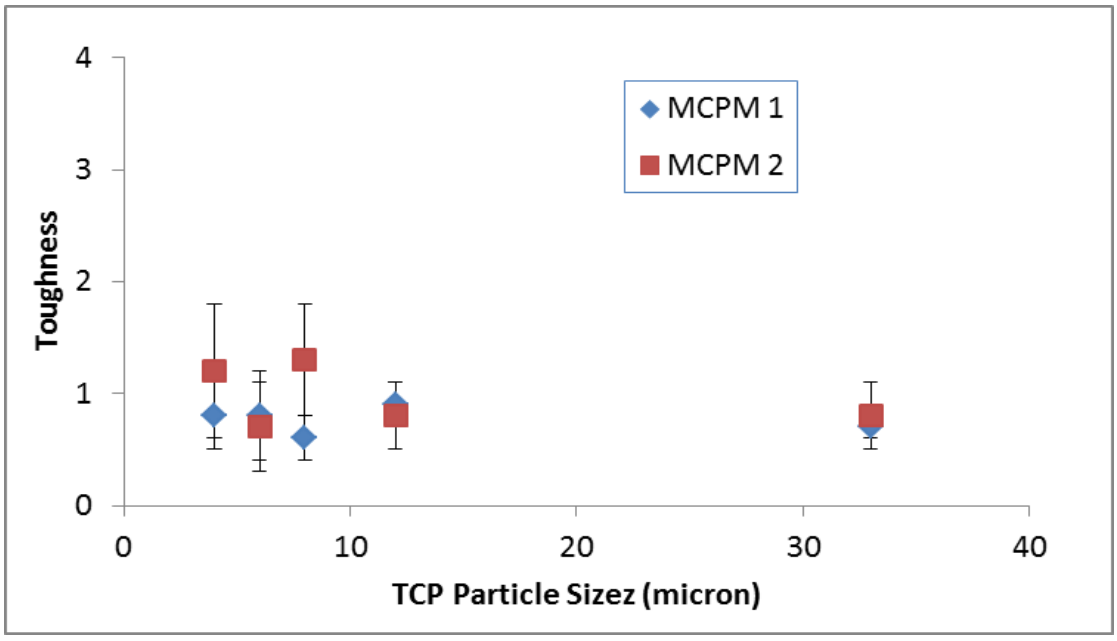

Figure 5-7: Toughness (error bars are 95% CI with n=6) for different TCP and MCPM particle sizes with CA 800mM (n=6).

5.1.3.2 Toughness of different powder to liquid ratio (PLR)

The mean and 95% confidence intervals of toughness for dry samples with increase percentage of ε-polylysine (PLS) and different PLR 3.3:1 and 4:1 are presented in Table and Figure 5.8. All formulations were prepared with MCPM 2, β-TCP 34 micron and CA 800mM with increase wt % PLS. Increasing PLR or PLS had no significant effect ($p > 0.05$) on the toughness as seen in appendix 2.

Table 5-8: Toughness for dry samples with different PLR 3.3:1 and 4:1 (n=6) with increase wt % PLS.

	Toughness (95% CI)	
Cement code (PLS %)	PLR 3.3:1	PLR 4:1
PLS 0%	1.0 (0.6)	1.7 (0.3)
PLS 10%	1.1 (0.2)	1.2 (0.3)
PLS 20%	1.9 (0.9)	1.2 (0.2)
PLS 30%	1.3 (0.5)	1.8 (0.5)
PLS 40%	1.5 (0.6)	1.2 (0.2)
PLS 50%	1.7 (0.4)	1.6 (0.2)
Gradient (95% CI)	1.2 (1.4)	0.1 (1.4)
Intercept (95% CI)	1.1 (0.4)	1.4 (0.4)

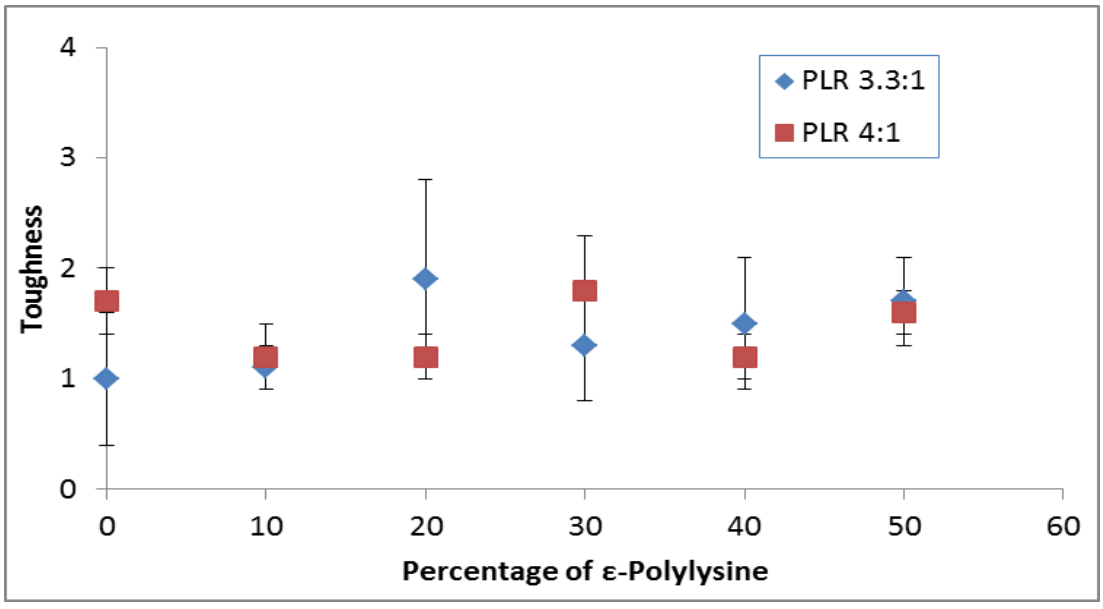

Figure 5-8: Toughness (error bars are 95% CI with n=6) for different powder to liquid ratio with increase wt % PLS.

5.1.3.3 Toughness of wet and dry samples

The mean and 95% confidence intervals of toughness for wet and dry samples with ε-polylysine (PLS) are presented in Table and Figure 5.9. Cements were prepared by using MCPM 2, β-TCP 34 micron and CA 800 mM with increase wt % PLS at PLR 4:1. The trend line showed that on average the dry samples had higher toughness than the wet samples. However both wet and dry samples toughness did not depend on the level of PLS.

Table 5-9: Toughness of dry samples and wet samples with PLR 4:1 (n=6) with increase percentage of PLS. *indicates results in two columns are significantly different.

	Toughness (95% CI)	
Cement code (PLS %)	Dry samples	Wet samples
PLS 0%	1.7 (0.3)	0.8 (0.2) *
PLS 10%	1.2 (0.3)	1.0 (0.4)
PLS 20%	1.2 (0.2)	0.8 (0.2)
PLS 30%	1.8 (0.5)	0.8 (0.2) *
PLS 40%	1.2 (0.2)	0.7 (0.1) *
PLS 50%	1.6 (0.2)	0.6 (0.1) *
Gradient (95% CI)	0.1 (1.6)	-0.5 (0.4)
Intercept (95% CI)	1.4 (0.4)	0.9 (0.1)

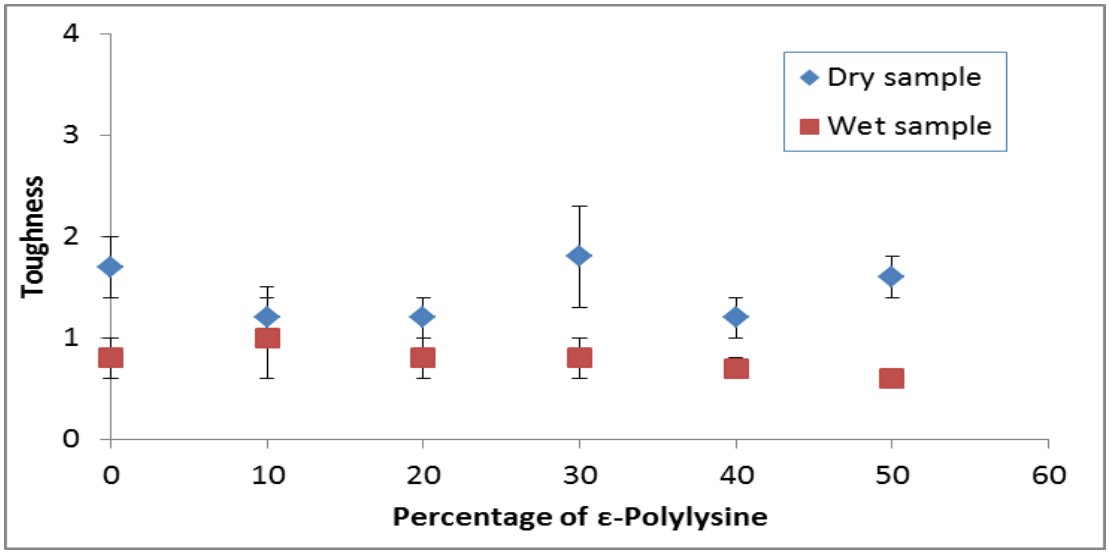

Figure 5-9: Toughness (error bars are 95% CI with n=6) for dry and wet samples with increase wt % PLS.

5.2 Microstructure study using scanning electron microscopy (SEM)

5.2.1 Microstructure study of MCPM powder

SEM image of MCPM 1 and 2 are shown in figure 5.10 and 5.11 respectively. MCPM 1 is a ground powder that appeared as spherical, rounded particles. They look as if they have been milled smoothing their edges and producing many smaller fine particles. Some particles are less than a few microns but attracted to the larger particle surfaces. MCPM 1 had broader distribution of particle size compared to MCPM 2. MCPM 2 had narrow distribution of particle size and appears as flat, rhombohedra or diamond crystal shapes. MCPM 2 also showed slightly larger size with a much smoother surface.

5.2.2 Microstructure study of β-TCP powder

SEM images of β-TCP with sizes from 4 micron to 34 micron are shown in figure 5.12 to 5.16. The smaller β-TCP particles (4 micron to 8 micron) appear very similar with small particles clumping to bigger particles. The texture was quite porous and dull. With β-TCP size 12 micron however, the surface appears much smoother and glossier. For β-TCP powder with 34 micron, the shape appears larger and irregular, less spherical and with a surface that was smooth. All β-TCP appeared smaller compared with the MCPM's.

5.2.3 Microstructure study of ε-polylysine powder

Figure 5.17 shows an SEM image of ε-polylysine (PLS) powder. PLS also had smaller particle size compared to MCPM. PLS particles appear as spherical particles with dimples similar to those observed with golf balls.

.

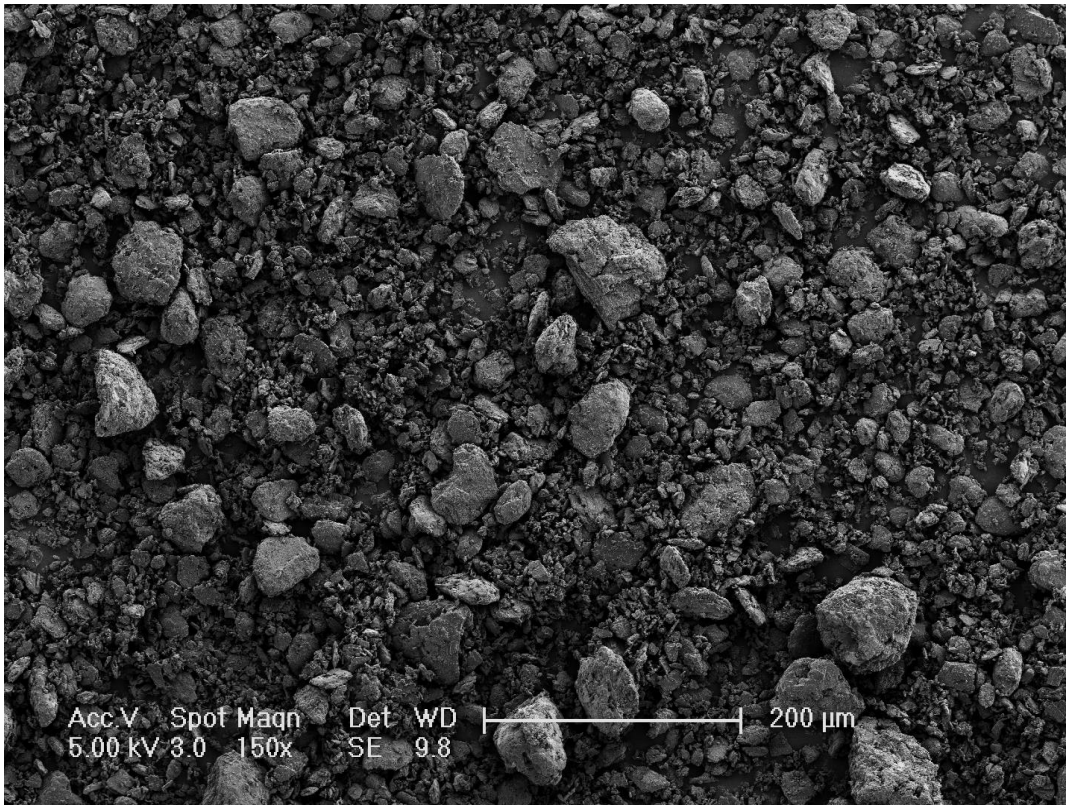

Figure 5-10: SEM image of MCPM 1 (HIMED) taken at x100 magnification

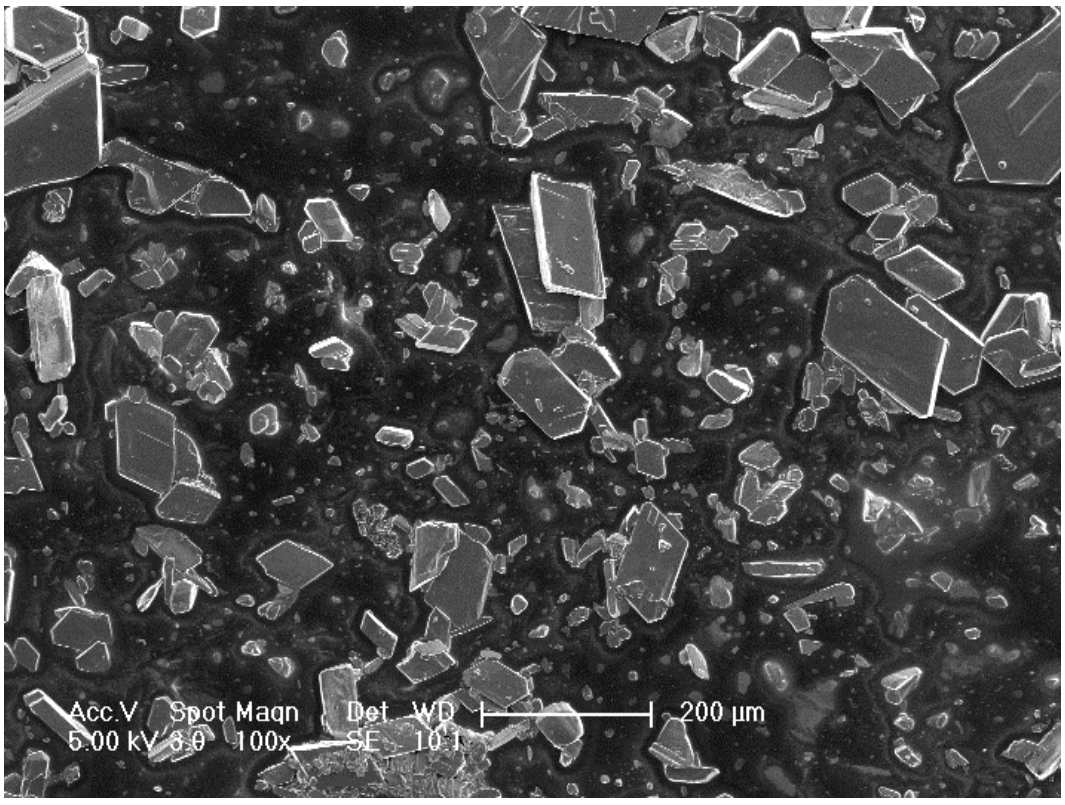

Figure 5-11: SEM image of MCPM 2 (SIGMA) taken at x100 magnification

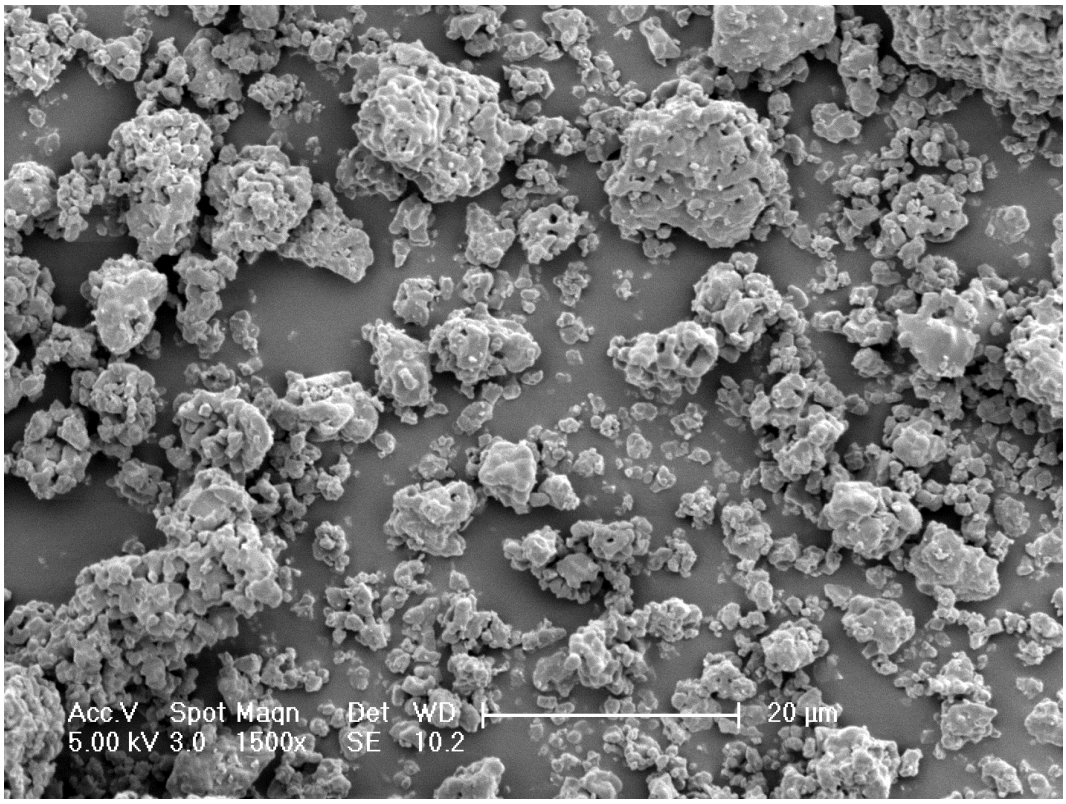

Figure 5-12: SEM image of β-TCP 4.0 micron taken at x1500 magnification

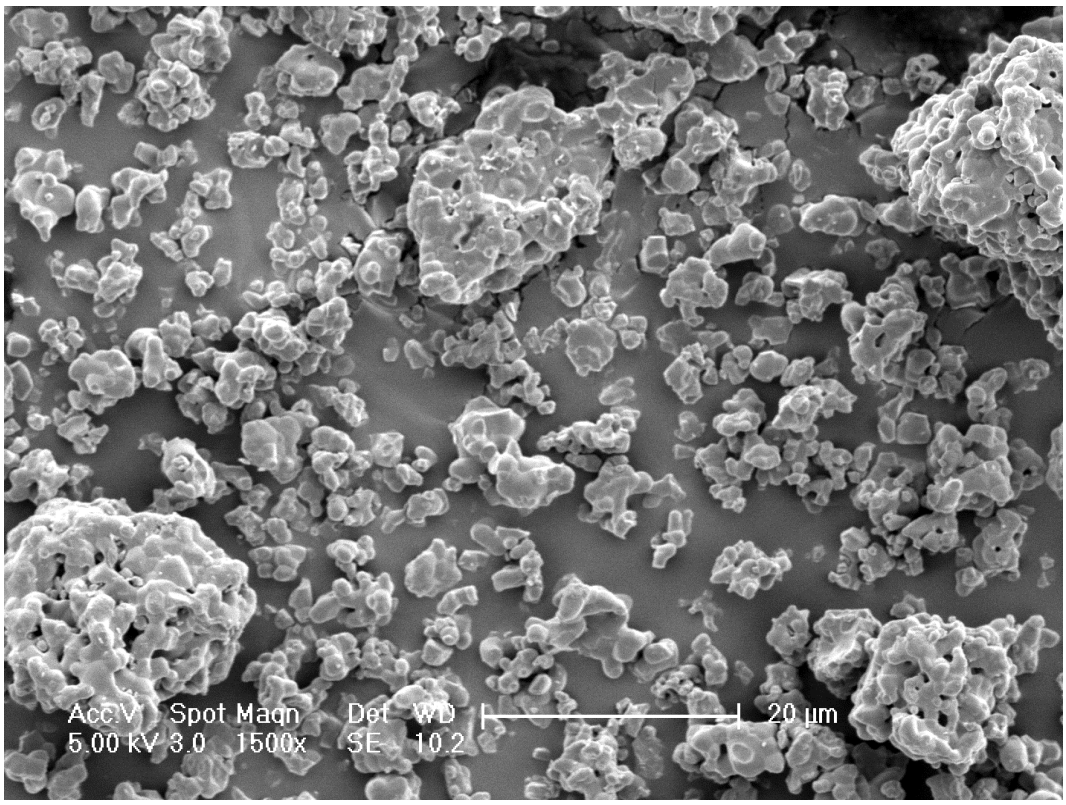

Figure 5-13: SEM image of β-TCP 6.0 micron taken at x1500 magnification

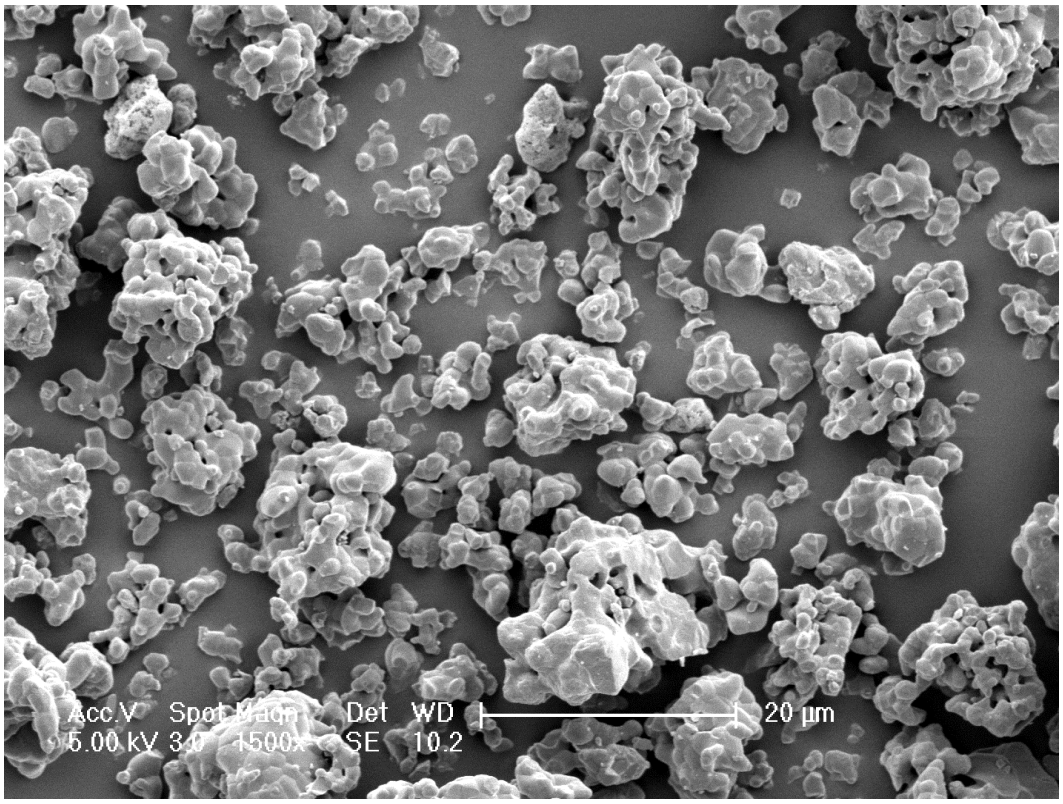

Figure 5-14: SEM image of β-TCP 8.0 micron taken at x1500 magnification

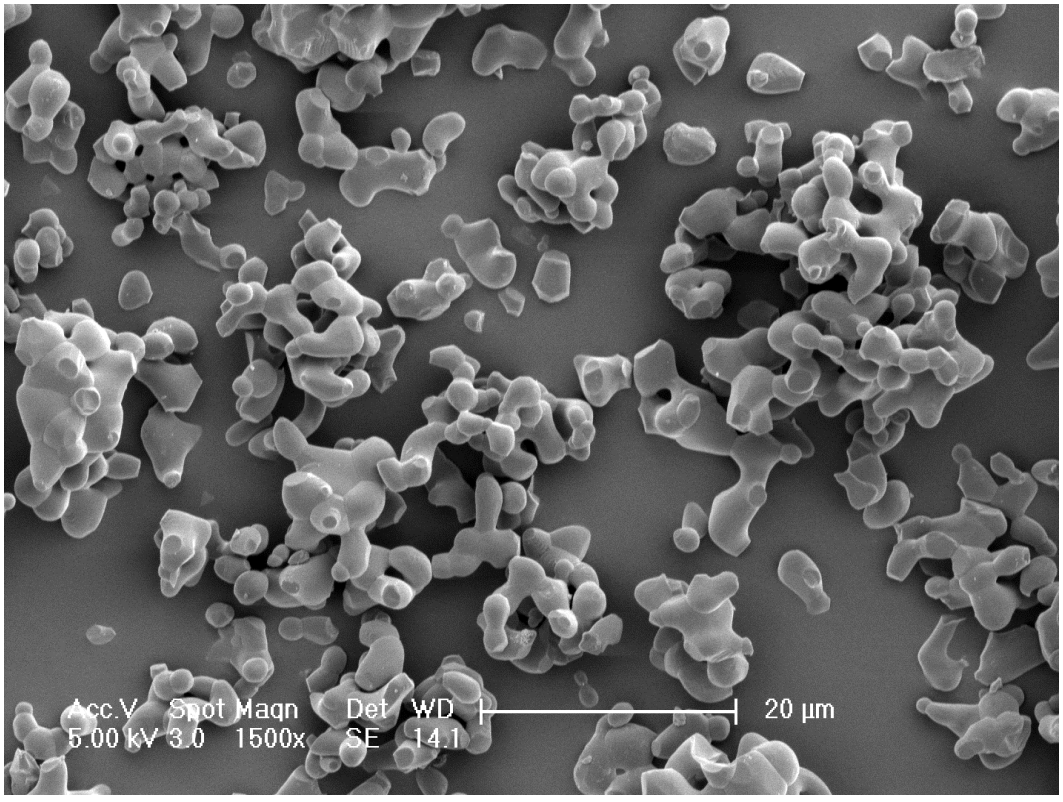

Figure 5-15: SEM image of β-TCP 12.0 micron taken at x1500 magnification

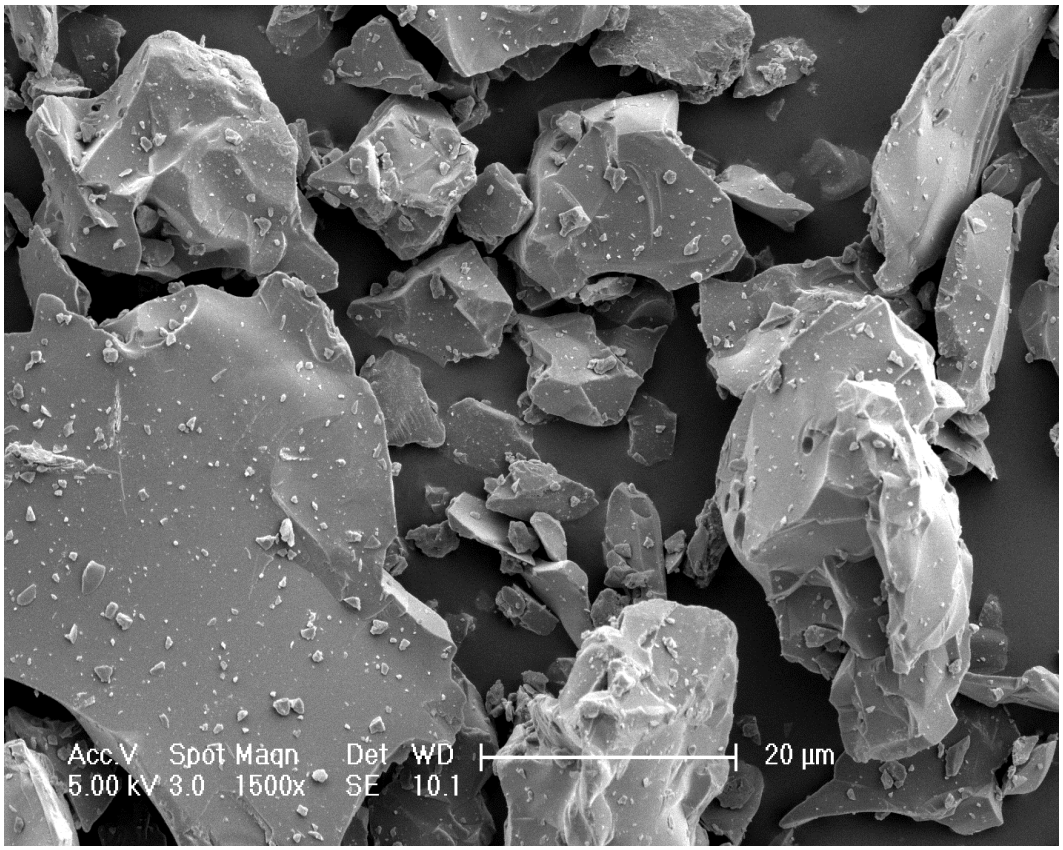

Figure 5-16: SEM image of β-TCP 34.0 micron taken at x1500 magnification

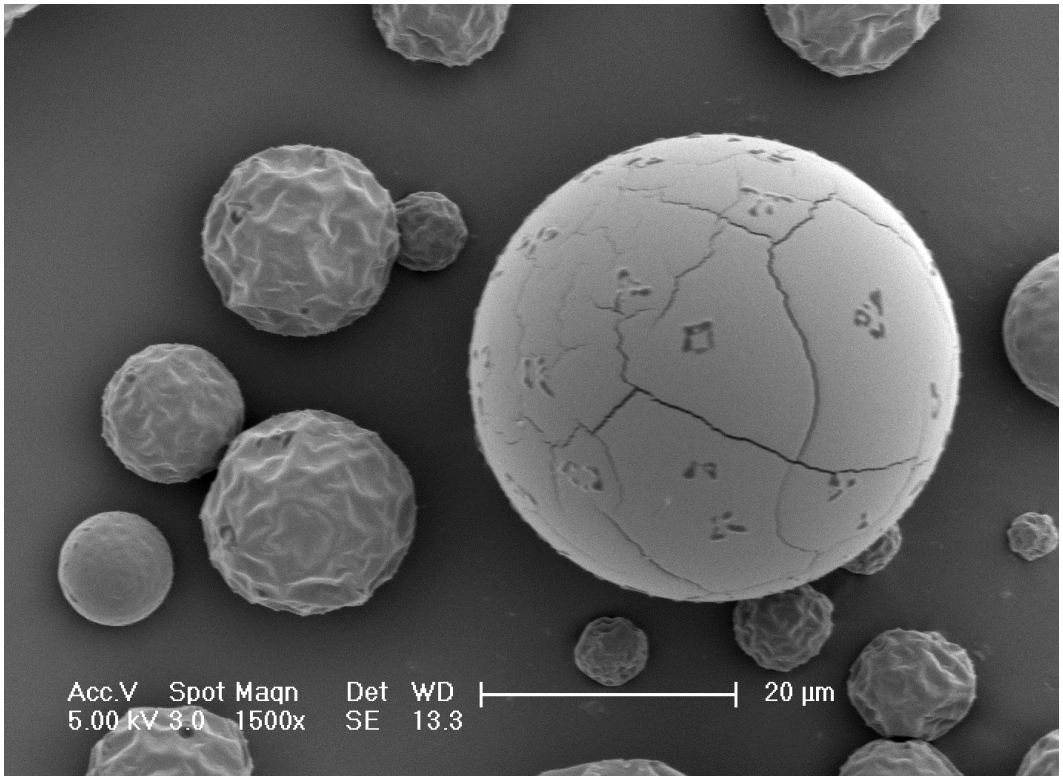

Figure 5-17: SEM image of ε-polylysine taken at x1500 magnification

5.2.4 Microstructure study of the set cements

The top surface and fracture surface microstructure of the set cements was observed under scanning electron microscopy (SEM) at different magnification (x50, x150, x350, x500, x1500, x3500 and x5000). At first specimens were scanned dry and then scanned again after being immersed in distilled water for 24 hours.

5.2.4.1 Brushite cements prepared with water

Figure 5.18 and figure 5.19 shows the morphology of the fracture and top surfaces of the brushite cements produced using no citric acid, MCPM 2 and TCP of 34 micron at x1500 and x500 magnification. The images for wet and dry samples were comparable both on the top and fracture surface. The cement surface appeared as non – homogenous with areas of porosity with comparable shape and dimension to the original MCPM 2 crystals. The brushite crystals were like flat plates stacked on each other in the denser parts of the structure. In porous regions, however, large well-defined 20 to 50 micron long hexagonal rod – like crystals could be observed jutting into the large cracks left by the flat MCPM crystals

5.2.4.2 MCPM and citric acid effects on cements microstructure

Figures 5.20 to 5.25 shows the morphology of the surfaces of brushite cements prepared with MCPM 2 and MCPM 1 (wet samples) with 34 micron TCP and 800 mM citric acid at different magnifications. Changing the MCPM particles had a much greater effect on SEM images than addition of citric acid or placement in water. Differences were more easily observed on the fracture surfaces at low magnification. With MCPM 2 a lot of long cracks of up to 500 micron length and typically 20-50 micron width were observed.

The cracks were of comparable shape and dimension as the original MCPM 2 particles suggesting that MCPM had dissolved slowly into the water and reprecipated away from the resultant crack area. Jutting into the cracks were larger brushite hexagonal prisms of the order of 20 to 50 µ in length. Obvious regions where the MCPM 2 crystals had been lying flat can also be seen. Within these regions, a layer of larger crystals is seen on the fracture surface. On fracture surfaces in other regions between cracks, the crystals were more densely packed.

On top surfaces more small pores could be detected. With MCPM 1 more spherical pores could be observed in fracture surfaces with no long cracks. These spherical pores were comparable in size and shape to the original MCPM particles again suggesting they are formed by slow dissolution of MCPM away from the original particles and precipitation elsewhere.

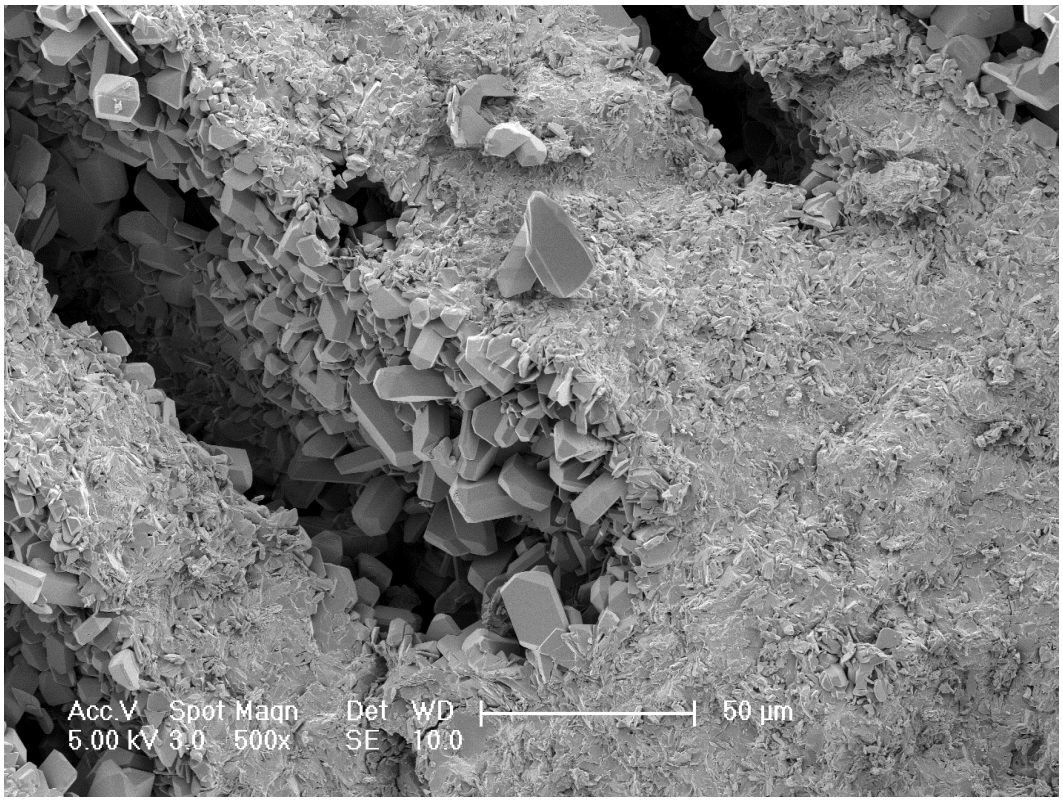

Figure 5-18: SEM image of fracture surface brushite cement (wet sample) taken at x500 magnifications (MCPM 2 + β-TCP 34.0 micron + water)

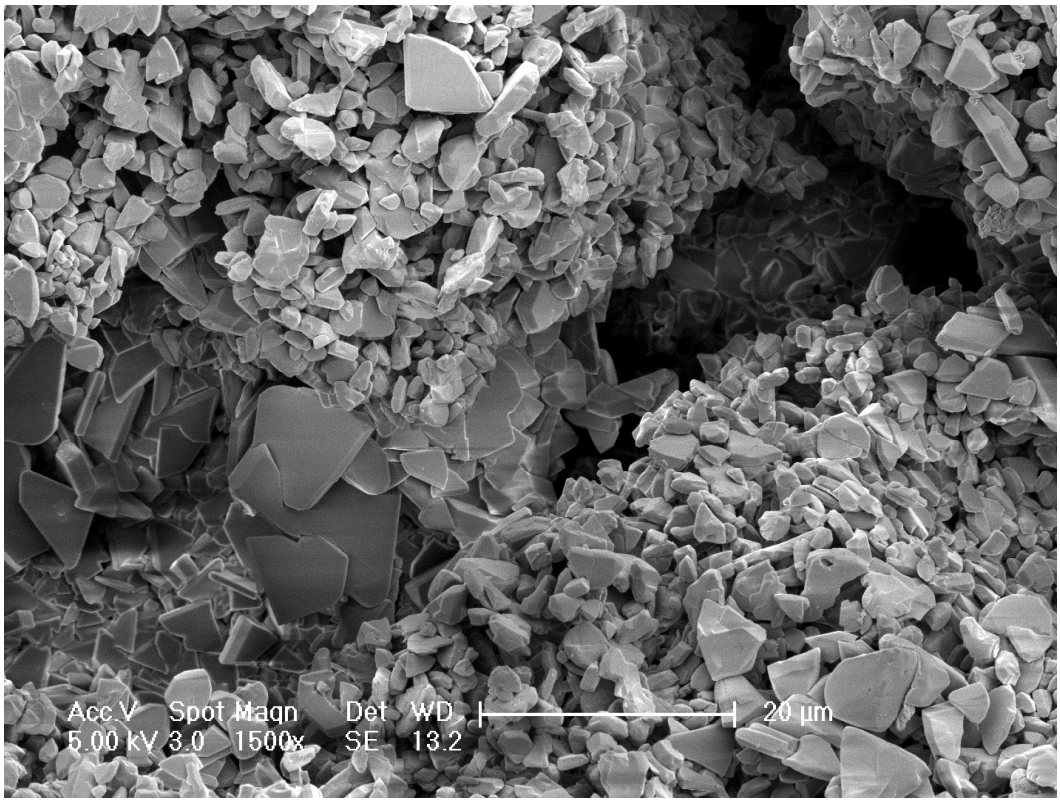

Figure 5-19: SEM image of surface (wet sample) taken at x1500 magnification (MCPM 2 + β-TCP 34.0 micron + water)

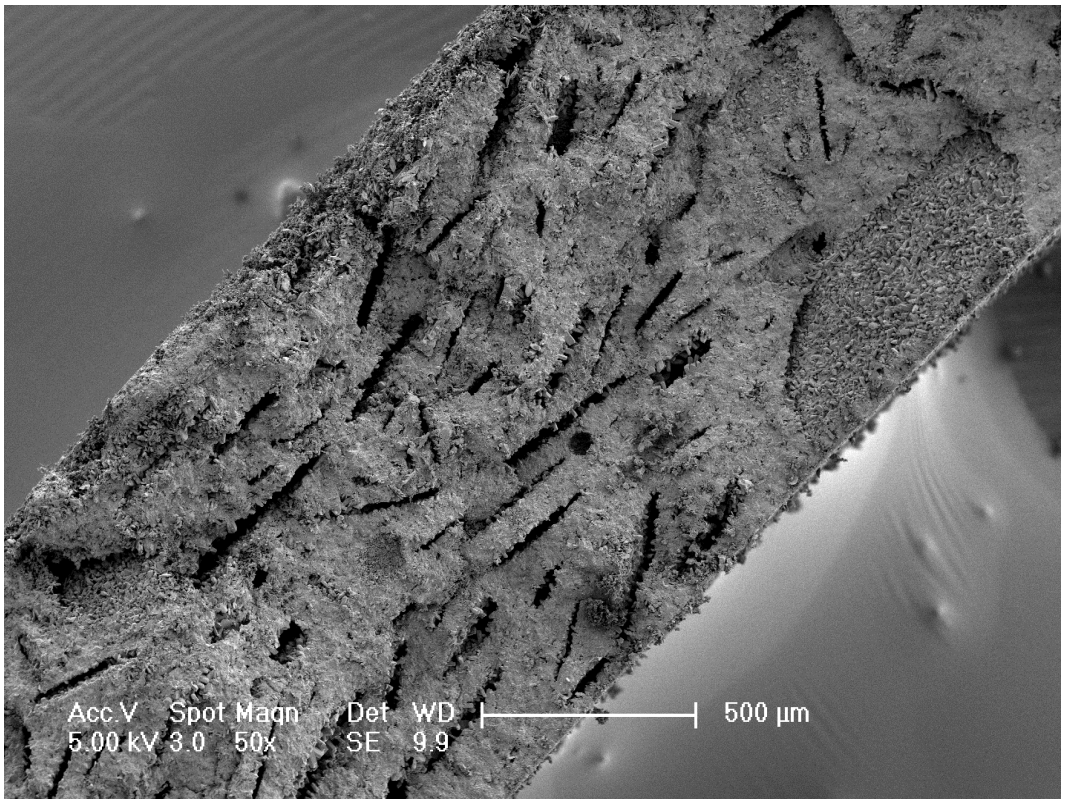

Figure 5-20: SEM image of fracture surface (wet sample) taken at x500 magnification (MCPM 2 + β-TCP 34.0 micron + citric acid)

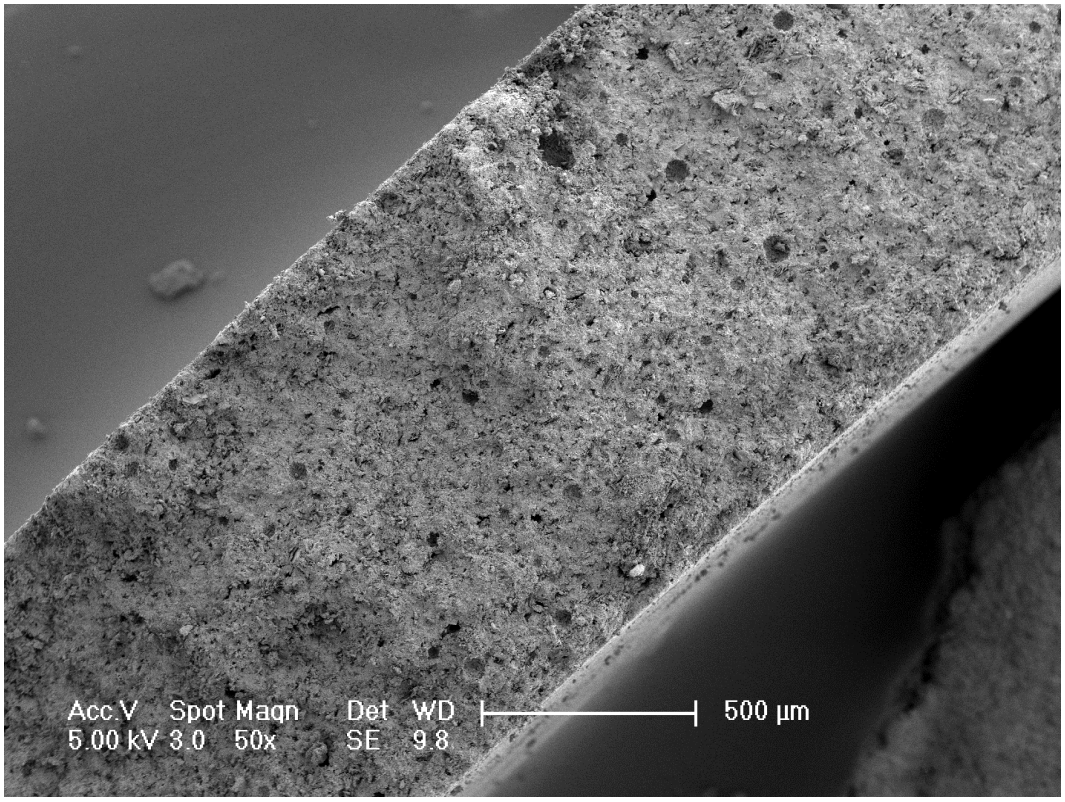

Figure 5-21: SEM image of fracture surface cement (wet sample) taken at x500 magnification (MCPM 1 + β-TCP 34.0 micron + citric acid)

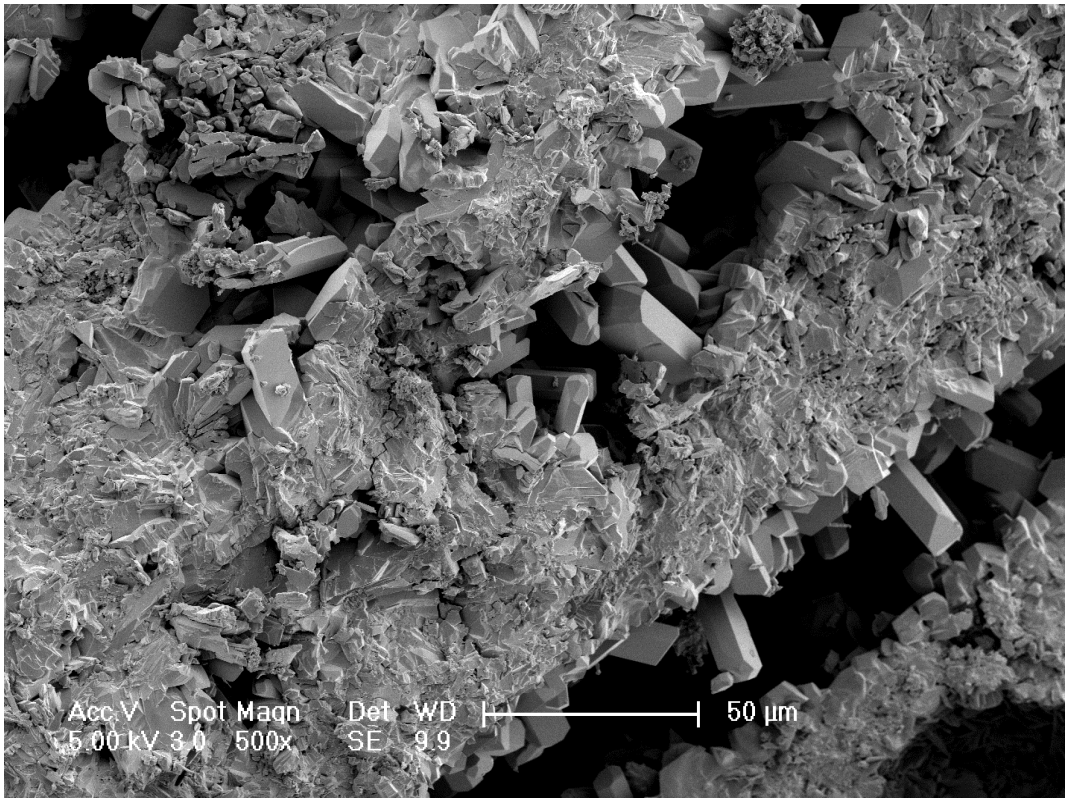

Figure 5-22: SEM image of fracture surface cement (wet sample) taken at x500 magnification (MCPM 2 + β-TCP 34.0 micron + citric acid)

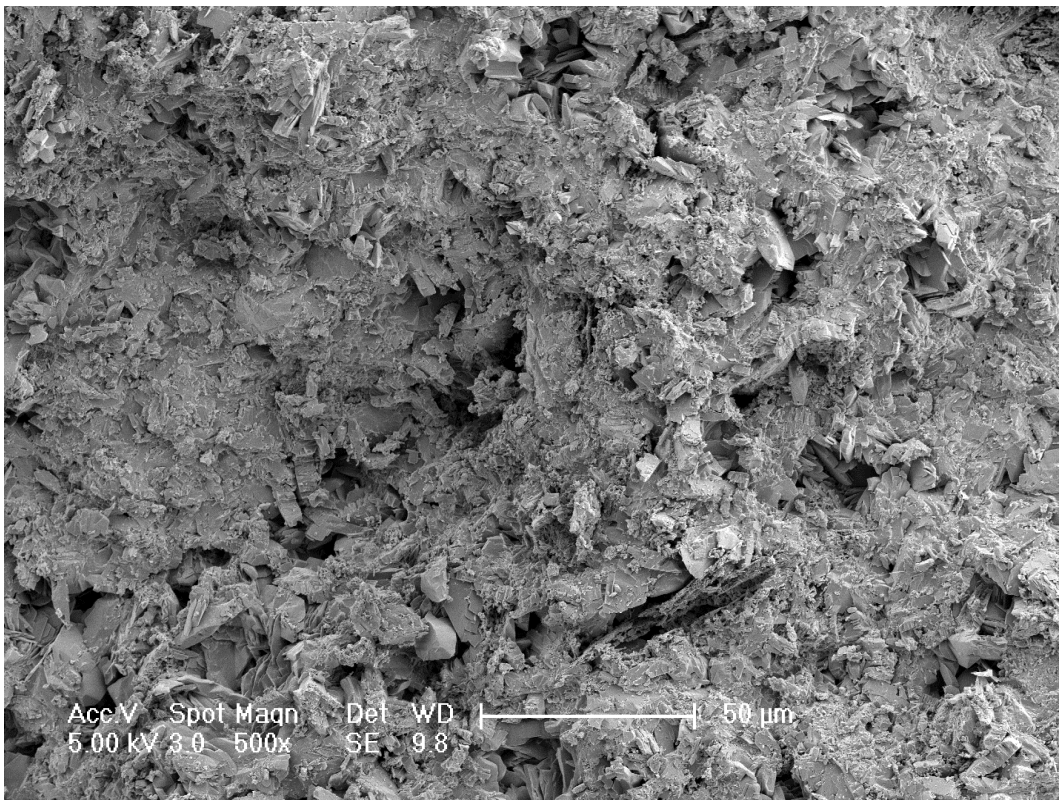

Figure 5-23: SEM image of fracture surface cement (dry sample) taken at x500 magnification (MCPM 1 + β-TCP 34.0 micron + citric acid)

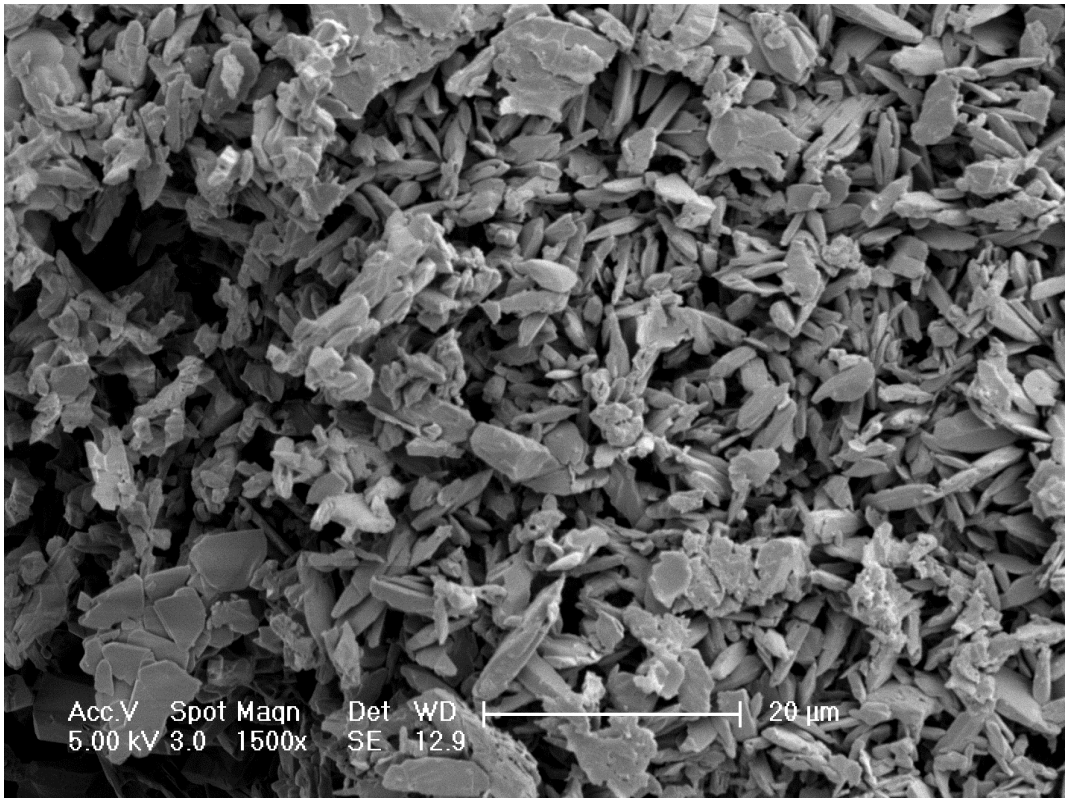

Figure 5-24: SEM image of surface (wet sample) taken at x1500 magnification (MCPM 2 + β-TCP 34.0 micron + citric acid)

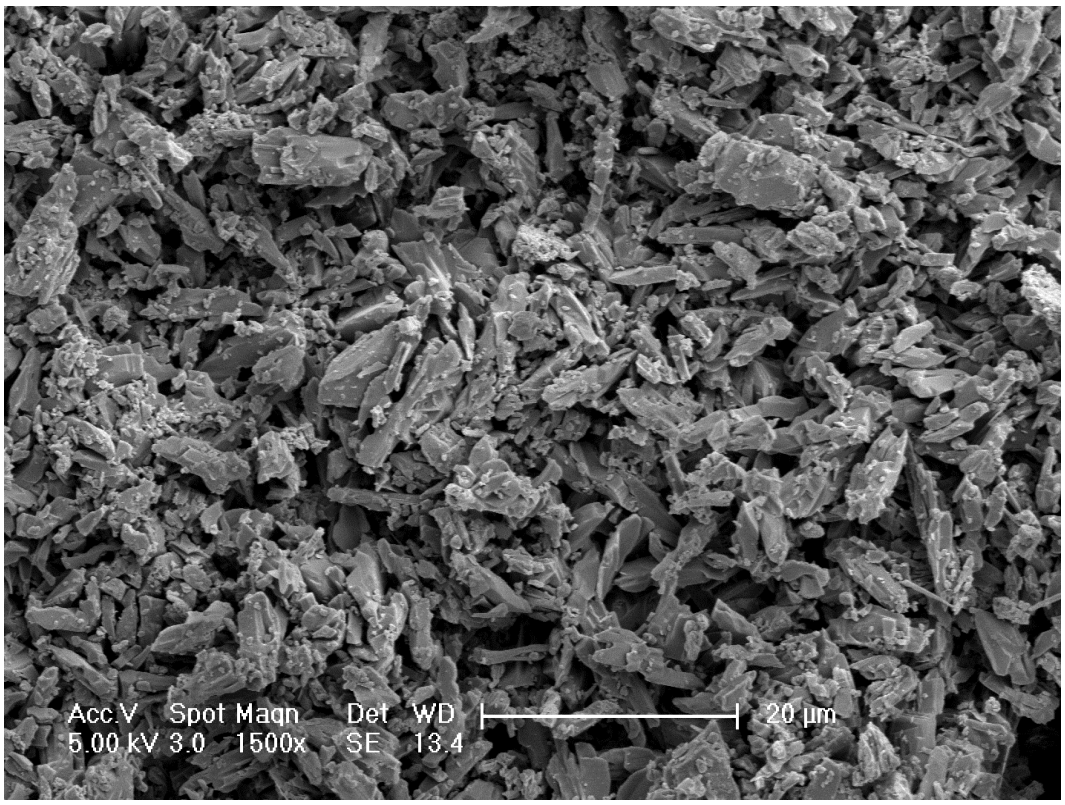

Figure 5-25: SEM image of surface cement (wet sample) taken at x1500 magnification (MCPM 1 + β-TCP 34.0 micron + citric acid)

5.2.4.3 ε-Polylysine effect on cements microstructure

Figures 5.26 to 5.30 show SEM images of set cements with ε-polylysine (PLS) (10%, and 50%). Even with the highest level of PLS in the formulation, no obvious effect of on structures can be seen except possibly more spherical air bubbles.

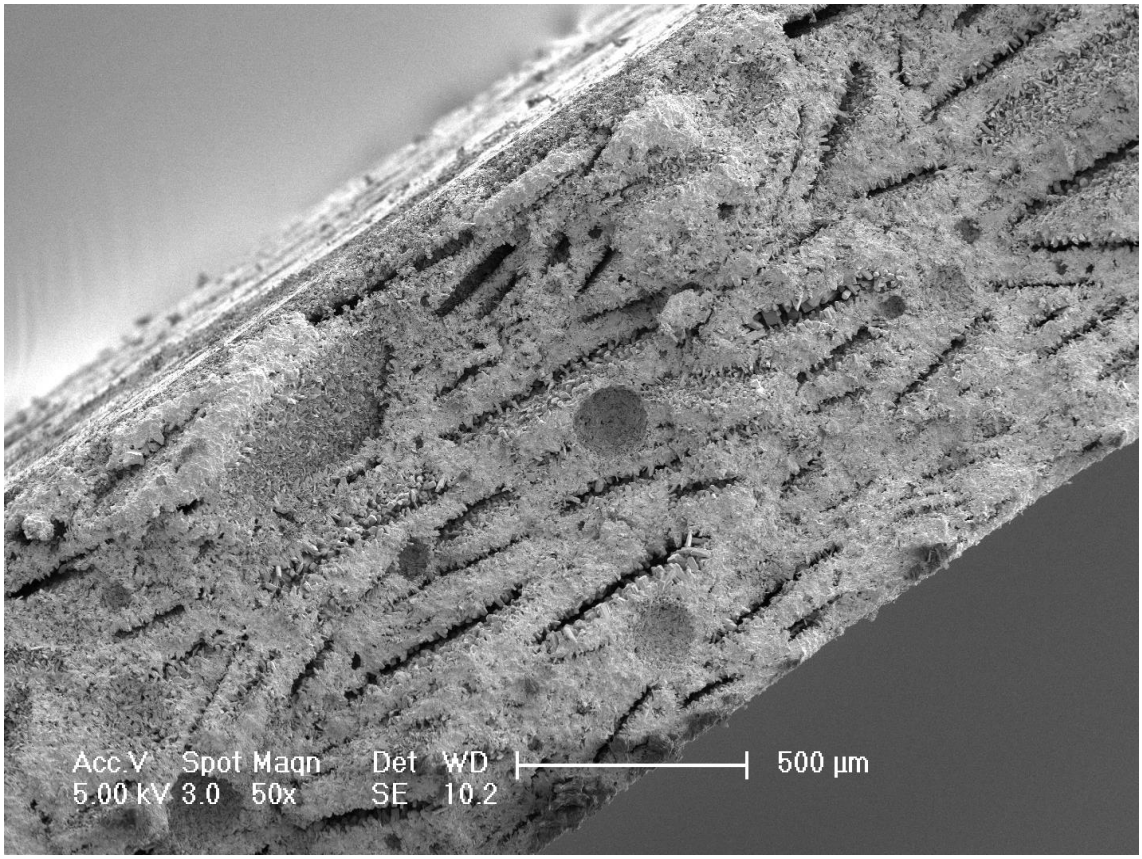

Figure 5-26: SEM image of fracture surface (wet sample) taken at x500 magnification (MCPM 2 + β-TCP 34.0 micron + 50 wt % PLS in citric acid)

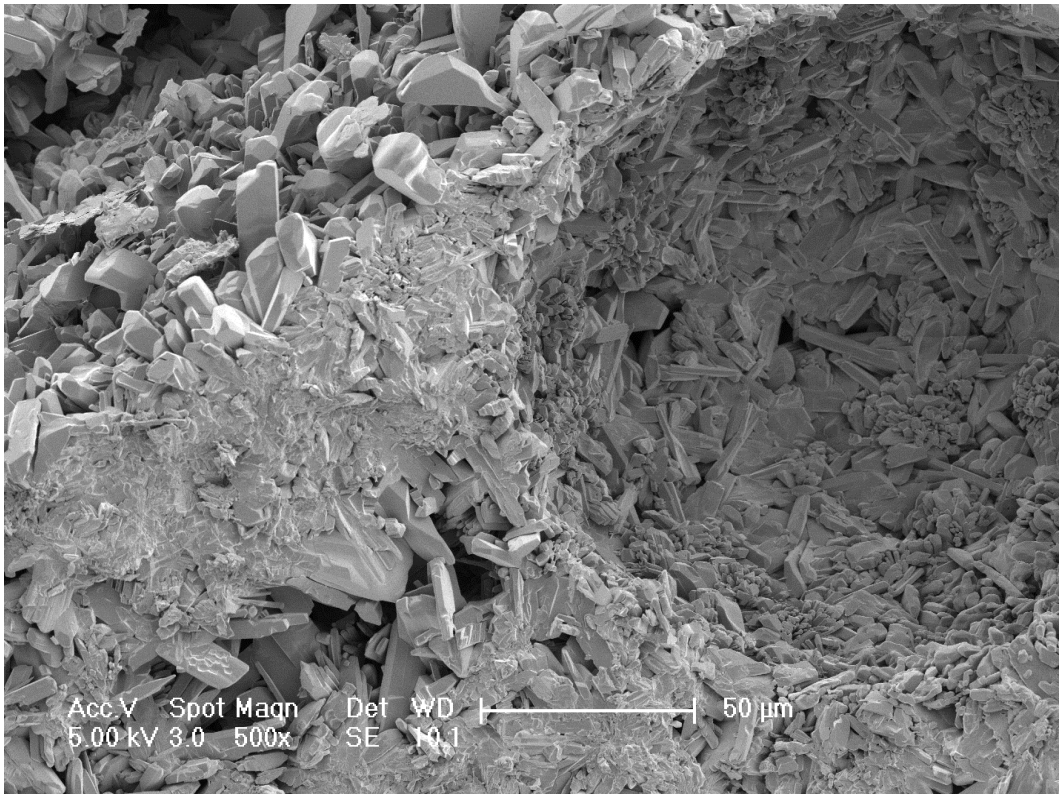

Figure 5-27: SEM image of fracture surface cement (wet sample) taken at x500 magnification (MCPM 2 + β-TCP 34.0 micron + citric acid + 50 wt % PLS)

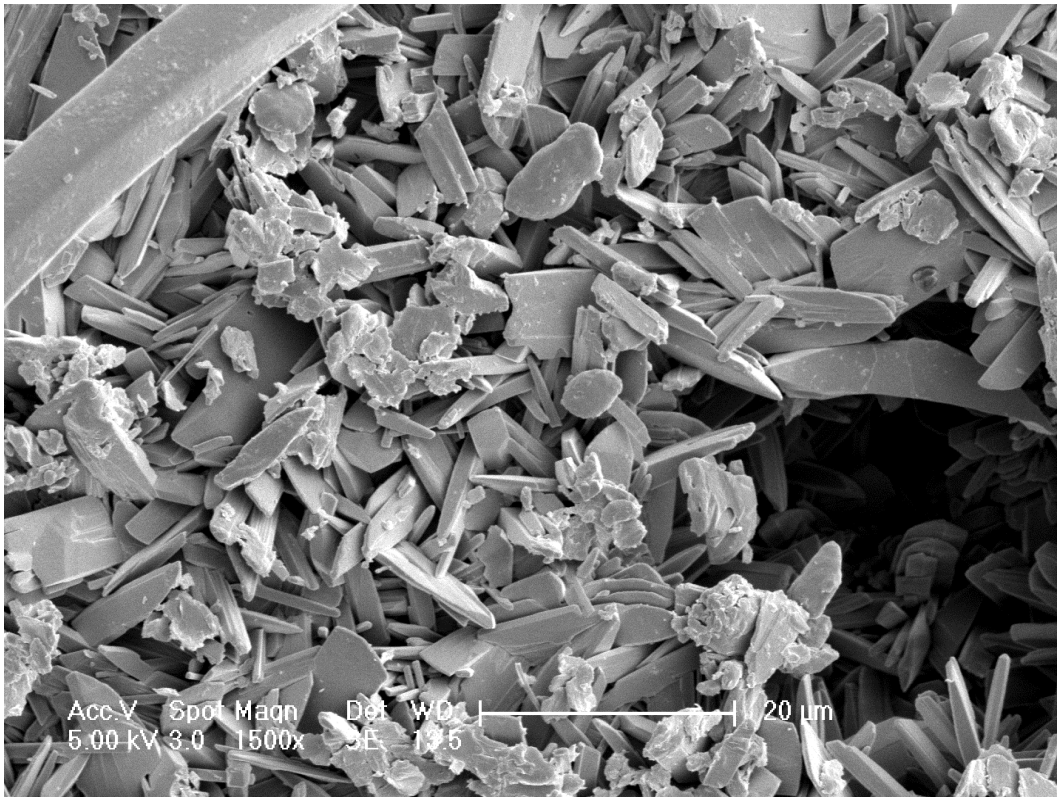

Figure 5-28: SEM image of surface cement (wet sample) taken at x500 magnification (MCPM 2 + β-TCP 34.0 micron + citric acid + 50 wt % PLS)

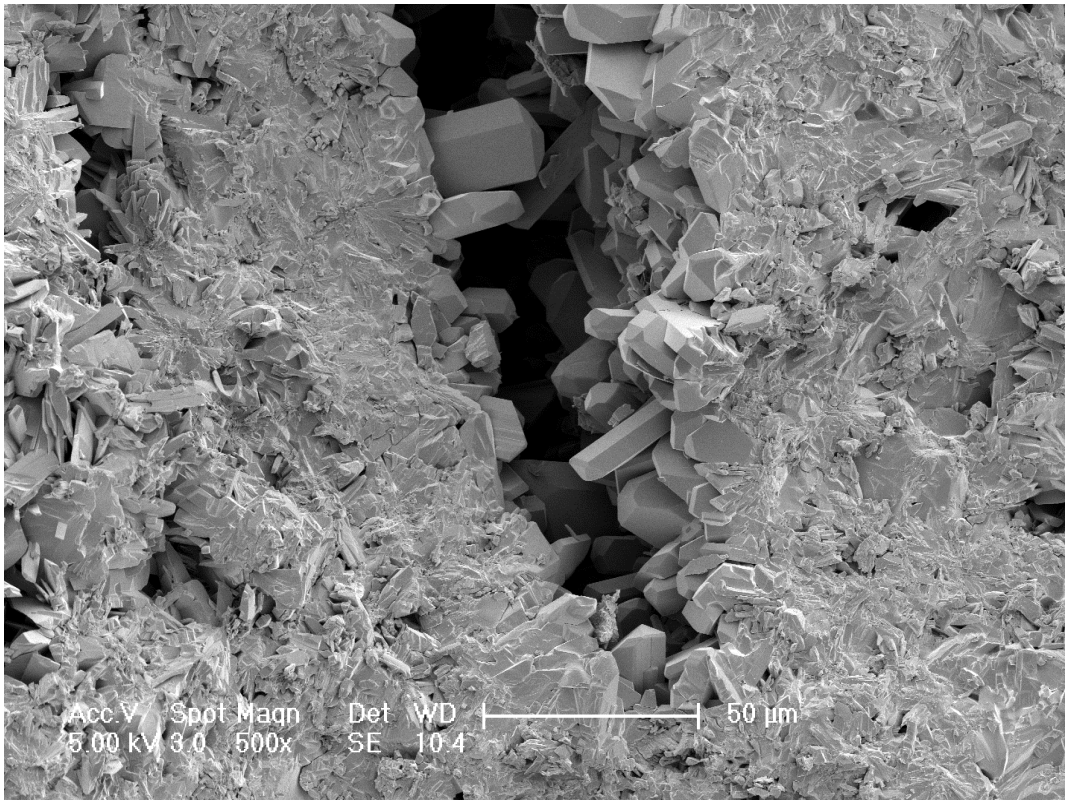

Figure 5-29: SEM image of fracture surface cement (wet sample) taken at x500 magnification (MCPM 2 + β-TCP 34.0 micron + citric acid + 10 wt % PLS)

Figure 5-30: SEM image of surface (wet sample) taken at x1500 magnification (MCPM 2 + β-TCP 34.0 micron + citric acid + 10 wt % PLS)

5.3 Handling properties

Upon mixing with smaller MCPM 1 (HIMED) particles, the cement paste became more viscous upon increasing the β-TCP particle size. With MCPM 2 (SIGMA) with more crystalline structure, the cement paste remained more fluid like even with the largest TCP particle size. This enabled an increase in PLR from 3.3:1 to 4:1 whilst maintaining better handling properties. Upon initial increase in wt % of PLS, the paste become more viscous and cohesive but the paste become too viscous upon reaching 50 wt % PLS.

.

5.4 Setting kinetics

5.4.1 Reference spectra

FTIR reference spectra for the reactants used in this experiment are shown in Figures 5.31 to 5.34. The reference spectrum for monocalcium phosphate monohydrate (MCPM) illustrated in figure 5.31 has strong P - O stretch peaks at 1075 and 955 cm^{-1} and a moderate peak observed at 850 cm^{-1} (Hofmann et al., 2006).

β – tricalcium phosphate (β-TCP) spectrum is illustrated in Figure 5.32. The spectrum consists of a broad P-O stretch at 1000 cm^{-1}. Figure 5.33 shows the reference spectrum for water. There was a sharp peak observed at 1640 cm^{-1} and broad peak at 3300 cm^{-1} that's indicating O – H stretching (Hofmann et al., 2006, Young et al., 2008).

The reference spectrum for 800mM citric acid is illustrated in figure 5.34. The spectrums consist of water O – H stretching at 1640 and 3300 cm^{-1}. There were additional peaks at 1420 and 1532 cm^{-1} due to symmetric and asymmetric COO^- stretching. There were also moderate peak corresponding with C = O and C – O stretching at 1720, 1016 and 1096 cm^{-1} (Hofmann et al., 2006, Young et al., 2004).

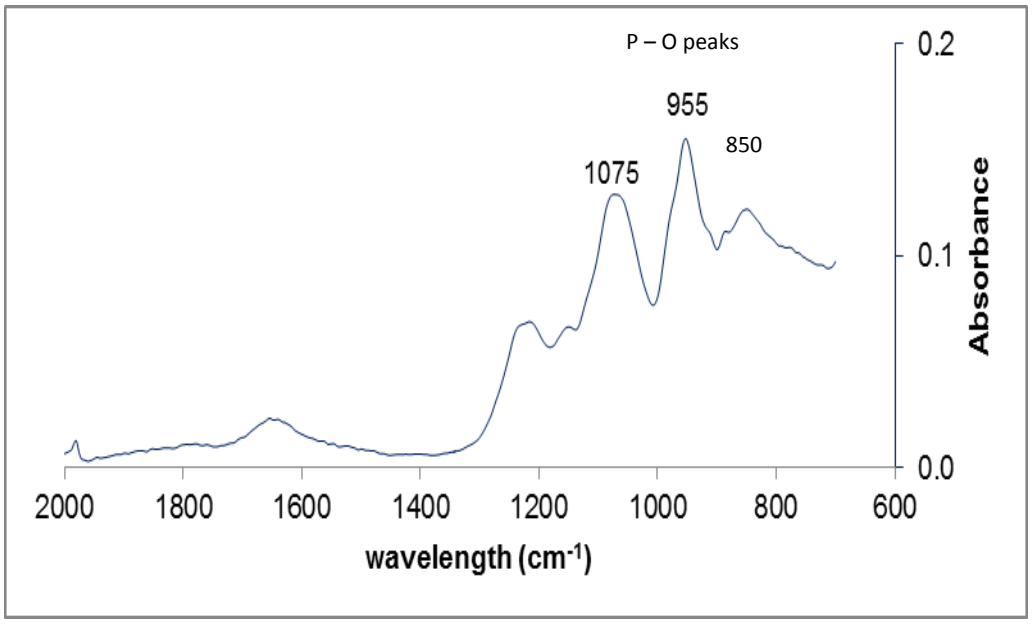

Figure 5-31: Reference spectrum of MCPM (powder phase).

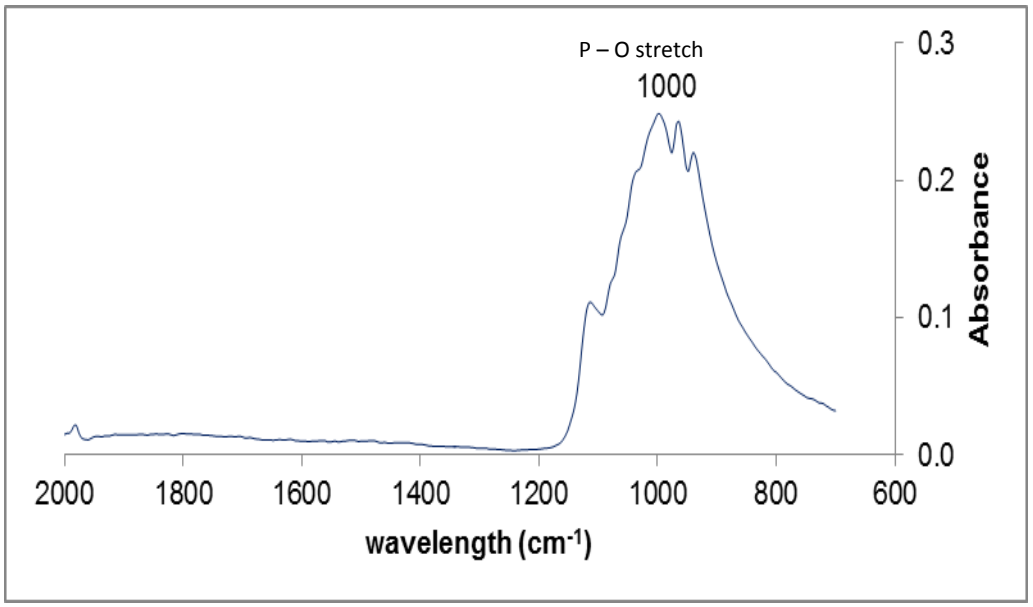

Figure 5-32: Reference spectrum of β - TCP (powder phase)

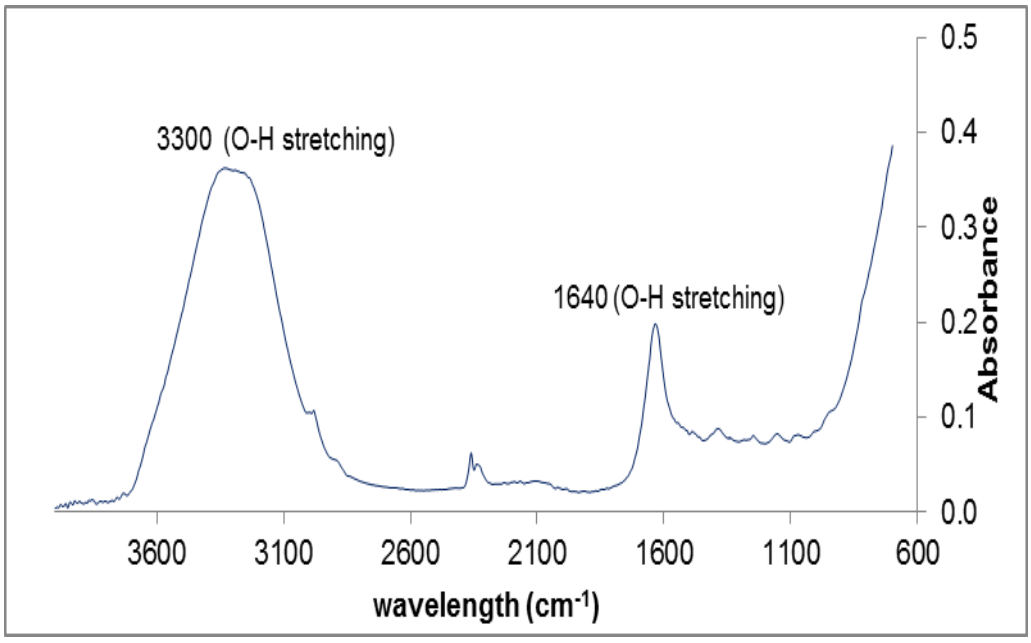

Figure 5-33: Reference spectrum of water (aqueous phase).

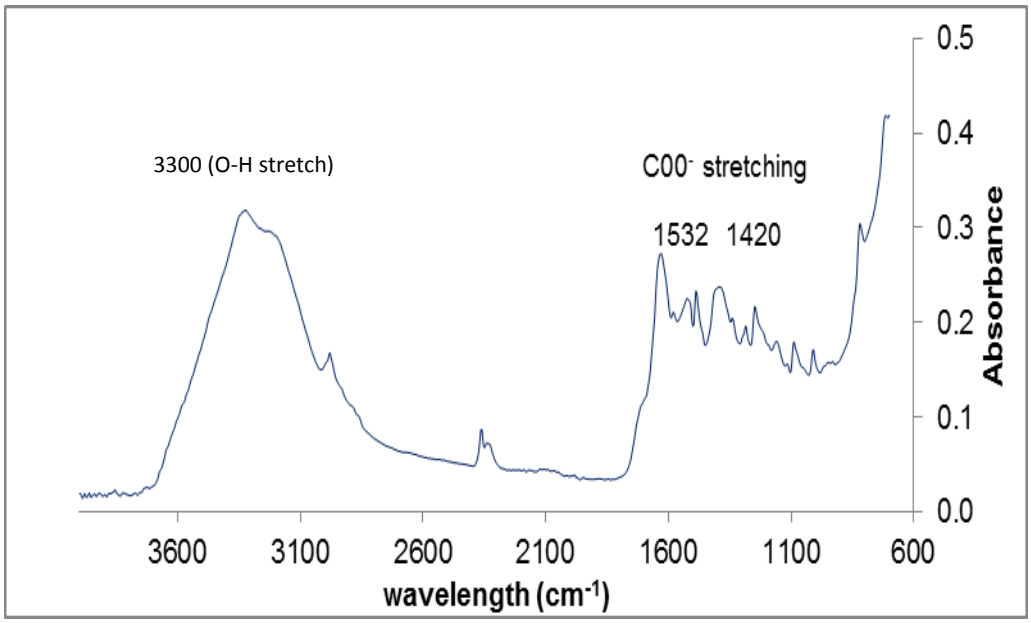

Figure 5-34: Reference spectrum of citric acid (aqueous phase).

5.4.2 Setting reaction

5.4.2.1 Setting reaction of brushite cements

FTIR spectroscopy was used to monitor brushite cements setting reactions and setting kinetics. Reference spectra for brushite cements with water at PLR 4:1 and 37^{o}C shown in figure 5.35. For control formulation the setting reaction was well underway at 100 s and practically complete at 3000 s. Three strong peaks (P-O peaks), consistent with brushite formation were noted at 1116, 1052 and 980 cm^{-1}. O-H peak, which suggest water incorporated during setting reaction, is noted at 1652, 3540 and 3480 cm-1 (sharp peak) and also 3280 and 3172 cm-1 (broad peak).

5.4.2.2 ε-Polylysine (PLS) effect on setting reaction

The absorbance spectra for the cements prepared with water and 50 wt % PLS are given in figure 5.36. The formulation was prepared at 37^{0}C with MCPM 2 without CA. These spectra are weaker than in figure 5.35. This could be due to poorer contact with the FTIR diamond and / or much less reaction. Lower reaction might be due to reduced water level available for reaction.

5.4.2.3 Combination effect of citric acid with different PLR on setting reaction

Example time – dependent absorbance spectra for cements with PLR 3.3:1 and 4:1 are illustrated in figure 5.37 and 5.38 respectively. The entire specimens were prepared at 37^{0}C with CA 800 mM. These spectra show all the main features for a brushite reaction. The peaks between 1200 and 1600 that appear and disappear are citrate - dicalcium phosphate complex intermediate peaks. The sharp key brushite peaks around 3000, 1640 and 980 appear as the intermediate peaks disappear. These indicate water binding. With 4:1 PLR the intermediate peaks are more difficult to detect possibly because of faster reaction.

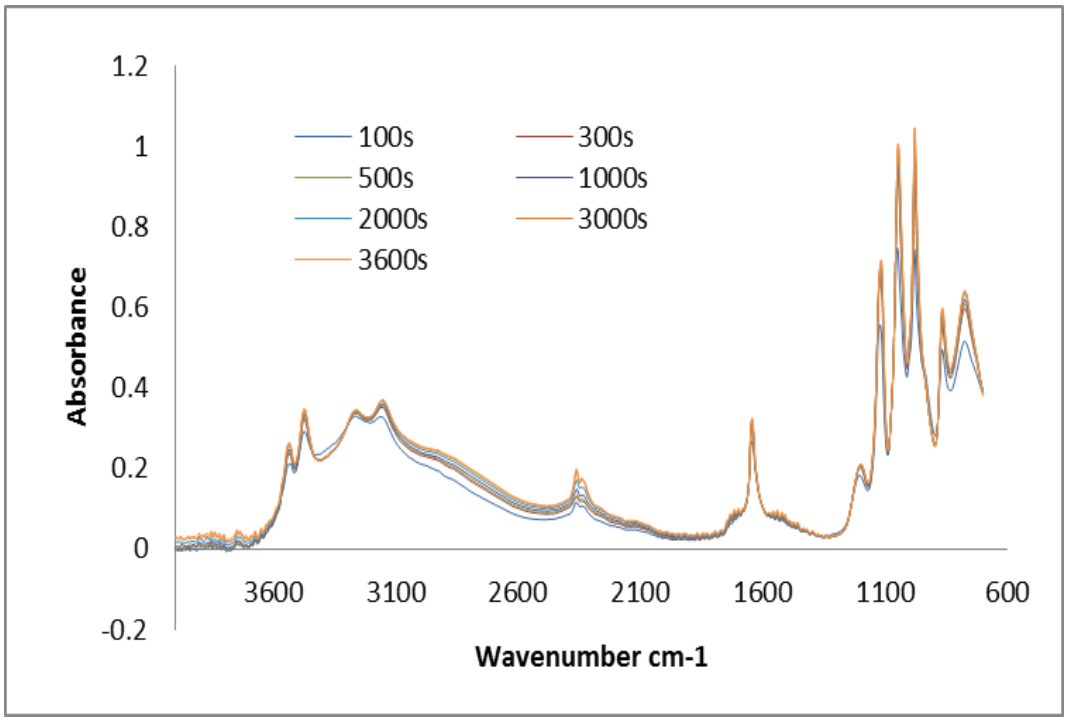

Figure 5-35: FTIR spectra versus time for brushite cement with PLR 4:1, MCPM 2, β-TCP 34 micron and water

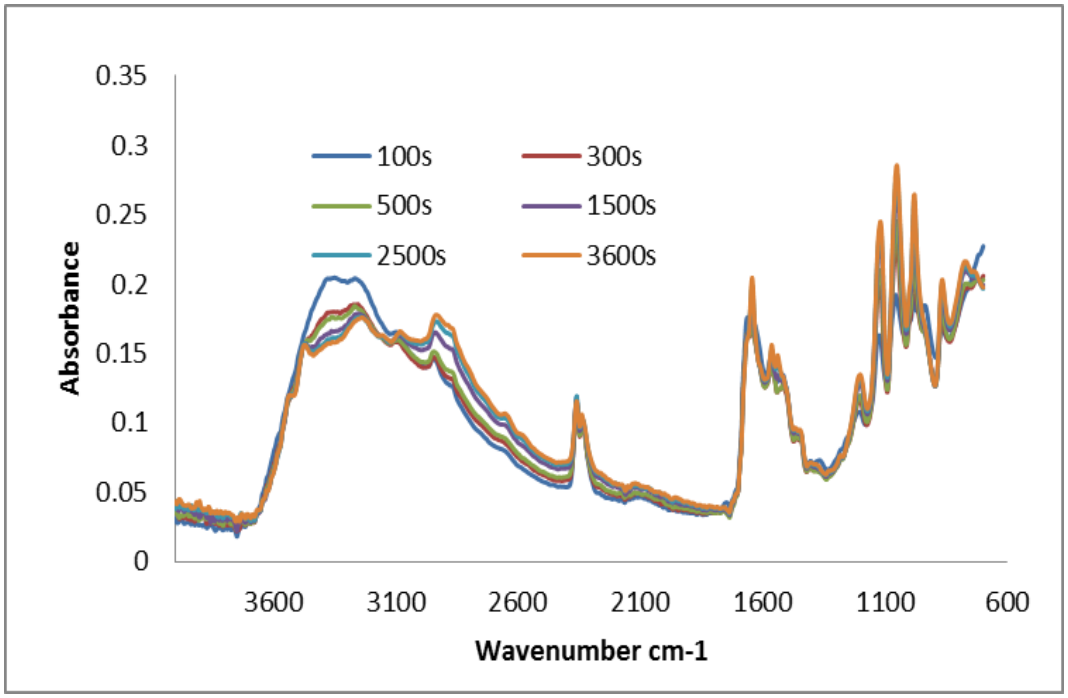

Figure 5-36: FTIR spectra versus time for brushite cement with PLR 4:1, MCPM 2, β-TCP 34 micron and water with 50 wt % PLS

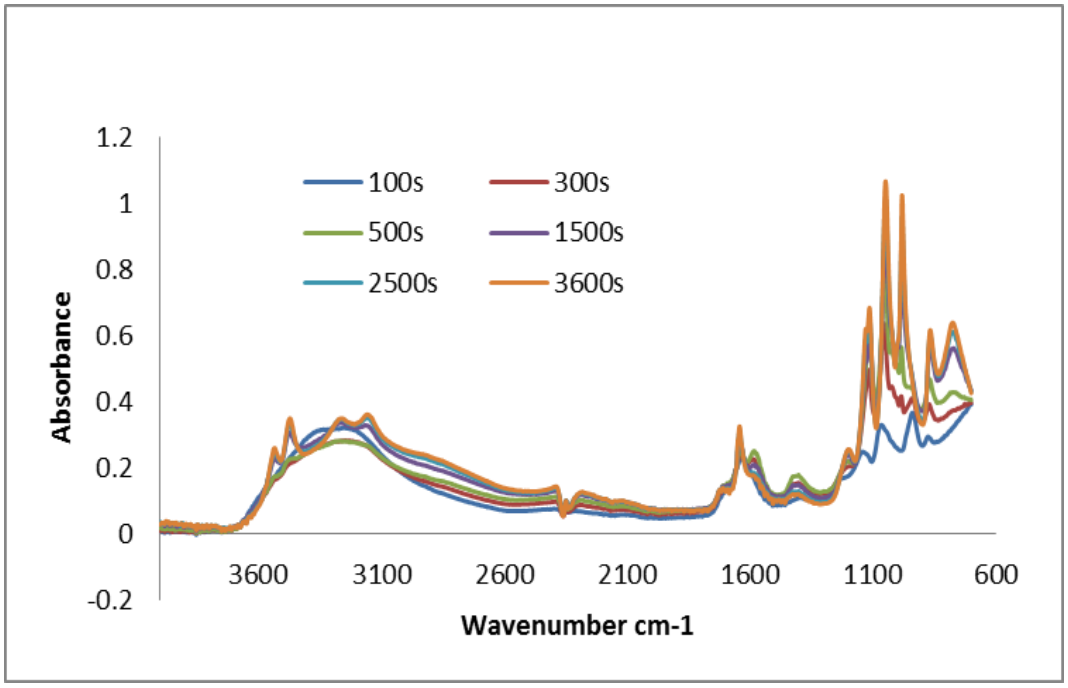

Figure 5-37: FTIR spectra versus time for brushite cement with PLR 3.3:1, MCPM 2, β-TCP 34 micron and CA

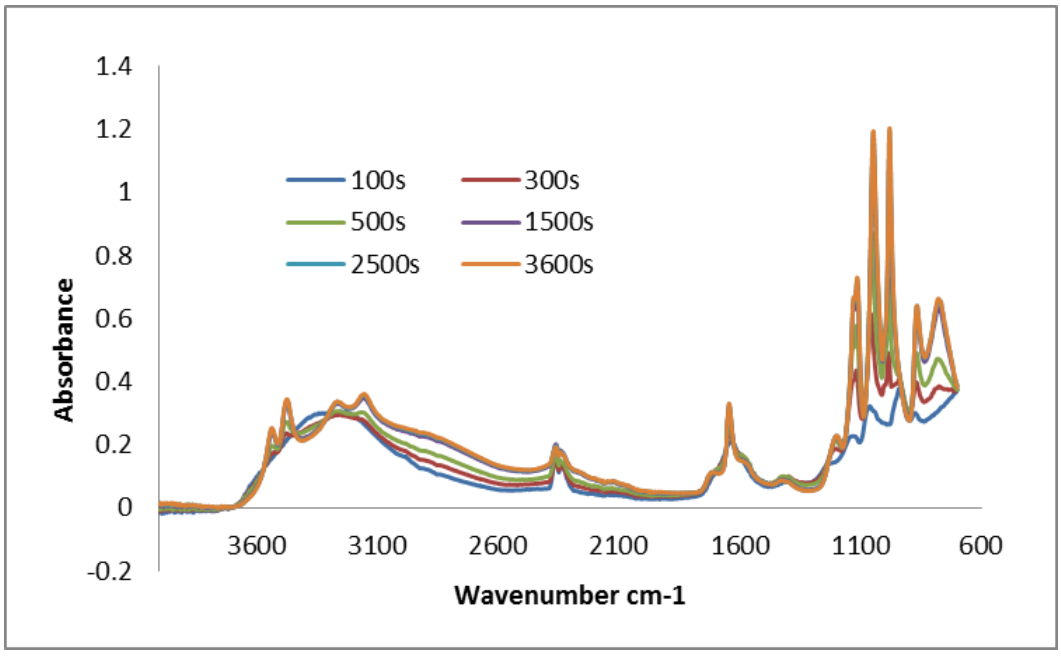

Figure 5-38: FTIR spectra versus time for brushite cement with PLR 4:1, MCPM 2, β-TCP 34 micron and CA

5.4.2.4 Combination effect of citric acid and increase wt % of ε-polylysine (PLS) on setting reaction

Figure 5.39 to figure 5.43 show the absorbance spectra for the cements prepared with increasing wt % of PLS from 10 wt % to 50 wt %. The entire formulations were prepared at 37^{o}C with MCPM 2 and CA 800 mM. All these figures show that increasing PLS caused an increase in the formation of dicalcium phosphate complexes. Unlike with citric acid alone these peaks do not disappear with time. The complex peaks may be due to NH and CN stretches or COO symmetric and asymmetric stretch peaks dependent upon whether the complexes form with PLS or citrate ions. Note as the complex peaks increase in intensity the water binding brushite peaks decrease as does the absorbance change for other peaks. This could be because either less dicalcium phosphate forming or because when it complexes the product causes less absorbance change.

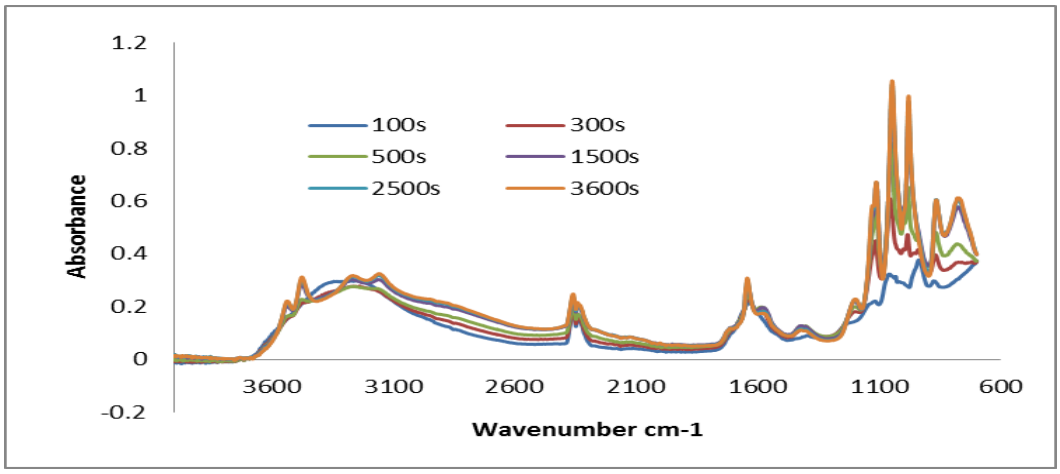

Figure 5-39: FTIR spectra versus time for brushite cement with PLR 4:1, MCPM 2, β-TCP 34 micron and CA with 10 wt % PLS

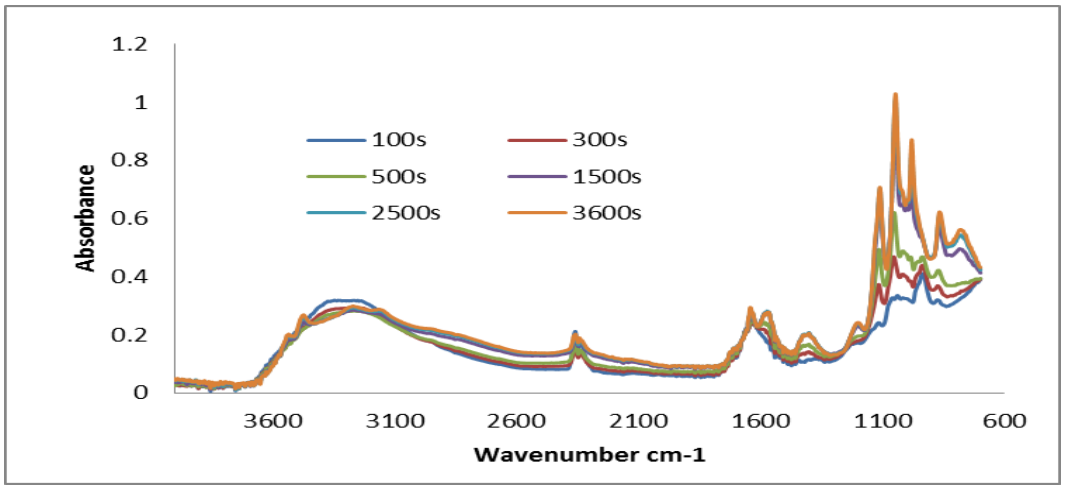

Figure 5-40: FTIR spectra versus time for brushite cement with PLR 4:1, MCPM 2, β-TCP 34 micron and CA with 20 wt % PLS

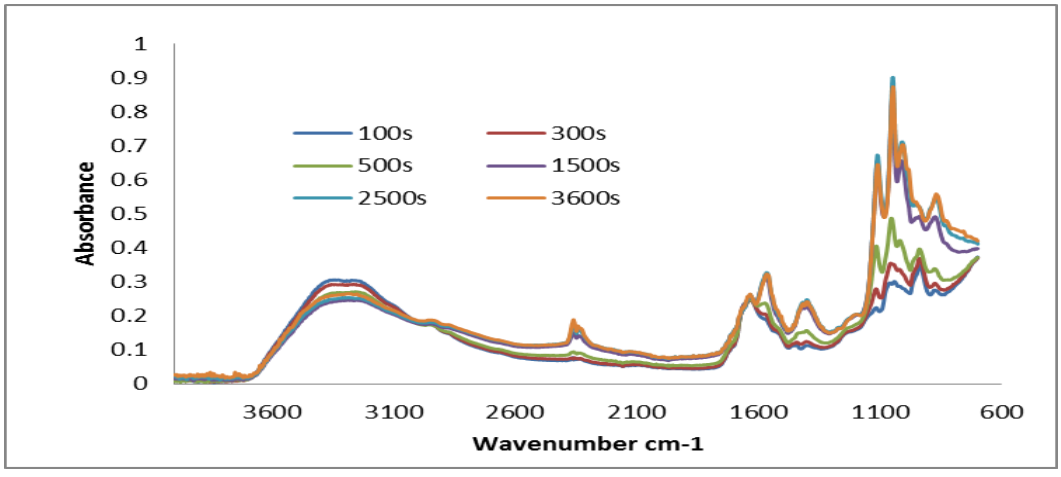

Figure 5-41: FTIR spectra versus time for brushite cement with PLR 4:1, MCPM 2, β-TCP 34 micron and CA with 30 wt % PLS

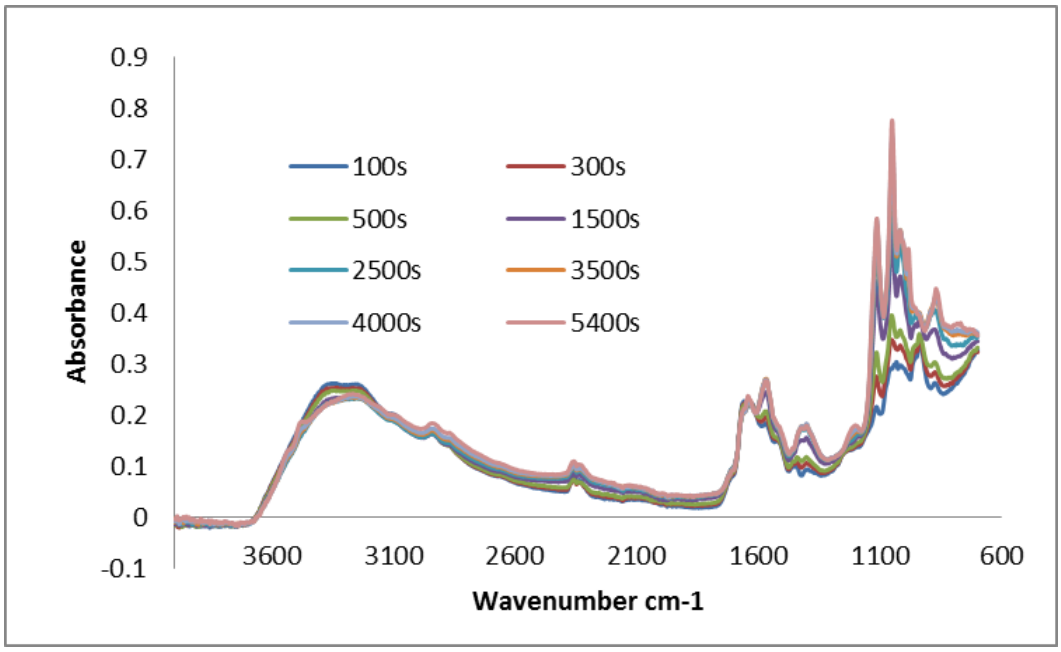

Figure 5-42: FTIR spectra versus time for brushite cement with PLR 4:1, MCPM 2, β-TCP 34 micron and CA with 40 wt % PLS

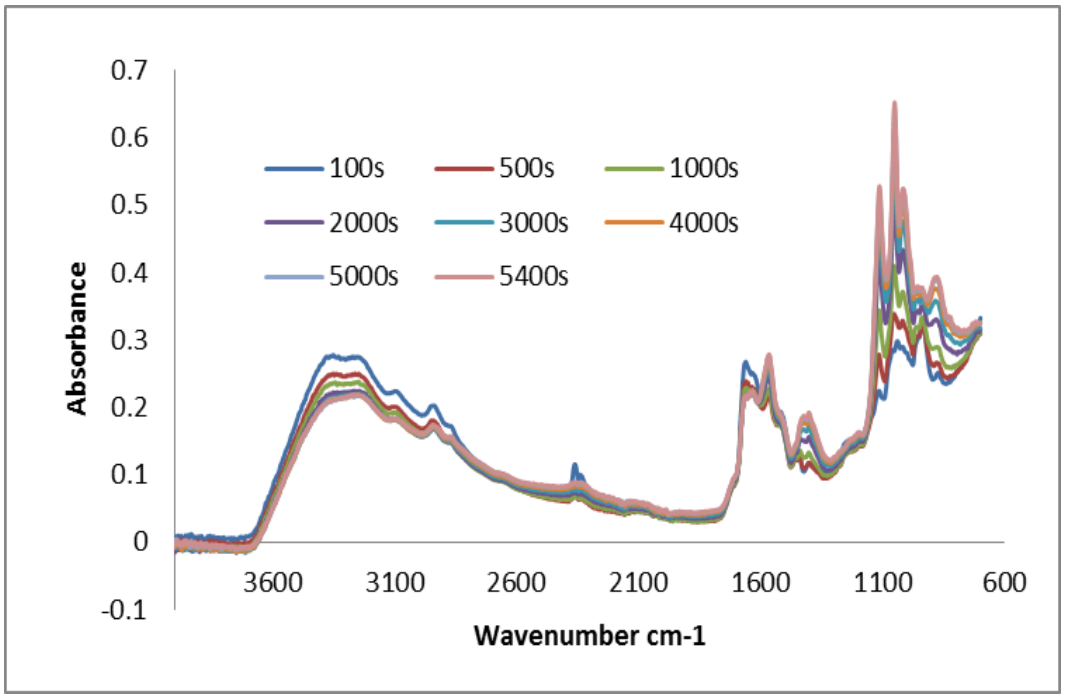

Figure 5-43: FTIR spectra versus time for brushite cement with PLR 4:1, MCPM 2, β-TCP 34 micron and CA with 50 wt % PLS

5.4.3 Difference spectra

Difference spectra were obtained by subtracting each spectrum from the first at 100 s. The absorbance changes obtained are characteristic of the reactions taking place. The following figures from 5.44 to 5.55 represent difference spectra for all formulations. All formulations were prepared at 37^{o}C with or without citric acid (CA) 800 mM.

5.4.3.1 Absorbance change for brushite cements prepared with water and ε-polylysine (PLS)

Figures 5.44 to 5.46 show the difference spectra of compositions prepared with no citric acid and 0, 20 or 50 wt % PLS. In these formulations no intermediate peaks are observed. Dicalcium P-O peaks (1100, 1052 and 980 cm^{-1}) and bound water O-H peaks (1640 and 3100 to 3600 cm-1) are obtained.

5.4.3.2 MCPM and PLR effect on absorbance change

Figures 5.47 to 5.50 shows difference spectra of cements prepared with CA and different PLR or MCPM. The setting reaction involves two processes. The first process is observed most readily in Figure 5.47 with MCPM 1 and PLR 3.3. This gives strong absorbance increase at 1052, 1100, and between 1200 and 1600 cm^{-1}. Those between 1200 and 1600 are lost as the water binding peaks at 980 and around 3000 develop. With higher PLR or MCPM 2 the peak changes are comparable but the intermediate peaks are more difficult to detect and the reaction rate is changed.

5.4.3.3 Combined effect of ε-polylysine (PLS) and citric acid on absorbance change

The difference spectra for compositions with different wt % of PLS are demonstrated from figure 5.51 to 5.55. These show the gradual change from brushite to complex formation with increasing PLS.

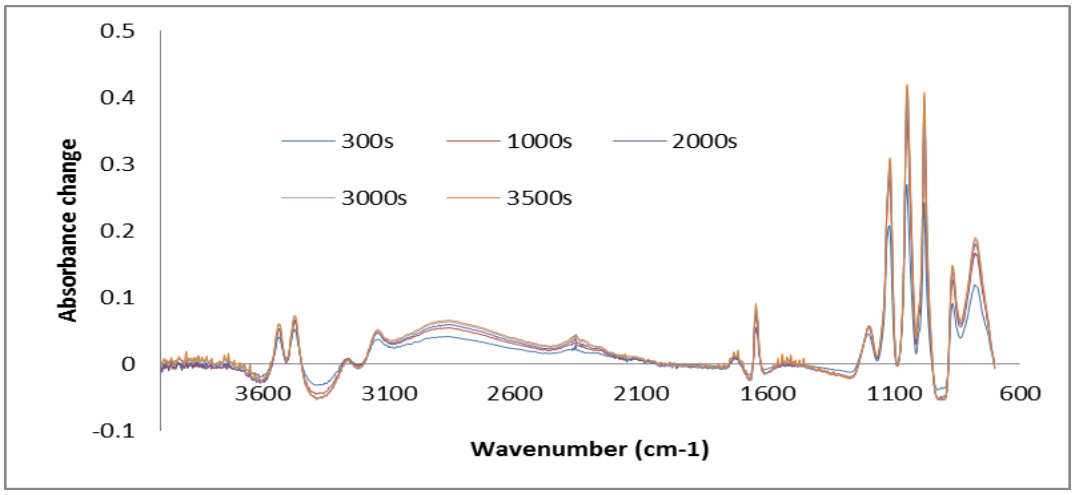

Figure 5-44: Effect of time on FTIR difference spectra of brushite cement with PLR 4:1 MCPM 2, β-TCP 34 micron and water

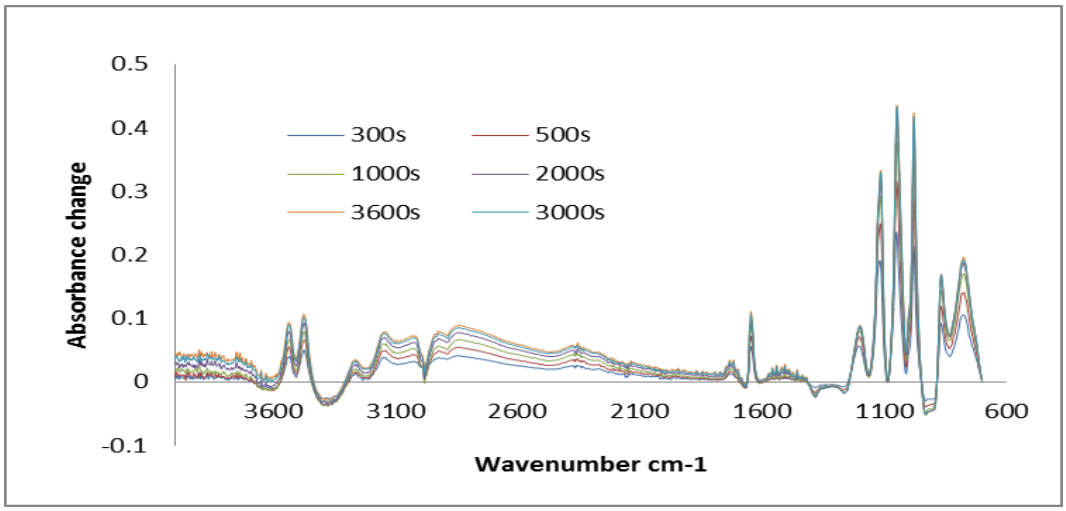

Figure 5-45: Effect of time on FTIR difference spectra of brushite cement with PLR 4:1 MCPM 2, β-TCP 34 micron and water with 20 wt % PLS

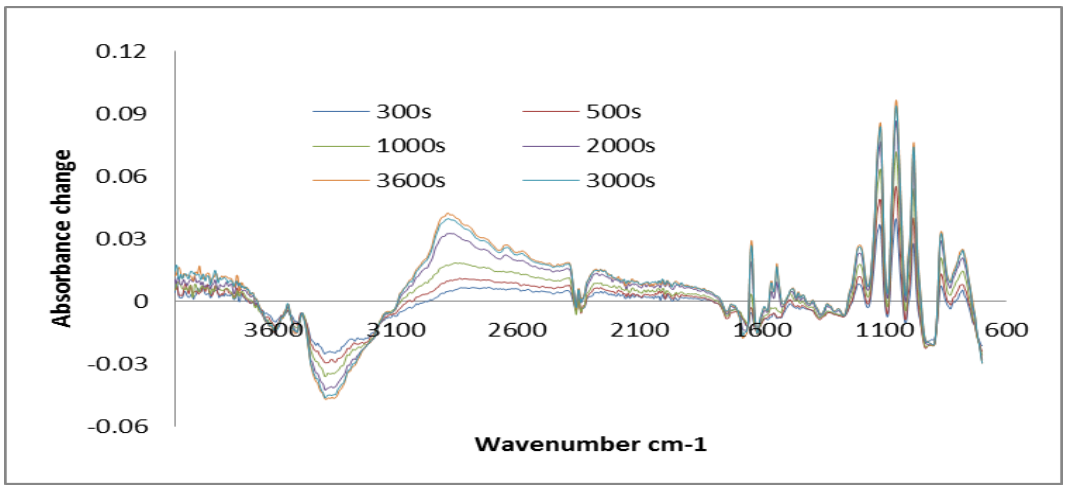

Figure 5-46: Effect of time on FTIR difference spectra of brushite cement with PLR 4:1 MCPM 2, β-TCP 34 micron and water with 50 wt % PLS

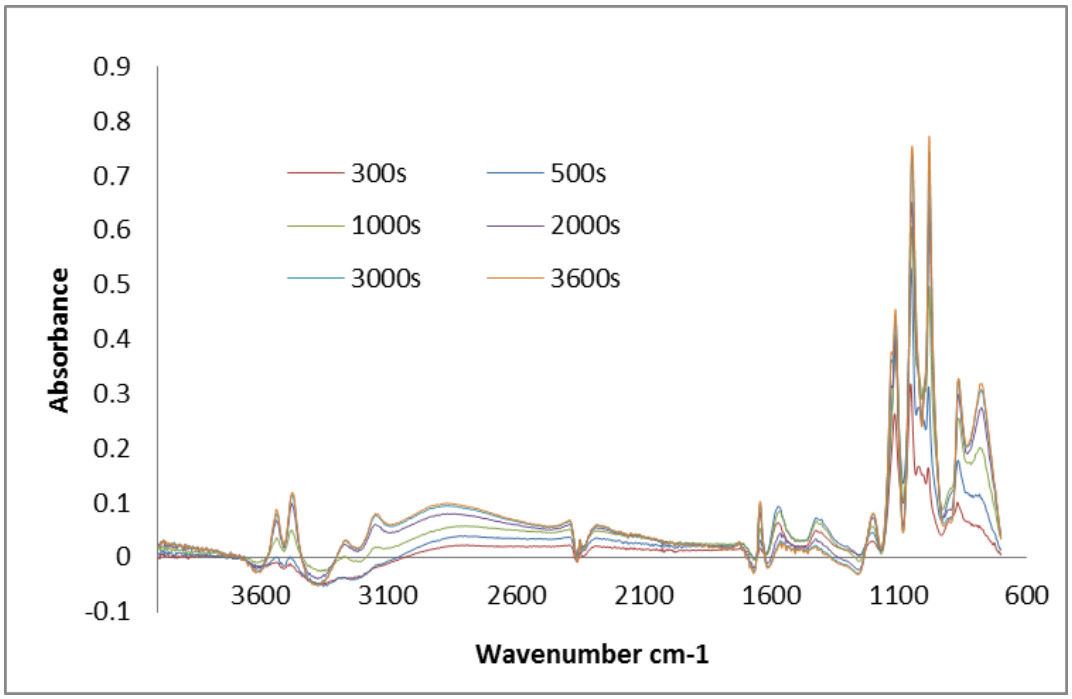

Figure 5-47: Effect of time on FTIR difference spectra of brushite cement with PLR 3.3:1 MCPM 1, β-TCP 34 micron and CA

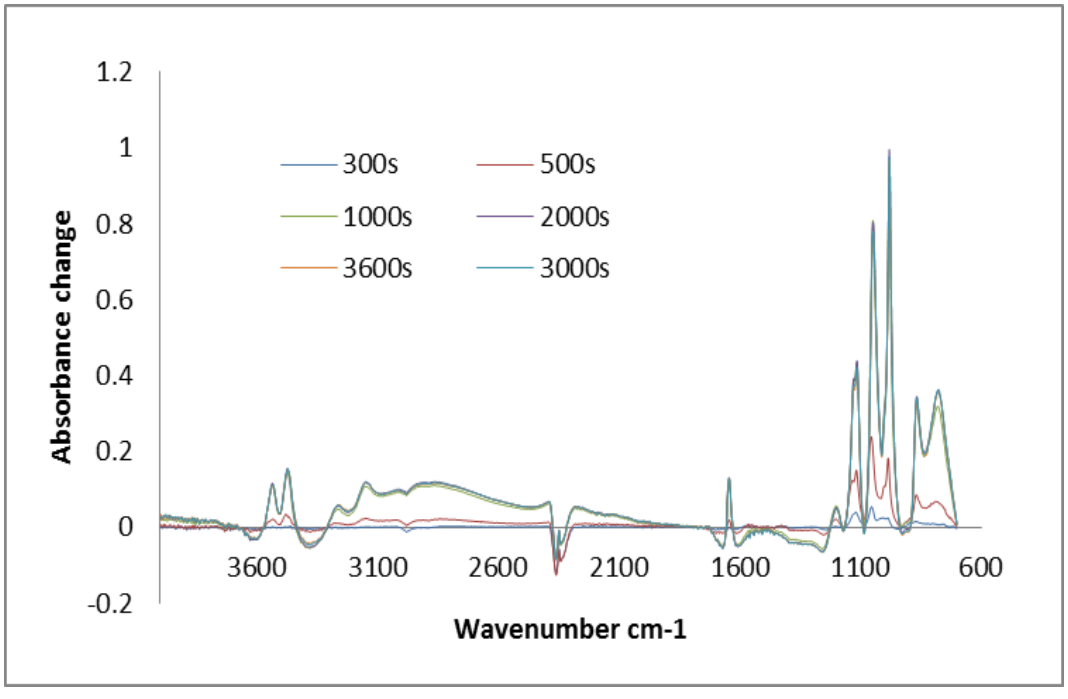

Figure 5-48: Effect of time on FTIR difference spectra of brushite cement with PLR 3.3:1 MCPM 2, β-TCP 34 micron and CA

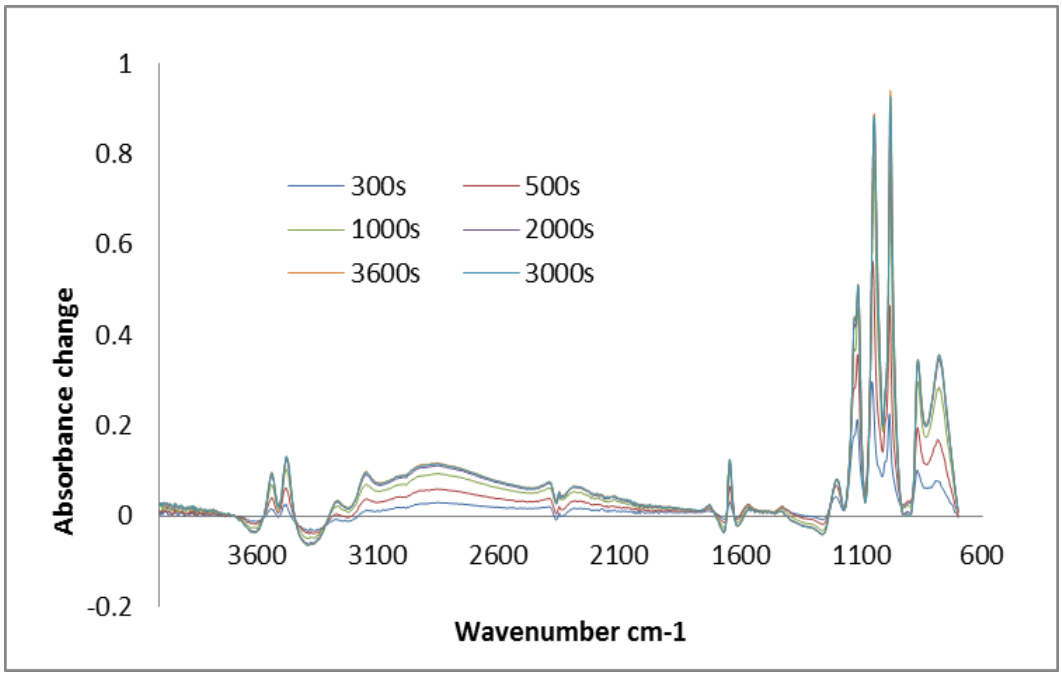

Figure 5-49: Effect of time on FTIR difference spectra of brushite cement with PLR 4:1 MCPM 1, β-TCP 34 micron and CA

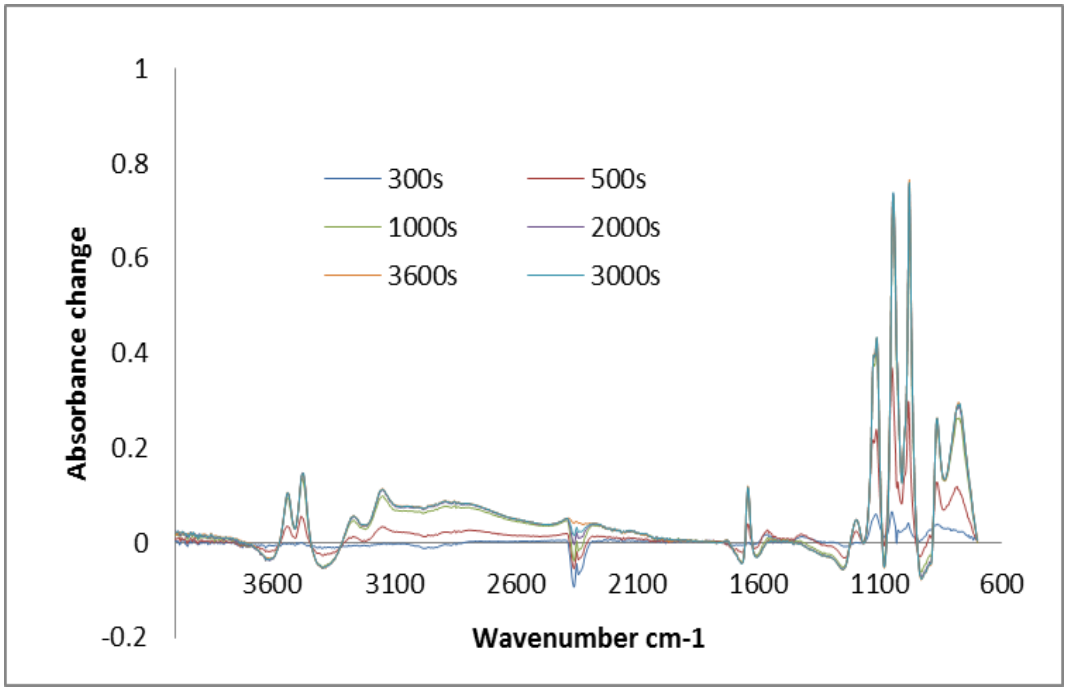

Figure 5-50: Effect of time on FTIR difference spectra of brushite cement with PLR 4:1 MCPM 2, β-TCP 34 micron and CA

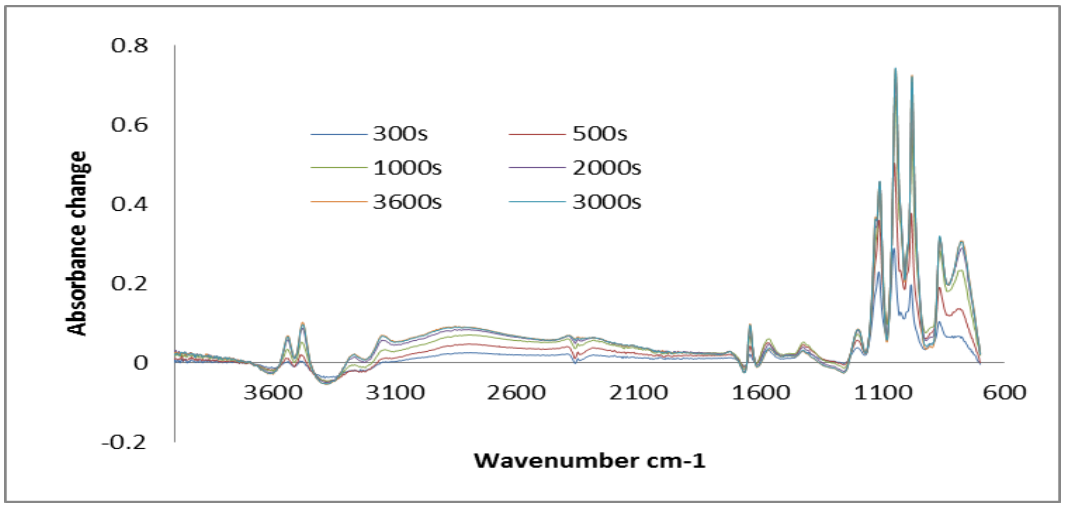

Figure 5-51: Effect of time on FTIR difference spectra of brushite cement with PLR 4:1 MCPM 2, β-TCP 34 micron and CA with 10 wt % PLS

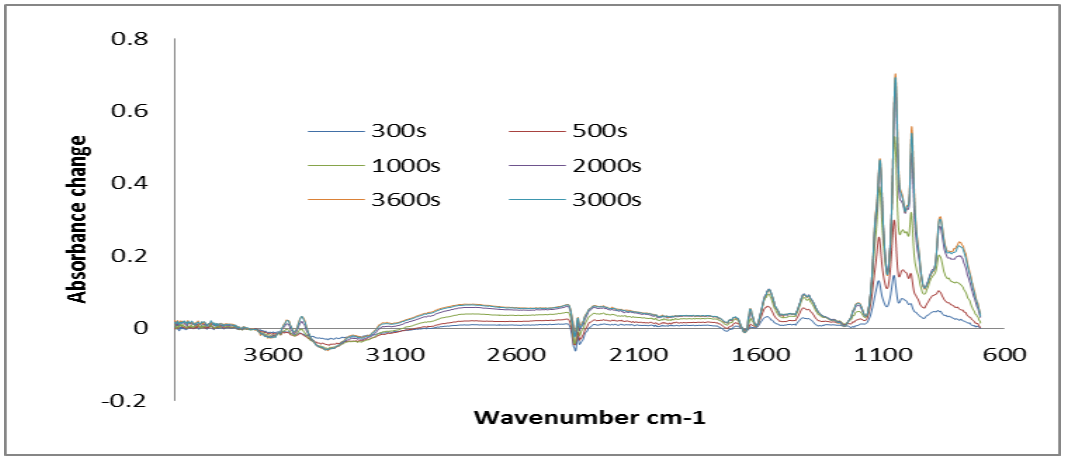

Figure 5-52: Effect of time on FTIR difference spectra of brushite cement with PLR 4:1 MCPM 2, β-TCP 34 micron and CA with 20 wt % PLS

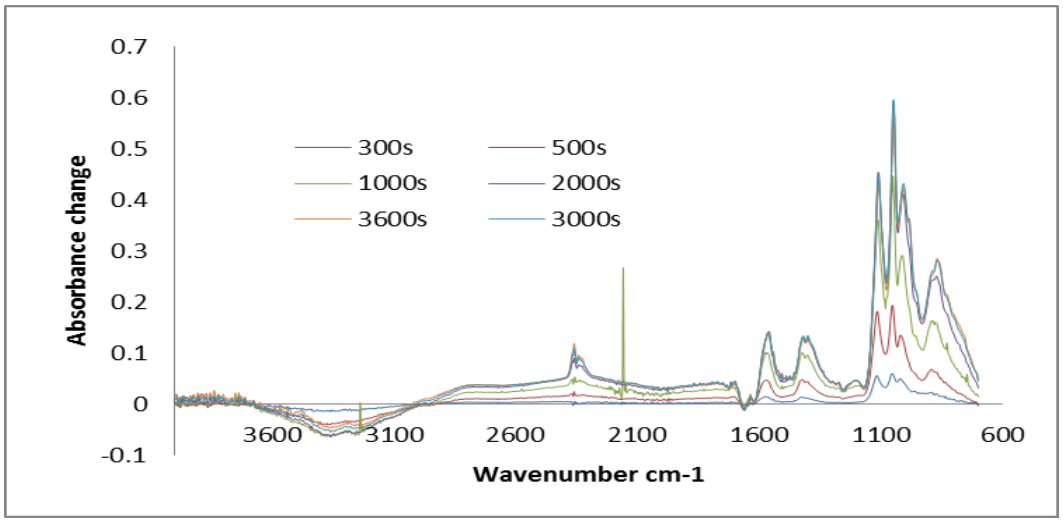

Figure 5-53: Effect of time on FTIR difference spectra of brushite cement with PLR 4:1 MCPM 2, β-TCP 34 micron and CA with 30 wt % PLS

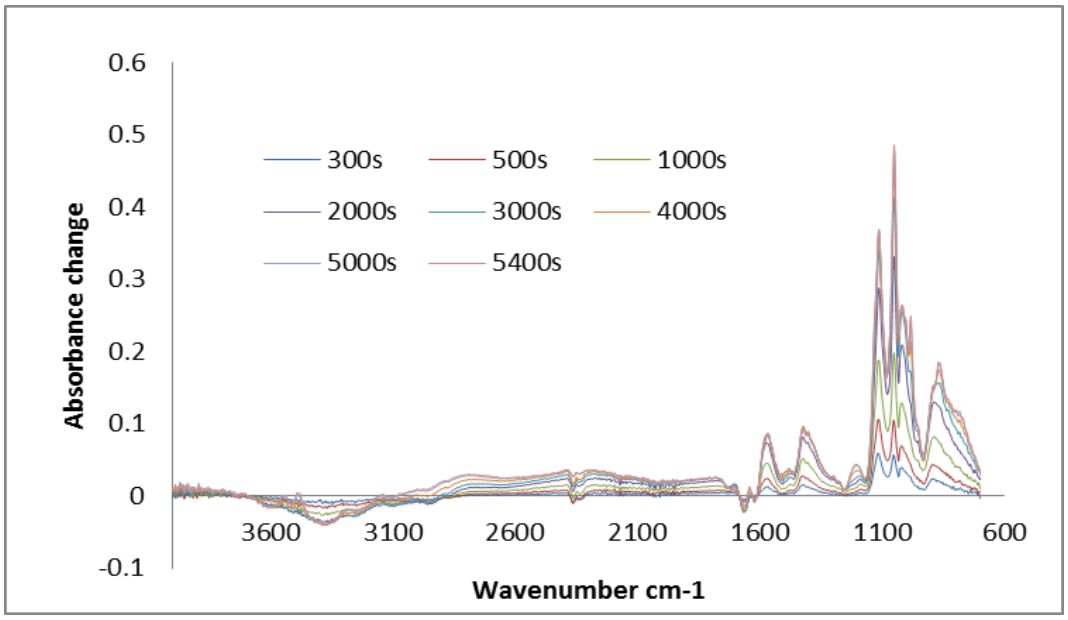

Figure 5-54: Effect of time on FTIR difference spectra of brushite cement with PLR 4:1 MCPM 2, β-TCP 34 micron and CA with 40 wt % PLS

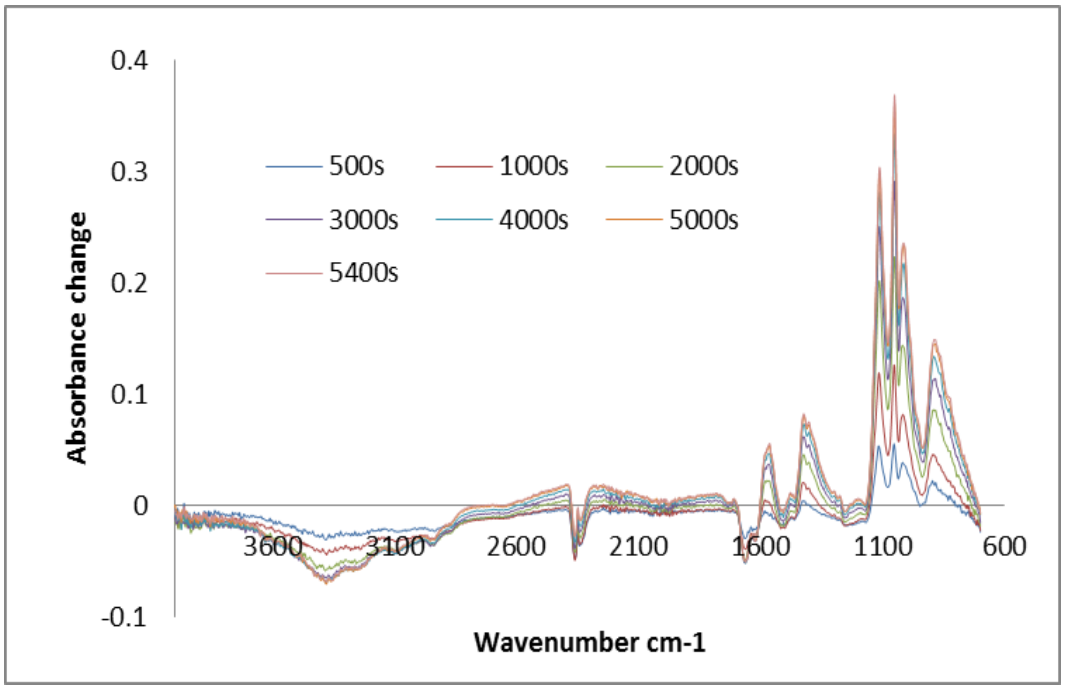

Figure 5-55: Effect of time on FTIR difference spectra of brushite cement with PLR 4:1 MCPM 2, β-TCP 34 micron and CA with 50 wt % PLS

5.4.4 Absorbance change

Absorbance change profiles at 980 cm^{-1} and 1050 cm^{-1} were obtained by using Time base software and subtracting initial absorbance values from all time points. The following figures from 5.56 to 5.61 represent the different absorbance profiles for each composition of cement prepared at 37^{o}C with or without CA 800 mM.

5.4.4.1 Different MCPM and PLR effect on absorbance change

Figure 5.56 and 5.57 shows absorbance profiles at 980 cm^{-1} and 1050 cm^{-1} for the 2 different MCPM's and PLRs. All formulations were prepared with CA 800 mM. Greater maximum change was seen with higher PLR possibly due to increased brushite density. With higher PLR, more powder was available and less water thereby reducing porosity and increasing the amount of brushite in contact with the FTIR diamond. Furthermore, using different MCPM gave obvious changes in setting profiles.

With MCPM 1, CA appears more readily able to interact with the cement reactants. CA was therefore able to delay the set and provide a snap set. With MCPM 2 with more crystalline structure there was no clear delay before reaction but the 1050 peak reached its maximum value more quickly than the 980 peak. By comparison with Figures 5.56 and 5.57 it can be observed that with MCPM 2 the presence of CA both enhances the maximum absorbance change and slows down the absorbance change particularly at 980 cm^{-1}.

5.4.4.2 ε-Polylysine (PLS) effect on absorbance change

Figure 5.58 and 5.59 shows brushite cements setting profile at 980 cm^{-1} and 1050 cm^{-1} with different wt % of PLS without CA. All formulations were prepared with MCPM 2. Cements prepared with 20 wt % of PLS showed similar absorbance change with sample prepared with only water. Absorbance changes of cements prepared with 50 wt % of PLS however had much reduced maximum change particularly at 980 cm^{-1}. This suggests less brushite in contact with the FTIR diamond.

5.4.4.3 Combined effect of ε-polylysine (PLS) and citric acid (CA) on absorbance change

The 980 and 1050 cm^{-1} profiles with different wt % of PLS and CA are shown in figures 5.60 and 5.61. All formulations were prepared with MCPM 2, β-TCP 34 micron and CA 800 mM. By increasing the wt % of PLS both the rate of reaction and maximum absorbance changes declined. The effects were reduced at the higher wave number. After running the experiment for 3600 seconds, the cements with 50 wt % ε-polylysine had an absorbance of 0.6, which only accounts for 1/3 of brushite cements with 10 wt % of PLS for the same period of time. The setting of cements with 50 wt % of PLS was delayed beyond 3000 seconds.

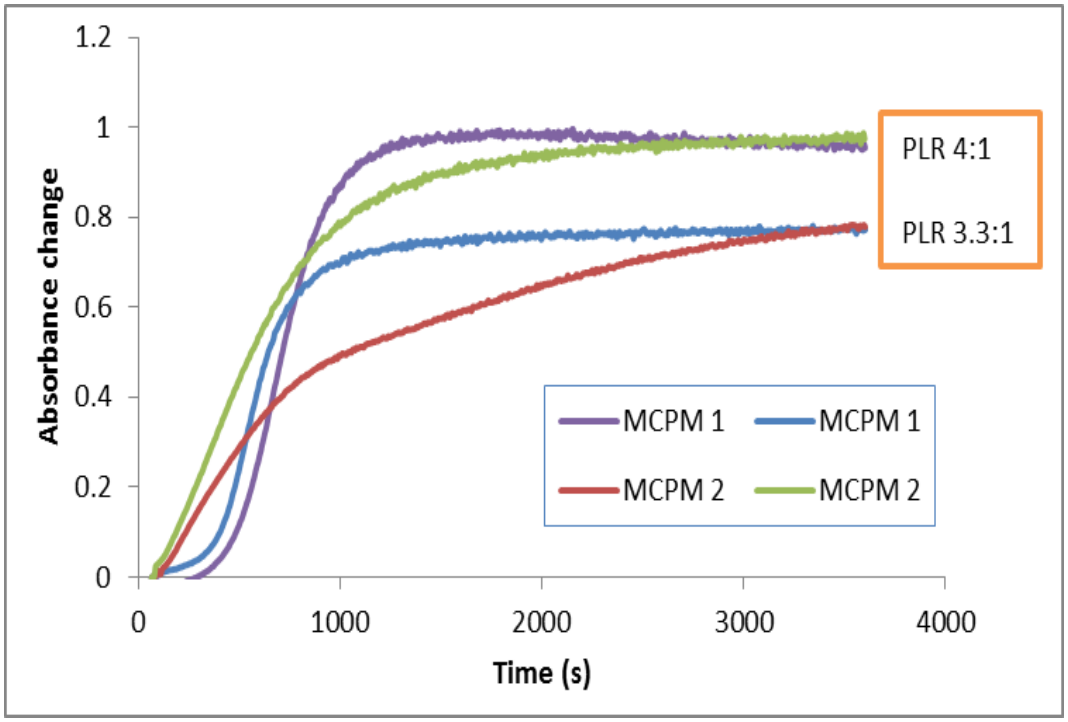

Figure 5-56: Brushite cements setting profile at 980 cm^{-1} with different MCPM (1 or 2), β-TCP 34 micron and CA at PLR (3.3:1 or 4:1)

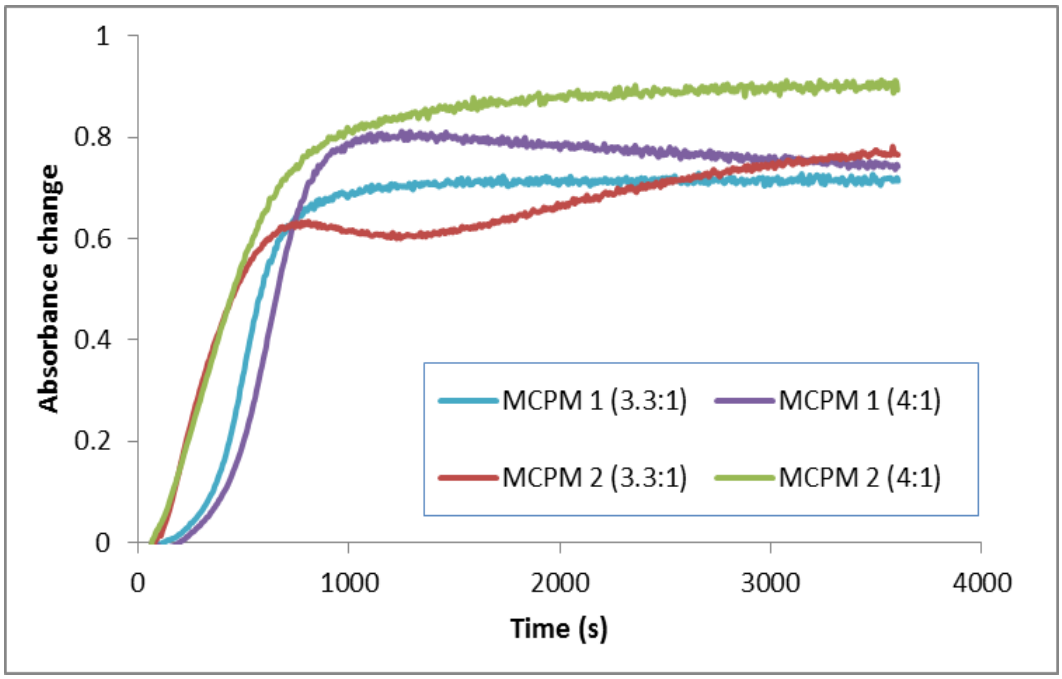

Figure 5-57: Brushite cements setting profile at 1050 cm^{-1} with different MCPM (1 or 2), β-TCP 34 micron and CA at PLR (3.3:1 or 4:1)

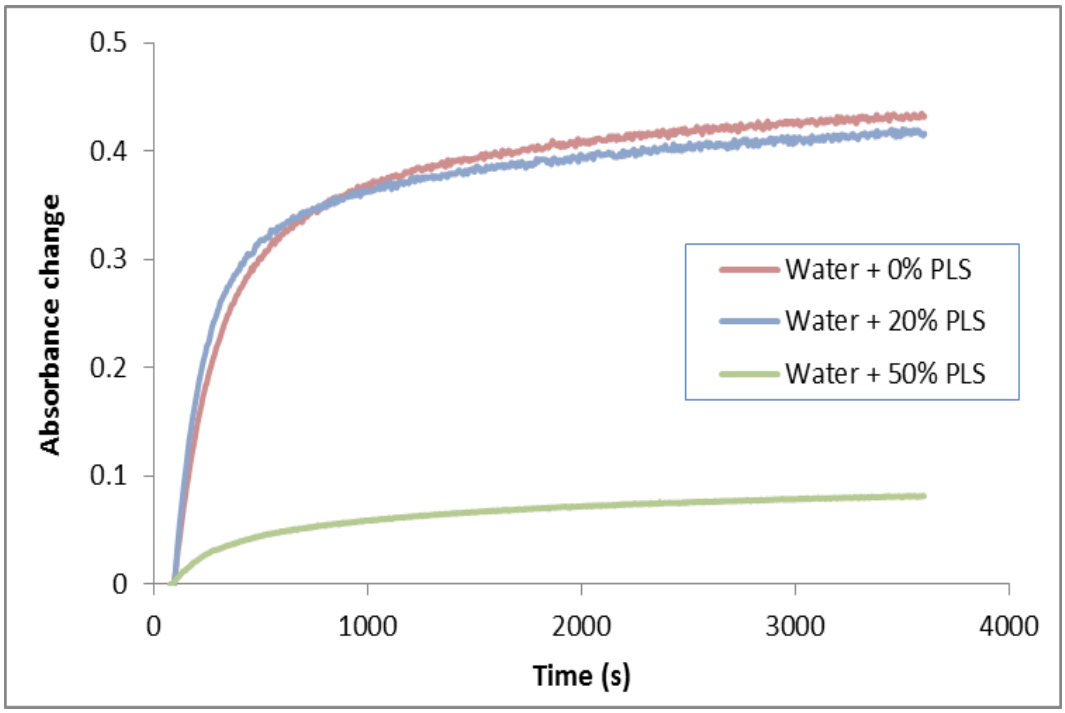

Figure 5-58: Brushite cements setting profile at 980 cm^{-1} with different wt % of PLS, PLR 4:1 and without CA (MCPM 2 + β-TCP 34 micron + water)

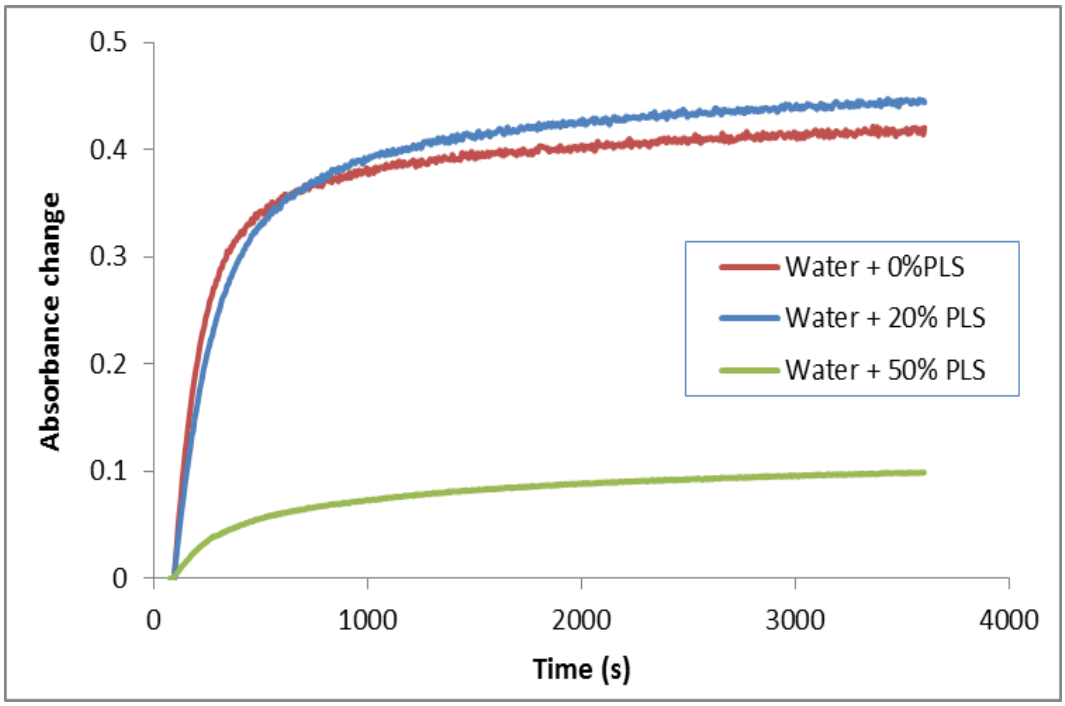

Figure 5-59: Brushite cements setting profile at 1050 cm^{-1} with different wt % of PLS, PLR 4:1 and without CA (MCPM 2 + β-TCP 34 micron + water)

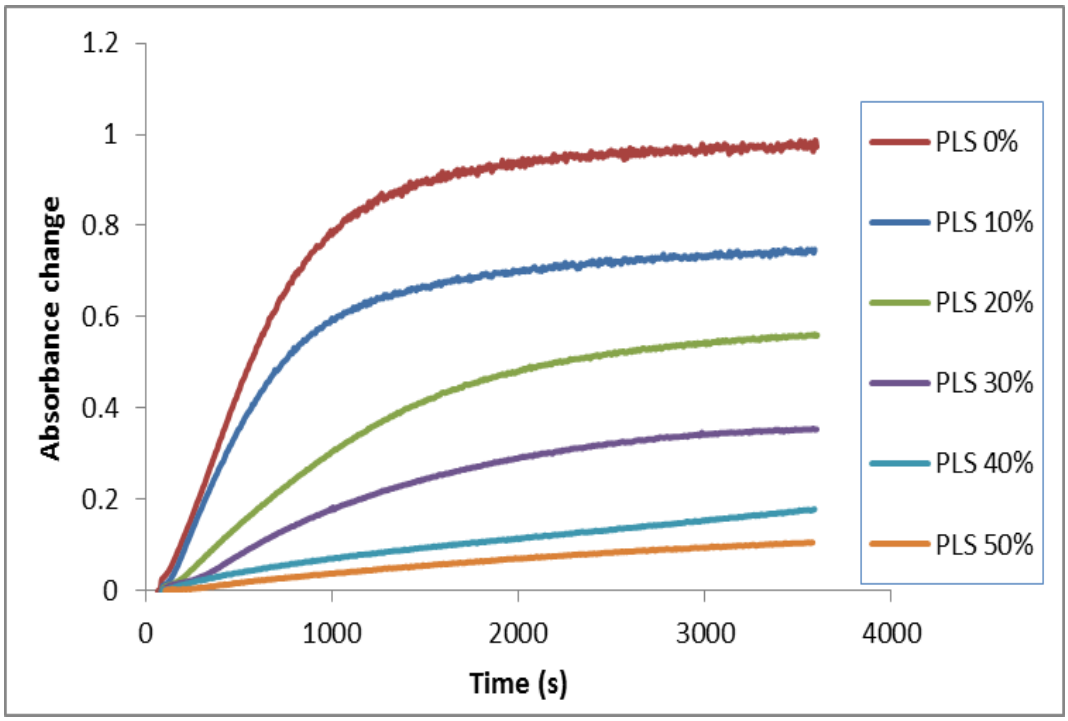

Figure 5-60: Brushite cements setting profile at 980 cm^{-1} with MCPM 2, β-TCP 34 micron and CA with increase wt % PLS.

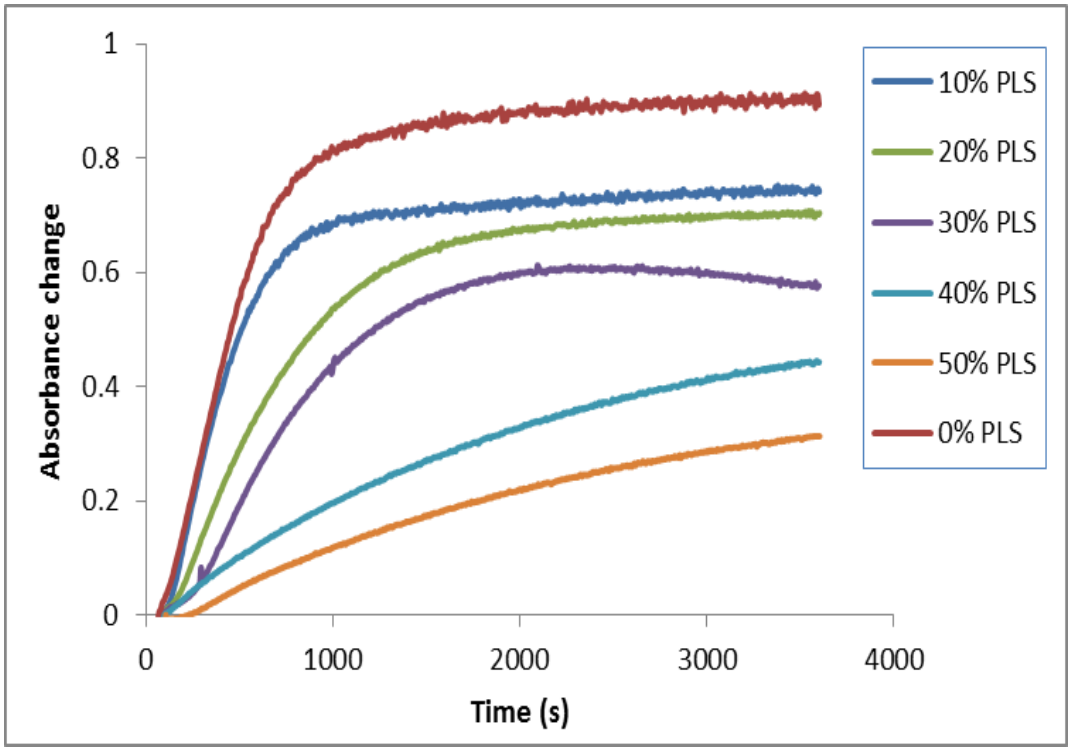

Figure 5-61: Brushite cements setting profile at 1050 cm^{-1} with MCPM 2, β-TCP 34 micron and CA with increase wt % PLS.

5.5 Degradation study

5.5.1 Mass loss of set cements with different MCPM

Figure 5.62 shows the percentage of mass loss time (hours) in water for cements with different MCPM, β-TCP particle size of 34 micron and CA 800 mM. The first 24 hours showed rapid mass loss for cements with MCPM 2. Cements prepared with MCPM 1 overall degraded less than cements prepared with MCPM 2. There was significant difference in mass loss between composition with MCPM 1 and MCPM 2. Mass losses for both MCPM were increase with time.

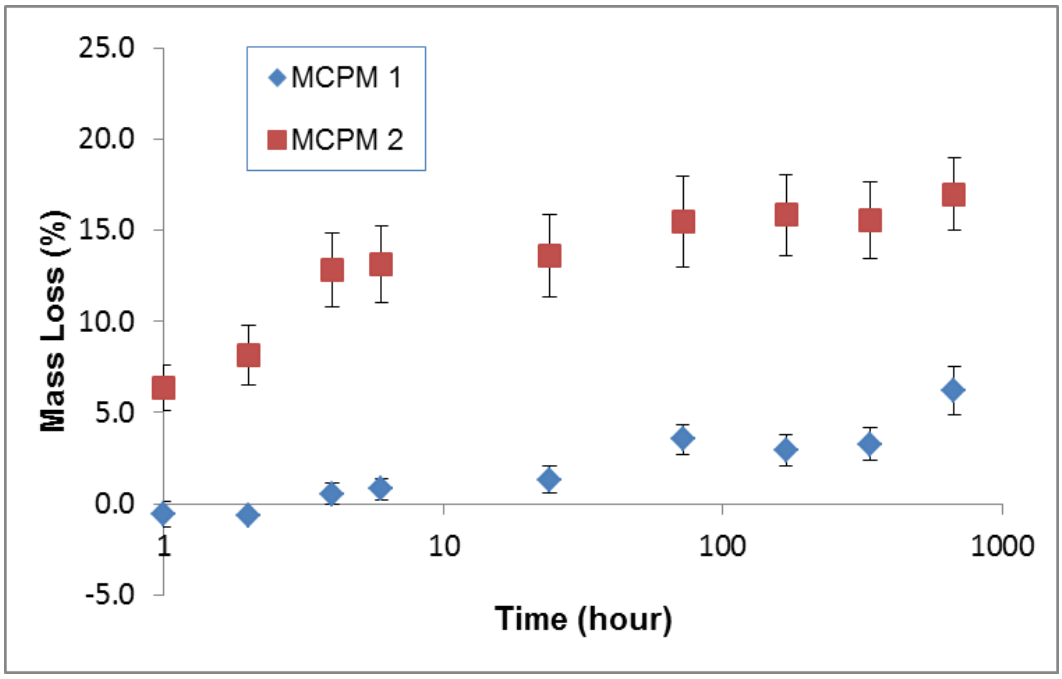

Figure 5-62: Mass loss vs $\log_{10}$ for cements composition with MCPM 1 and MCPM 2. Error bars shown are 95% CI (n = 5). None overlapping indicates significantly different results ($p < 0.05$).

5.5.2 Mass loss of set cements with increase wt % of ε-polylysine (PLS)

Cumulative mass loss was linear with time (hours) with a burst material release in the first 24 hours for all formulations containing PLS (Figure 5.63). The plotted graph shows that there was still increase in mass loss after 24 hours but it was very slow. The overall mass loss was increasing for cements with formulation of 0 wt % of PLS to 40 w% of PLS. Cements with 50 wt % PLS also showed increase in mass loss but become more stable after 72 hours.

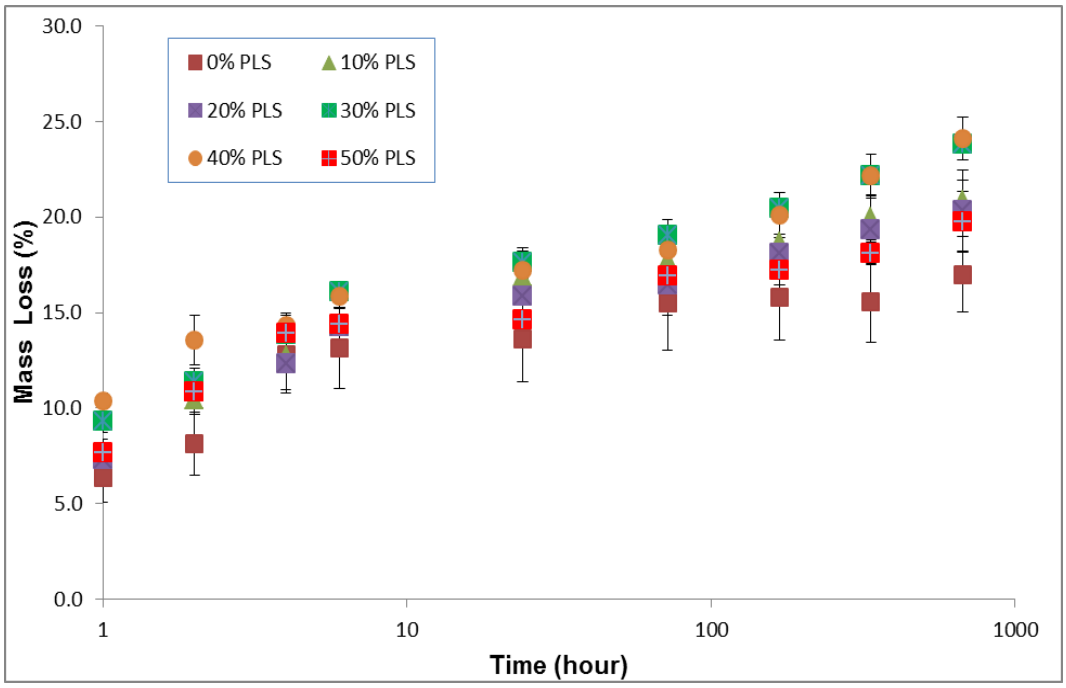

Figure 5-63: Mass loss vs $\log_{10}$ for cements composition with increase wt % of PLS (MCPM 2 + β-TCP 34.0 micron + citric acid 800 mM + increase wt % of PLS). Error bars shown are 95% CI (n = 5).

5.6 pH study

5.6.1 pH study for formulation with different MCPM's

pH of storage solutions were analysed after 1, 2, 4, 6, 24 hours, 48 hours, 72 hours, one week, two weeks and 4 weeks. Samples were placed in fresh water at each time point. All formulations were prepared with different MCPM, β-TCP 34 micron and CA 800 mM. Figure 5.64 shows the changes in the pH levels of distilled water with square root of time in the presence of cements prepared with different MCPM. Generally, the pH levels were slightly acidic initially but neutral after 24 hours. The pH values ranged from 3.8 to 7.2. Figure 5.65 shows the cumulative acid release of cement with different MCPM versus square root of time. Effects of changing MCPM were not highly significant.

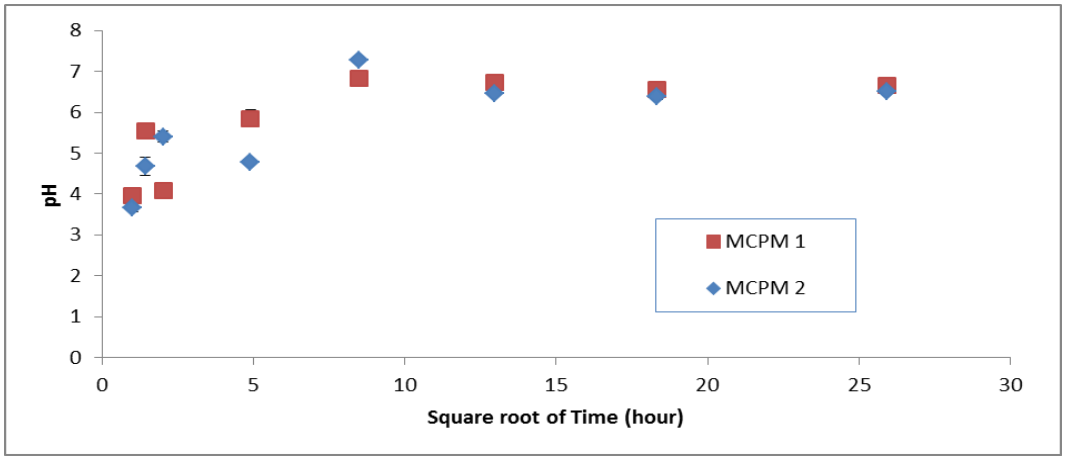

Figure 5-64: pH level of composition with MCPM 1 and MCPM 2 at different time point. Error bars shown are 95% CI (n = 5).

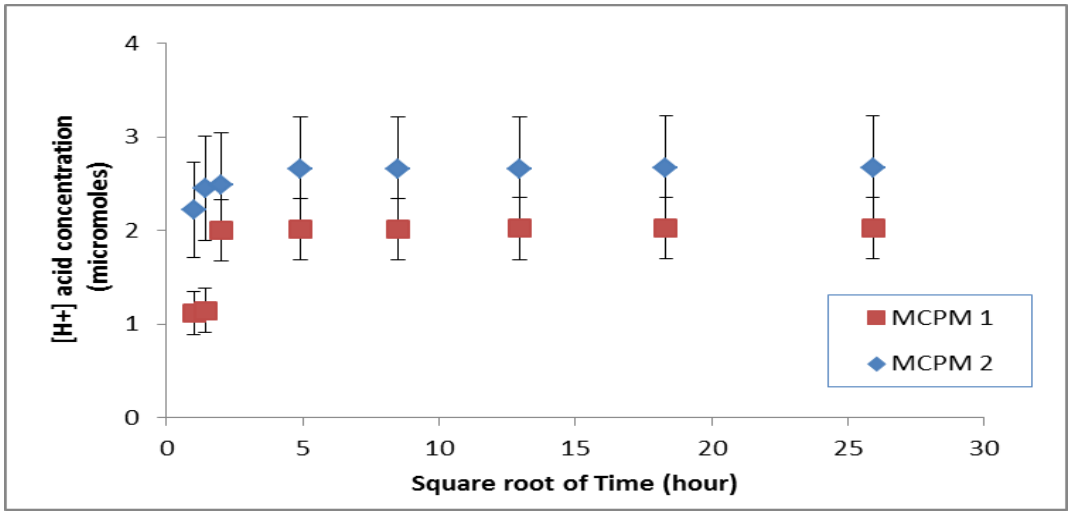

Figure 5-65: Cumulative acid released with MCPM 1 and MCPM 2 at different time point. Error bars shown are 95% CI (n = 5)

5.6.2 pH study for formulation with increase wt % of ε-polylysine (PLS)

Figure 5.66 shows the changes of storage solution pH with time and with increasing wt% of PLS. Error bars shown are 95% CI with n = 5. Overall all formulations were slightly acidic initially with pH ranges from 3.7 to 7.0.

Figure 5.67 shows the cumulative acid release with different wt % of PLS versus square root of time. Acid release with 10 to 30 wt % PLS was not significantly different from that with no PLS. Formulations with 40% and 50% PLS, however, did produce less acid.

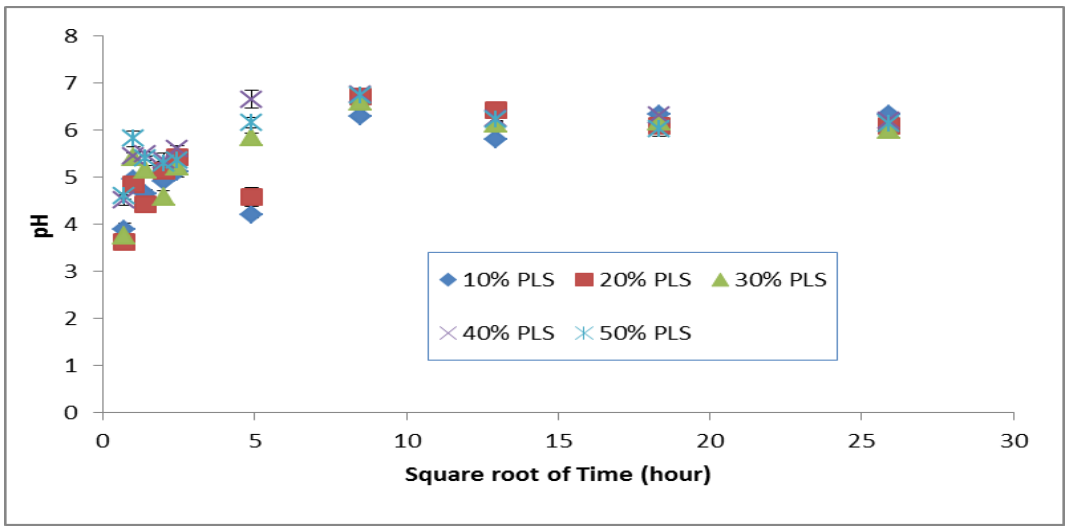

Figure 5-66: pH level for cements composition with increase wt % of PLS (MCPM 2 + β-TCP 34.0 micron + citric acid 800 mM + increase wt % of PLS).

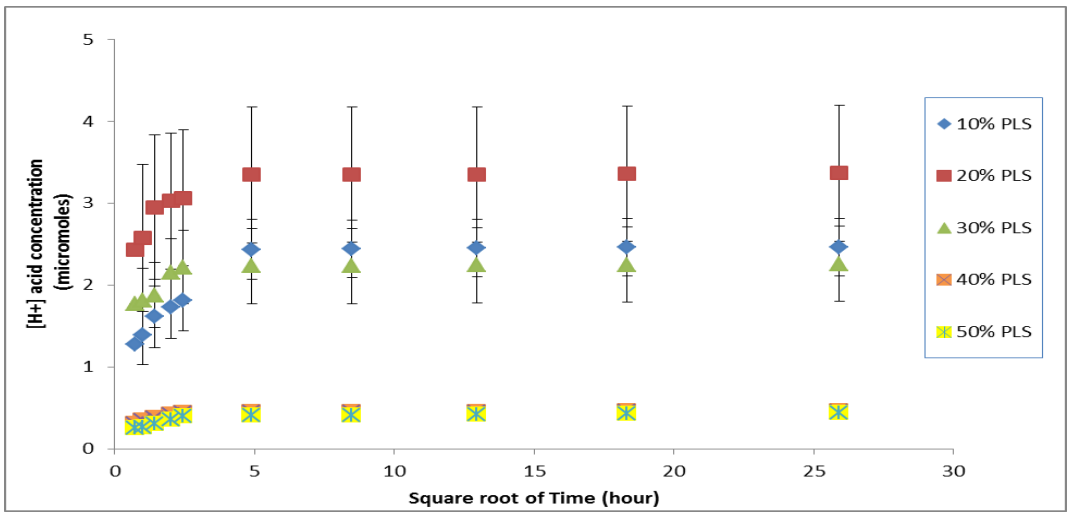

Figure 5-67: Cumulative acid released with increase wt % of PLS (MCPM 2 + β-TCP 34.0 micron + citric acid 800 mM + increase wt % of PLS).

5.7 ε-Polylysine release profile

5.7.1 Calibration curve of ε-polylysine

Table 5.10 shows the average absorbance due to the blue dye trypan blue after its reaction with increasing concentrations of ε-polylysine (PLS) from 1 ppm to 10 ppm. This dye has peak absorbance at 580 nm and upon reaction with PLS forms a precipitate that was removed by centrifugation. The calibration curve was obtained by plotting the absorbance at 580 nm against the various level of PLS concentration in aqueous solutions (Figure 5.68).

Table 5-10: The average absorbance of various concentration of ε-polylysine at 580 nm

Concentration of ε-polylysine (ppm)	Average absorbance at 580 nm (n=3)
1	0.18
2	0.36
4	0.51
5	0.73
7	0.78
9	0.85
10	0.96

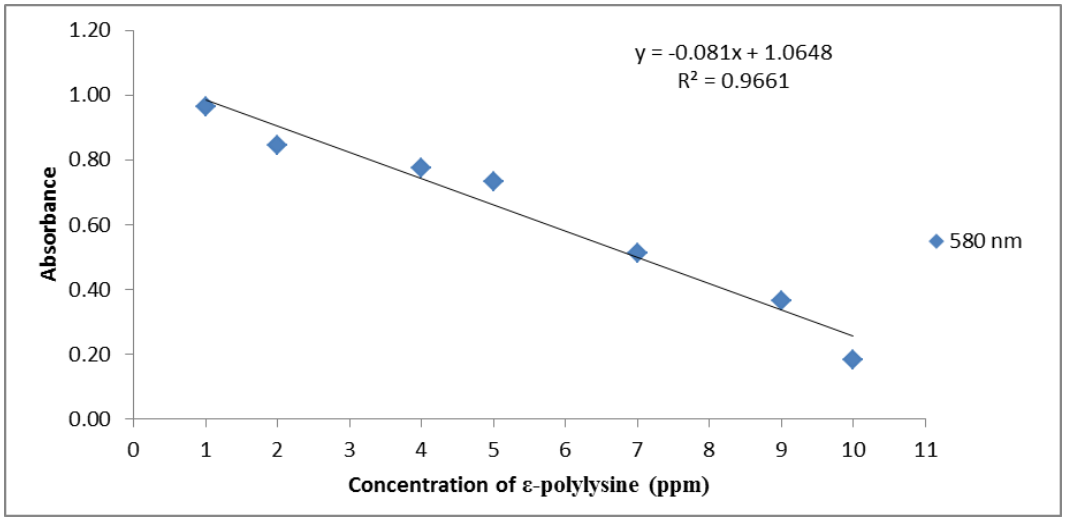

Figure 5-68: Calibration curve ε-polylysine at 580 nm (n=3).

5.7.2 ε-Polylysine release in water

Figure 5.69 shows the cumulative percentage of ε-polylysine (PLS) release rapidly reaches a maximum value in 24 hours. This release percentage is calculated according to equation 6 and 7. It shows that cement containing lower level of PLS has higher level of release. It decreases with increase wt % of PLS. Around 4 to 27 % total release was observed. Cement formulations with 10 wt % showed significant highest release of PLS compared to other formulation. The PLS percentage release dropped dramatically between formulations with 10 wt % of PLS to formulations with 20 wt % of PLS.

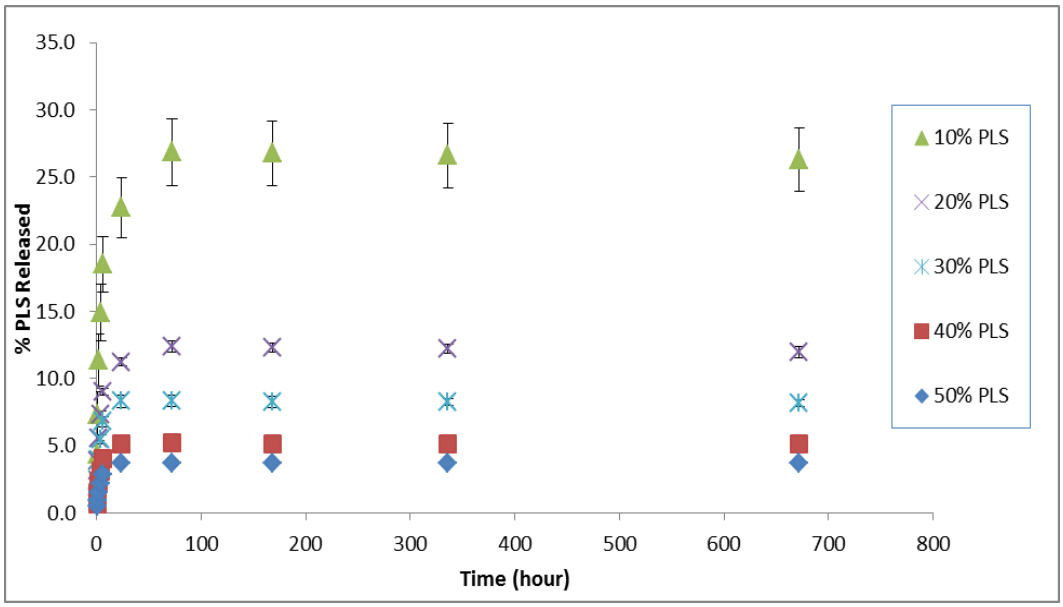

Figure 5-69: % of PLS released for cements composition with increase wt % of PLS (MCPM 2 + β-TCP 34.0 micron + citric acid 800 mM + increase wt % of PLS).

CHAPTER 6
DISCUSSION AND CONCLUSION

6 DISCUSSION

Brushite cements, one of the end products of CPC, have potential as drug carriers and bone filling materials. They can also act as a reservoir for calcium and phosphate ions for the remineralisation of hard tissues. However, their applications might be limited due to a number of issues including low strength, high modulus and brittle fracture. Brushite cements may also suffer from poorly controlled setting, degradation and drug release.

6.1 Mechanical properties of brushite cements

6.1.1 Biaxial flexural strength (BFS)

Strength is the ability of a material to resist deformation under load. The original brushite cement formulations had very poor mechanical properties and a number of approaches have been explored to address this. Early BFS ranged from 0.7 to 4.5 MPa (Bohner et al., 1996). Compressive strength has been reported to range from 1 to a maximum of 52 MPa (Gbureck et al., 2005; Hofmann et al., 2009). The highest 24 hour wet compressive strength obtained in the study of Hofmann et al. was obtained using CA at 800 mM, PLR 4:1, MCPM sieved below 63 micron and 11 micron TCP. Using similar powders and liquid but lower PLR (3.3:1) a recent study demonstrated a 24 hour wet flexural strength of 5 – 8 MPa. This increased up to 10 MPa with the addition of polyacrylic acid (Xia et al., 2014).

In this thesis the difference MCPMs used were much larger than those of Hofmann and Xia. The thesis showed that changing MCPM from powder to crystal – like did not provide any significant effect on the flexural strength. However, an increased in TCP particle sizes did provide a small but significant increase in flexural strength. The highest result for dry materials was 30.0 MPa with TCP particle size of 34 micron. This was much higher than previously observed by Hofmann and Xia and comparable to that of glass Ionomer cements (GIC) that have flexural strength between 20 MPa to 40 MPa (Xie et al., 2000). To optimize the powder to liquid ratio in the above thesis, brushite cements were prepared by using MCPM 2, TCP particle size 34 micron and increasing percentage of ε-polylysine (PLS). Our study showed that increasing the powder to liquid ratio from 3.3:1 to 4:1 increases the flexural strength.

This is due to lower porosity by increasing the PLR in cements, thereby helps to increase the mechanical properties (Hofmann et al., 2009). It is also observed that the strength declined slightly with increased percentage of PLS. FTIR result showed that increasing PLS changes chemistry and formed complex rather than brushite, thus reducing strength.

The BFS of wet samples was used to mimic what happens with time in a clinical environment. As water immersion can strongly affect mechanical properties (Charriére et al., 2001), dry strength alone may be misleading with regards to clinical performance (Barralet et al., 2004). Wet sample data showed that the strength does not depend on the level of PLS. One possible explanation might be due to the surrounding water providing more water for the formulation to complete its setting reaction. Even with the wet samples however, the flexural strength achieved was still high compared to the previous studies mentioned above, 18 MPa with the formulation without PLS and 14 MPa with 50 wt % of PLS. This new cement will be able to provide support where previously brushite cements would not be considered to be able to support any significant load. This will help to widen the application of brushite cements to more load bearing areas.

6.1.2 Biaxial flexural modulus (BFM)

Young's modulus is a measurement of stiffness of an elastic material. Flexural modulus was increased by increasing the β-TCP particle size with MCPM 2 but not with MCPM 1. Addition of higher percentage of PLS also resulted in decrease of the modulus. The decrease in modulus for the wet samples cements is statistically significant when compared to dry samples. Flexural modulus achieved from this study was 5 times higher for wet samples compared to a recent study (Xia et al., 2014). The strength is also 5-6 time higher. That means the new cements have similar strain at break to Xia's study. This could attribute to the denser crystals formed in this study.

6.1.3 Toughness

Toughness was determined by measuring the area underneath the stress-strain curve. Brushite cements are brittle materials. The toughness is therefore proportional to strength squared divided by modulus.

From this study it was concluded that there were no significant differences in the toughness either by changing MCPM and PLR or by adding increase wt % of PLS. Any decreases in strength were therefore compensated by decrease in modulus.

6.2 Setting kinetics

Brushite cement is precipitated through acid – base reaction with the presence of an aqueous phase. In MCPM and β-TCP system, brushite cements setting reaction begins by the dissolution of MCPM which causes a rapid decrease in pH followed by dissolution of β-TCP and uptake of hydrogen ions to precipitate more brushite crystal (Bohner and Gbureck, 2008, Mirtchi et al., 1989). The setting reaction of the original composition of brushite cements is very rapid, approximately 30 seconds which limits the time for manipulation and placement of the cement (Mirtchi et al., 1991). Adding any additive to brushite cement such as citric acid (Bohner et al., 2008) or tartaric acid (Alkhraisat et al., 2008a) can affect the dissolution of the reagent, precipitation of the brushite crystal or both thereby altering the setting reaction time. Another way to control the setting reaction of brushite cements is by manipulating powder to liquid ratio.

As the profile at 980 cm^{-1} reflects the forming of brushite cement as a function of time, so the value of absorbance will indicate the amount of brushite crystal formed. It is generally considered that the forming of brushite crystal is responsible for the setting of cement. Brushite formation was marked by formation of strong 980 cm^{-1} and sharpened O – H peaks in the final spectra. In this study, absorbance changes showed that the setting reaction was faster without the addition of citric acid. Citric acid had the capability to chelate the calcium ions and cause delays in precipitation of brushite crystal. Incorporation of citric acid therefore helps to prolong the setting time. This also helps to form a workable cement paste (Grases et al., 2000, Barralet et al., 2004).

From the FTIR we can see that an intermediate complex formed with the addition of citric acid. When this occurred, the 1050 cm^{-1} peak increased faster than the 980 cm^{-1} peak. The intermediate complex is also known as dicalcium citrate complex. Formation of an intermediate complex was due to interaction between negative charge citrate ions and positive charge calcium ions (Hofmann et al., 2006). The intermediate complex will later dissolve to allow precipitation of brushite crystals.

In this thesis the intermediate complex was observed more in the formulation with MCPM 1 and PLR 3.3:1. The intermediate peaks were observed at 1532 and 1420 cm^{-1} which is consistent with the formation of COO- symmetric and asymmetric stretching peak (Xia et al., 2014). Previous studies indicated that with higher PLR the dicalcium citrate complex was difficult to detect unless high concentration of citric acid greater than 1000 mM was used (Hofmann et al., 2006). This thesis also demonstrated, O – H peaks indicating water was bound into the composition. All final peaks were consistent with brushite cement (Hofmann et al., 2006). Therefore, addition of citric acid helps to delay the setting time but did not interfere with the formation of brushite cements.

PLR was then varied from 3.3:1 to 4:1. Formulations with PLR 4:1 reacted faster than 3.3:1. This was previously attributed to faster crystal precipitation (Hofmann et al., 2006). It also increased the maximum absorbance change presumably by increasing the amount of brushite in contact with the FTIR diamond. With higher PLR, more powder was available that provides more absorbance which indicates more brushite formation.

A major factor that affected the reaction profile was the type of MCPM. MCPM 1 showed very similar FTIR profile to that observed by Xia. The absorbance spectra were also very similar to those in the work by Hofmann (Xia et al., 2014, Hofmann et al., 2006). MCPM 1 which has a particle-like powder dissolved slowly, this helped to delay the setting time then provide a snap set. For formulations with MCPM 2, citric acid was not stopping the early reaction but did broaden the reaction. This showed that citric acid was able to delay the set but was not able to provide a snap set with MCPM 2 that had a crystalline structure. Varying MCPM had limited effect on maximum absorbance change suggesting final cements have similar brushite concentrations.

Upon increased percentage of PLS in the formulation, the absorbance was going down and the working time enhanced. The 980 cm^{-1} peak which indicated formation of brushite was decreasing. Adding PLS even at low levels demonstrated that the intermediate complex peak was readily detected by the FTIR and significantly higher when 50 wt % of PLS was used. The intermediate peak however was not strong in the formulation with PLS without citric acid. The intermediate complex form was stable and not dissolved over time unlike the dicalcium citrate complex.

The stability of such complex is probably attributed by both citric acid and larger molecular size of PLS. This indicates that PLS may become solid and interacts with the citric acid and formed a new intermediate phase. There may be possible ionic interactions which form the broad peaks at 1585 and 1500 – 1300. These would be consistent with the formation of NH^{+}_{3} (amine salt) symmetric and asymmetric stretching peaks. It is difficult, however, to distinguish these from the COO^{-} symmetric and asymmetric stretch peaks at 1460 – 1400 and 1610 – 1540.

The final spectra of all formulations with more than 20 wt % of PLS did not have characteristic water binding brushite peaks. This finding is similar to a previous study done with polyacrylic acid and chlorhexidine in brushite cements (Xia et al., 2014). Therefore incorporating PLS into the formulation does interfere with formation of brushite. The setting time was slowing down and the maximum absorbance was decreased with an increased percentage of PLS.

Another important factor regulating the setting time is the amount of water present in the cement paste. More water available for the setting reaction will favour a faster precipitation of brushite crystals hence accelerating the setting time. This is usually seen when cements with low PLR are used (Mirtchi AA et al., 1989, Alkhraisat MH et al., 2010, Tamimi-Marino F et al., 2007). However, our study shows that the setting rate not only depends on PLR, but also on the type of MCPM. Formulations with 50 wt % of PLS decreased the maximum absorbance. This could be because water is required to form the brushite cements and in this formulation, there was not enough water because PLS had replaced it. This explains the reason for reduction in the strength with cements that had same formulation. Also with this formulation, 50 wt % of citric acid had been removed and the setting time is expected to accelerate. The setting reaction however was slower with increased level of PLS suggesting that PLS may also act as a setting retardant.

6.3 Scanning electron microscopy (SEM)

In this study, the surface of brushite cements prepared with citric acid showed the characteristic of small needle-like crystal appearance. This is an expected finding as citric acid is known to decrease the crystal growth rate of brushite which results in smaller and thinner crystals (Bohner et al., 1996).

Smaller crystal sizes produced may result in reduced porosity of cement microstructure. SEM image of cements with MCPM 2 exhibit large cracks which had the same shape and dimension of the original MCPM 2 particles. The crystals formed in this crack were much larger indicating that slow dissolution of the larger MCPM particles may have happened in this region. MCPM dissolved into the water and precipitate away from the crack area. This crack was a new finding and had never been observed with any brushite cements before. The crack may help as a channel for PLS to be released.

By adding increase wt % of PLS into the formulations with MCPM 2, few changes were observed by SEM. This is possibly due to PLS acting as a setting retardant and causing a delay in the setting reaction and affecting the crystal precipitation in a similar manner to citric acid (Tamimi et al., 2008). Furthermore, cements prepared with MCPM 2 did not show any difference when either dry or wet samples were observed by SEM. This showed that high levels of PLS can be added without interfering with crystal formation and the cements produced will be stable in any surrounding environment. Only pores structure is different between MCPM 1 and MCPM 2. From the fracture surface, no large cracks were seen with cement produced by MCPM 1 as seen in the formulation with MCPM 2. Very large brushite crystal can be observed in the large cracks produced by MCPM 2.

Therefore further research should be done to assess the effect of wt % of PLS on crystal structure with MCPM 1 and if this also will improve other properties of brushite cements produced. From SEM image done in this study at both high and low magnifications, all formulations showed porosities on the fracture surface. Quantitave method such as porosity measurement with Archimedes principles could be carried out for accurate measurement of porosity (Matejicek et al., 2006).

6.4 Degradation

Initial, rapid decrease in mass for all cements composition had been observed. The same result was reported by previous study (Young et al., 2008). In this study, formulations prepared with MCPM 1 were shown to be degradable at a much lesser rate compared to cement prepared with MCPM 2. SEM results show that cement prepared with MCPM 2 has much more pores left by dissolving MCPM. This indicates that more MCPM 2 is dissolving than MCPM 1.

This also indicates that MCPM 1 can produce more uniformed cement. This may be an advantage because of the concern that brushite cements may disperse before they can set in clinical application. Therefore further study with MCPM 1 will be an interesting field for future work. However, more degradable cements produced with MPCM 2 promise more antimicrobial release.

Addition of PLS showed overall increase degradation for cements prepared with up to 40 wt % PLS. The degradation was less with 50 wt % of PLS. Mass loss was independent of drug content as expected from other work (Young et al., 2008). From this study, the continuity of total weight loss at the end of the study period suggest that both dissolution of brushite or complex and release of PLS.

6.5 ε-polylysine release study

ε-Polylysine (PLS) was added as an antibacterial agent to produce a new cement formulation with antimicrobial properties. Brushite is resorbable but the rate of drug release from the system is much higher than the rate of matrix degradation. There are various factors involved to determine the drug release kinetics from its carrier. These include microstructure of the carrier and degradation of the matrix. Other factors to consider are the interaction and bonding between the drugs and the matrix which holds it (Ginebra et al., 2006a). Previous studies showed 2 % to 9 wt % of chlorhexidine could be incorporated into a brushite cement system (Hofmann et al., 2008, Young et al., 2008). These formulations released all their antibacterial within a few days.

Our study showed that when 50 wt % of PLS was added into the aqueous phase of the brushite cement there were significant effects on setting chemistry. 50 wt % PLS corresponds with 10 wt % of the total with PLR 4:1. Much less than 30% of the drug was released, however, in a few days. Drug release can be controlled by reducing the porosity (Bohner et al., 1997a, Hofmann et al., 2009, Tamimi et al., 2008). From the FTIR studies, however, it is more likely that slow PLS release is a result of stronger interactions between the brushite cement and drug particularly as it increasingly replaces the citric acid retardant.

There was a critical point between 20 and 30 wt % PLS. This is interesting because there will be equal number of moles acidic (3 per molecule of citric acid) and lysine (1 per mole of lysine) reactive groups at 26 wt %.

Before this concentration acid release is approximately constant. After this point, both acid release and PLS release are very low. Additionally, brushite no longer forms and absorbance profile was very different. Burst release of antimicrobial agents often occurs at an early time followed by a longer duration of persistent but reduced release. In this study, the high initial release of PLS was noticed in the first hours of soaking them in water. This early diffusion could have an effect on the microorganisms and colonization particularly if these drugs were entrapped inside the injected area or in gaps between the tooth and restoration.

Between 75 – 95 wt % of PLS load in the cements was not released during the release study. The PLS release below 30% PLS was approximately proportional to level in the cement indicating that the same amount of PLS is being released irrespective of its concentration in the formulation. At later times PLS release and degradation *in vitro* were both very slow. Brushite cements can degrade more rapidly *in vivo* than *in vitro* due to the action of cells and enzymes from the body (Constantz et al., 1998, Grover at al., 2003). Therefore the degradation of brushite cements *in vivo* would be expected to lead to faster release of PLS.

6.6 Conclusion

This study firstly focused on assessing the effect of different monocalcium phosphate monohydrate (MCPM) and β -tricalcium phosphate (β-TCP) particle sizes on brushite cement formation.

Afterwards, the effects of varying the powder to liquid ratio (PLR) and concentration of ε-polylysine (PLS) on brushite cements was assessed. The following conclusions can be drawn from this study.

6.6.1 Mechanical properties

The largest particle size of (34 micron) produced the highest flexural strength of 32.5 MPa at PLR 4 to 1. The handling of brushite cements is better with MCPM 2 (Sigma) that has crystalline shape. Strength of brushite cements can be decreased by decreasing the β-TCP particle sizes and PLR. Decreasing the level of PLS helps to produced higher strength cements.

Placement of set cements in water will result in decreased in strength down to 14 MPa. Increase in biaxial flexural strength overall lead to increase in biaxial flexural modulus. On average, there is slightly increased in biaxial modulus by increasing PLR but increased the wt % of PLS does not had any significant effect on modulus. Cement toughness however does not depend with any factor, either different MCPM, PLR or level wt % of PLS.

6.6.2 Setting kinetic

High levels of PLS can be added with only minor reduction in the strength but it does significantly delayed the setting time and reduced the brushite cement formation.

6.6.3 Microstructure of the cement

Adding high level of PLS does not interfere with crystal formation within the brushite cement. Cements prepared with MCPM 2 do not showed any obvious difference by adding citric acid or adding increase wt % level of PLS. The crystal formed also did not changed either in dry condition or placement of the samples in water.

6.6.4 Cement degradation

Set cements with MCPM 1 are less degraded. Incorporation of PLS into the composition with MCPM 2 resulted in more degradation except for formulation with 50 wt % of PLS.

6.6.5 pH and drug release study

pH study showed that acid released took place within 1 week and stabilised afterwards. Up to 30% of PLS was released within 1 month. Remaining PLS is still bound within the cements.

6.7 Summary

Brushite cements has a great potential in dental application and as bone substitute may offer clinicians the opportunity of preserving alveolar bone. The combination of self – setting nature, mouldability, injectability, biocompatibility, bioresorbable, has the osteoconductive properties and remineralising antibacterial effect suggests a great potential of brushite cements in regenerative therapy. The findings of this research demonstrated that brushite cements produced with MCPM 2 which has crystalline shape, β-TCP 34 micron and citric acid 800 mM produced the highest dry and wet flexural strength of 32 MPa and 14 MPa respectively. Very high levels of PLS could be introduced into brushite cements without serious detrimental effects on mechanical properties. PLS, however, did delay the setting time and altered the final chemistry and microstructure of the dicalcium phosphate product.

CHAPTER 7
FUTURE WORK

7 FUTURE WORK

7.1 Investigate effect of MCPM Himed

Mechanical test study showed that MCPM Himed produced BFS with β-TCP size 34 micron of 28.5 MPa and comparable to MCPM Sigma that gave 30.0 MPa. Setting kinetic result showed that citric acid (CA) readily interacted with the powder type of MCPM Himed and was able to delay the setting time. Mass study showed that brushite cements produced were more stable. Therefore, it is interesting to know whether by using MCPM from Himed with addition of ε-polylysine (PLS) will improve properties of brushite cements better than MCPM from Sigma.

7.2 Investigate effect of Strontium

Strontium can replace calcium to some extent in various biochemical processes in the body, including replacing small proportions of the calcium in hydroxyapatite crystals of calcified tissues such as bones and teeth. Strontium is believed to impart additional strength to these calcified tissues and draw extra calcium into the bones. Studies have showed that administering strontium results in reduction of cavities incidence (Lippert, 2012, Koletsi-Kounari et al., 2012). To extend the above work in this thesis, new formulation was design by using Sr. The initial aim was to keep the moles and PLR constant. However, the powder phase failed to mix with the liquid phase indicating inadequate liquid available to produce set cements. Further study will need to be modified by lowering PLR to assess the effect of Sr into the formulation with the same method as had been done in this thesis.

7.3 Cohesion study

Study has reported data suggesting thrombosis can possibly be due to the released of calcium phosphate particles in the blood stream (Bohner et al., 2006). Therefore, it is important to improve the cements paste resistance to disintegration upon early contact with blood or other fluids. From this thesis it was observed that by increasing the PLR from 3.3:1 to 4:1, the brushite cements paste become less viscous indicating increase in cohesion. Cohesion had been observed to improve by adding increase level of PLS into the formulation. Three methods to determine cohesion had been suggested including visual inspection, measurement of geometrical size of the cement and a setting time test (Gilmore needle).

7.4 Cement adhesion to dentine and bone

Adhesion between the brushite cements and the tooth or bone is very important. Therefore, it is interesting to know whether the presence of PLS in the composition will improve the bonding capability. The potential chemical bonding capability from PLS might increase adhesive properties of the brushite cements. Adhesion properties of PLS could be assessed through a push out test.

7.5 Antibacterial study

This study has shown that PLS was released over a period of time. Therefore, it is important to understand if interaction between CA and PLS or the concentration of PLS is adequate for minimum inhibitory concentration required to exert an antibacterial activity. Subsequently effectiveness of antibacterial effect of PLS should be studied using various microbiology techniques (e.g MIC and agar diffusion test).

7.6 Cement injectibility

It is important to have good cement injectability particularly for minimal invasive surgical procedures that required injection of the cements into the bone defect (Baroud et al., 2005). During the injection process, the liquid to powder ratios should not change in order to be capable for injectability but many brushite cements were found to suffer from phase separation during injection thus making it hard for them to be injected. Development of injectable brushite cements with PLS releasing properties offers a quick and easy placement method for this material. From this study it had been showed that adding PLS can help to produce paste like cements. However, further study needs to be carried out to determine the injectability of the compositions used above.

7.7 Final composition of the cements

Further studies needs to be done using Raman to analyse final composition of the cements. Raman mapping is a technique for generating detailed chemical images based on a sample's Raman spectra. These spectra can then be used to generate images showing location and amount of different species.

7.8 Cement porosity

It has been shown that the mechanical performance of brushite cements is inversely correlated to its porosity. In addition, less porous cements have been shown to regulate better drug release (Hofmann et al., 2009). This study only provided a qualitative assessment of the cements microstructure with the SEM images. However, further studies need to be done as a quantitave analysis of cements porosity and to understand the effect of PLS on the microstructure and drug release properties.

7.9 Adding polyacrylic acid

Previous study by Mohd Razi (Xia et al., 2014) showed that polyacrylic acid (PAA) addition helped to slow down (possibly overly) the release kinetics of chlorhexidine and increase the flexural strength. The drug release kinetics was affected by addition of polymer to the composition. Hence, it is very interesting to observe the interaction of PAA with calcium phosphate and PLS.

7.10 Comparison to commercial product

Further studies need to be carried out to compare the modified brushite cements with other commercial brushite cements. Currently, brushite cements have been studied to be used as reinforcements of osteosynthesis screw. However, the current brushite cements still have poor mechanical properties, no or limited antimicrobial effect and short working time. Therefore, it is essential to investigate the above modified cements and assess whether it has properties comparable or better than available product.

7.11 *In vivo* assessment of brushite cements

Post – extraction, alveolar bone remodelling often results in aesthetic compromises in the area of tooth extraction due to alveolar ridge resorption. Techniques to preserve natural bone and soft tissue contours are of great interest to clinicians. Therefore, the above antibacterial releasing brushite cements offer possible bone substitute following tooth extraction. Ultimately, the final modified brushite cements formulation should be examined *in vivo*.

CHAPTER 8
REFERENCE

8 REFERENCES

ABERG, J., BRISBY, H., HENRIKSSON, H. B., LINDAHL, A., THOMSEN, P. & ENGQVIST, H. 2010. Premixed acidic calcium phosphate cement: characterization of strength and microstructure. *J Biomed Mater Res B Appl Biomater,* 93**,** 436-41.

ADAM LP & RJC, W. 1985. A photomicrogrammatic method for monitoring changes in the residual alveolar ridge form. *J Oral Rehabil* 443-50.

AHN, J., CHOI, J., JOO, C. H., SEO, I., KIM, D., YOON, S. Y., KIM, Y. K. & LEE, H. 2004. Susceptibility of mouse primary cortical neuronal cells to coxsackievirus B. *J Gen Virol,* 85**,** 1555-64.

ALKHRAISAT, M. H., MARINO, F. T., RETAMA, J. R., JEREZ, L. B. & LOPEZ-CABARCOS, E. 2008a. Beta-tricalcium phosphate release from brushite cement surface. *J Biomed Mater Res A,* 84**,** 710-7.

ALKHRAISAT, M. H., MARINO, F. T., RODRIGUEZ, C. R., JEREZ, L. B. & CABARCOS, E. L. 2008b. Combined effect of strontium and pyrophosphate on the properties of brushite cements. *Acta Biomater,* 4**,** 664-70.

ALKHRAISAT, M. H., RUEDA, C., CABREJOS-AZAMA, J., LUCAS-APARICIO, J., MARINO, F. T., TORRES GARCIA-DENCHE, J., JEREZ, L. B., GBURECK, U. & CABARCOS, E. L. 2010. Loading and release of doxycycline hyclate from strontium-substituted calcium phosphate cement. *Acta Biomater,* 6**,** 1522-8.

ALKHRAISAT, M. H., RUEDA, C., MARINO, F. T., TORRES, J., JEREZ, L. B., GBURECK, U. & CABARCOS, E. L. 2009. The effect of hyaluronic acid on brushite cement cohesion. *Acta Biomater,* 5**,** 3150-6.

AMBARD, A. J. & MUENINGHOFF, L. 2006. Calcium phosphate cement: review of mechanical and biological properties. *J Prosthodont,* 15**,** 321-8.

AMLER, M. H. 1969. The time sequence of tissue regeneration in human extraction wounds. *Oral Surg Oral Med Oral Pathol,* 27**,** 309-18.

ANDRESEN, J., ANDREASEN, F. M. & ANDERSSON, L. (eds.) 2007. *Textbook and color atlas of traumatic injuries to the teeth,* Copenhagen: Oxford: Blackwell Munksgaard.

ARAUJO, M. G. & LINDHE, J. 2009. Ridge preservation with the use of Bio-Oss collagen: A 6-month study in the dog. *Clin Oral Implants Res,* 20**,** 433-40.

ARTZI, Z., TAL, H. & DAYAN, D. 2000. Porous bovine bone mineral in healing of human extraction sockets. Part 1: histomorphometric evaluations at 9 months. *J Periodontol,* 71**,** 1015-23.

ASFTA, M. 1999. *Standard specification for acrylic bone cement, ASTM F451- 99a.,* West Conshohocken, PA, ASTM International.

ATWOOD, D. A. 1973. Reduction of residual ridges in the partially edentulous patient. *Dent Clin North Am,* 17**,** 747-54.

BAROUD, G., CAYER, E. & BOHNER, M. 2005. Rheological characterization of concentrated aqueous beta-tricalcium phosphate suspensions: the effect of liquid-to-powder ratio, milling time, and additives. *Acta Biomater,* 1**,** 357-63.

BARRALET, J. E., GROVER, L. M. & GBURECK, U. 2004. Ionic modification of calcium phosphate cement viscosity. Part II: hypodermic injection and strength improvement of brushite cement. *Biomaterials,* 25**,** 2197-203.

BATH, B.-M. & FEHRENBACH, M. J. (eds.) 2006. *Dental embryology, histology and anatomy*: Elsevier Saunders.

BELKOFF, S. M. & MOLLOY, S. 2003. Temperature measurement during polymerization of polymethylmethacrylate cement used for vertebroplasty. *Spine (Phila Pa 1976),* 28**,** 1555-9.

BERLEMANN, U., FERGUSON, S. J., NOLTE, L. P. & HEINI, P. F. 2002. Adjacent vertebral failure after vertebroplasty. A biomechanical investigation. *J Bone Joint Surg Br,* 84**,** 748-52.

BOANINIA, E., GAZZANOB, M. & BIGIA, A. 2009. Ionic substitutions in calcium phosphates synthesized at low temperature. *Acta Biomaterialia,* 6**,** 1882–1894.

BODIC, F., HAMEL, L., LEROUXEL, E., BASLE, M. F. & CHAPPARD, D. 2005. Bone loss and teeth. *Joint Bone Spine,* 72**,** 215-21.

BOHNER M, LEMAITRE J & TA, R. 1996. Effects of sulfate, pyrophosphate, and citrate ions on the physicochemical properties of cements made of beta-tricalcium phosphate-phosphoric acid-water mixtures. . *J Am Ceram Soc* 1427-34.

BOHNER, M., DOEBELIN, N. & BAROUD, G. 2006. Theoretical and experimental approach to test the cohesion of calcium phosphate pastes. *Eur Cell Mater,* 12**,** 26-35.

BOHNER, M. & GBURECK, U. 2008. Thermal reactions of brushite cements. *J Biomed Mater Res B Appl Biomater,* 84**,** 375-85.

BOHNER, M., GBURECK, U. & BARRALET, J. E. 2005. Technological issues for the development of more efficient calcium phosphate bone cements: a critical assessment. *Biomaterials,* 26**,** 6423-9.

BOHNER, M., LEMAITRE, J., VAN LANDUYT, P., ZAMBELLI, P. Y., MERKLE, H. P. & GANDER, B. 1997a. Gentamicin-loaded hydraulic calcium phosphate bone cement as antibiotic delivery system. *J Pharm Sci,* 86**,** 565-72.

BOHNER, M., MERKLE, H. P., LANDUYT, P. V., TROPHARDY, G. & LEMAITRE, J. 2000a. Effect of several additives and their admixtures on the physico-chemical properties of a calcium phosphate cement. *J Mater Sci Mater Med,* 11**,** 111-6.

BOHNER, M., MERKLE, H. P. & LEMAITRE, J. 2000b. In vitro aging of a calcium phosphate cement. *J Mater Sci Mater Med,* 11**,** 155-62.

BOHNER, M., VAN LANDUYT, P., MERKLE, H. P. & LEMAITRE, J. 1997b. Composition effects on the pH of a hydraulic calcium phosphate cement. *J Mater Sci Mater Med,* 8**,** 675-81.

BRESCIANI, E., BARATA TDE, J., FAGUNDES, T. C., ADACHI, A., TERRIN, M. M. & NAVARRO, M. F. 2004. Compressive and diametral tensile strength of glass ionomer cements. *J Appl Oral Sci,* 12**,** 344-8.

CAI, S., ZHAI, Y., XU, G., LU, S., ZHOU, W. & YE, X. 2011. Preparation and properties of calcium phosphate cements incorporated gelatin microspheres and calcium sulfate dihydrate as controlled local drug delivery system. *Journal of Materials Science: Materials in Medicine,* 22.

CALISKAN, M. K. & TURKUN, M. 1995. Clinical investigation of traumatic injuries of permanent incisors in Izmir, Turkey. *Endod Dent Traumatol,* 11**,** 210-3.

CAMA, G., BARBERIS, F., BOTTER, R., CIRILLO, P., CAPURRO, M., QUARTO, R., SCAGLIONE, S., FINOCCHIO, E., MUSSI, V. & VALBUSA, U. 2009. Preparation and properties of macroporous brushite bone cements. *Acta Biomater,* 5**,** 2161-8.

CAMELO, M., NEVINS, M. L., SCHENK, R. K., SIMION, M., RASPERINI, G., LYNCH, S. E. & NEVINS, M. 1998. Clinical, radiographic, and histologic evaluation of human periodontal defects treated with Bio-Oss and Bio-Gide. *Int J Periodontics Restorative Dent,* 18**,** 321-31.

CARLSSON, G. E. & PERSSON, G. 1967. Morphologic changes of the mandible after extraction and wearing of dentures. A longitudinal, clinical, and x-ray cephalometric study covering 5 years. *Odontol Revy,* 18**,** 27-54.

CARMAGNOLA, D., ADRIAENS, P. & BERGLUNDH, T. 2003. Healing of human extraction sockets filled with Bio-Oss. *Clin Oral Implants Res,* 14**,** 137-43.

CAWOOD, J. I. & HOWELL, R. A. 1988. A classification of the edentulous jaws. *Int J Oral Maxillofac Surg,* 17**,** 232-6.

CHERNG, A., TAKAGI, S. & CHOW, L. C. 1997. Effects of hydroxypropyl methylcellulose and other gelling agents on the handling properties of calcium phosphate cement. *J Biomed Mater Res,* 35**,** 273-7.

CHUNG, S. M., YAP, A. U., CHANDRA, S. P. & LIM, C. T. 2004. Flexural strength of dental composite restoratives: comparison of biaxial and three-point bending test. *J Biomed Mater Res B Appl Biomater,* 71**,** 278-83.

CONSTANTZ, B. R., BARR, B. M., ISON, I. C., FULMER, M. T., BAKER, J., MCKINNEY, L., GOODMAN, S. B., GUNASEKAREN, S., DELANEY, D. C., ROSS, J. & POSER, R. D. 1998. Histological, chemical, and crystallographic analysis of four calcium phosphate cements in different rabbit osseous sites. *J Biomed Mater Res,* 43**,** 451-61.

COSTANTINO, P. D. & FRIEDMAN, C. D. 1994. Synthetic bone graft substitutes. *Otolaryngol Clin North Am,* 27**,** 1037-74.

CYPHER, T. J. & GROSSMAN, J. P. 1996. Biological principles of bone graft healing. *J Foot Ankle Surg,* 35**,** 413-7.

DAY, P. F., KINDELAN, S. A., SPENCER, J. R., KINDELAN, J. D. & DUGGAL, M. S. 2008. Dental trauma: part 2. Managing poor prognosis anterior teeth--treatment options for the subsequent space in a growing patient. *J Orthod,* 35**,** 143-55.

DE LA RIVA, B., SANCHEZ, E., HERNANDEZ, A., REYES, R., TAMIMI, F., LOPEZ-CABARCOS, E., DELGADO, A. & EVORA, C. 2009. Local controlled release of VEGF and PDGF from a combined brushite-chitosan system enhances bone regeneration. *J Control Release,* 143**,** 45-52.

DESAI, S. & CHANDLER, N. 2009. Calcium hydroxide-based root canal sealers: a review. *J Endod,* 35**,** 475-80.

DOROZHKIN, S. 2008. calcium orthophosphate cements for biomedical application. *Journal of materials science,* 43.

FIALKOV, J. A., HOLY, C., FORREST, C. R., PHILLIPS, J. H. & ANTONYSHYN, O. M. 2001. Postoperative infections in craniofacial reconstructive procedures. *J Craniofac Surg,* 12**,** 362-8.

FICKL, S., ZUHR, O., WACHTEL, H., STAPPERT, C. F., STEIN, J. M. & HURZELER, M. B. 2008. Dimensional changes of the alveolar ridge contour after different socket preservation techniques. *J Clin Periodontol,* 35**,** 906-13.

FILIPPI, A., POHL, Y. & VON ARX, T. 2001. Decoronation of an ankylosed tooth for preservation of alveolar bone prior to implant placement. *Dent Traumatol,* 17**,** 93-5.

FLAUTRE, B., LEMAITRE, J., MAYNOU, C., VAN LANDUYT, P. & HARDOUIN, P. 2003. Influence of polymeric additives on the biological properties of brushite cements: an experimental study in rabbit. *J Biomed Mater Res A,* 66**,** 214-23.

FORSBERG, C. M. & TEDESTAM, G. 1990. Traumatic injuries to teeth in Swedish children living in an urban area. *Swed Dent J,* 14**,** 115-22.

FRAYSSINET, P., GINESTE, L. & ROUQUET, N. 1998. [Osseointegration of 2 different types of calcium phosphate materials: ceramics and ionic cements]. *Morphologie,* 82**,** 3-7.

FRAYSSINET, P., ROUDIER, M., LERCH, A., CEOLIN, J. L., DEPRES, E. & ROUQUET, N. 2000. Tissue reaction against a self-setting calcium phosphate cement set in bone or outside the organism. *J Mater Sci Mater Med,* 11**,** 811-5.

FUKUTOME, A., M, K. & AIUCHI, M. 1995. A combined chronic toxicity and carcinogenicity study of polylysine powder in rats by peroral dietary administration. Clinical report.

GALEA, H. 1984. An investigation of dental injuries treated in an acute care general hospital. *J Am Dent Assoc,* 109**,** 434-8.

GBURECK, U., DEMBSKI, S., THULL, R. & BARRALET, J. E. 2005. Factors influencing calcium phosphate cement shelf-life. *Biomaterials,* 26**,** 3691-7.

GINEBRA, M. P., ESPANOL, M., MONTUFAR, E. B., PEREZ, R. A. & MESTRES, G. 2010. New processing approaches in calcium phosphate cements and their applications in regenerative medicine. *Acta Biomater,* 6**,** 2863-73.

GINEBRA, M. P., TRAYKOVA, T. & PLANELL, J. A. 2006a. Calcium phosphate cements as bone drug delivery systems: a review. *J Control Release,* 113**,** 102-10.

GINEBRA, M. P., TRAYKOVA, T. & PLANELL, J. A. 2006b. Calcium phosphate cements: competitive drug carriers for the musculoskeletal system? *Biomaterials,* 27**,** 2171-7.

GIOCONDI, J. L., EL-DASHER, B. S., NANCOLLAS, G. H. & ORME, C. A. 2010. Molecular mechanisms of crystallization impacting calcium phosphate cements. *Philos Trans A Math Phys Eng Sci,* 368**,** 1937-61.

GRASES, F., RAMIS, M. & COSTA-BAUZA, A. 2000. Effects of phytate and pyrophosphate on brushite and hydroxyapatite crystallization. Comparison with the action of other polyphosphates. *Urol Res,* 28**,** 136-40.

GROSS, U., SCHMITZ, H. J. & STRUNZ, V. 1988. Surface activities of bioactive glass, aluminum oxide, and titanium in a living environment. *Ann N Y Acad Sci,* 523**,** 211-26.

GROSSARDT, C., EWALD, A., GROVER, L. M., BARRALET, J. E. & GBURECK, U. 2010. Passive and active in vitro resorption of calcium and magnesium phosphate cements by osteoclastic cells. *Tissue Eng Part A,* 16**,** 3687-95.

GROVER, L. M., GBURECK, U., WRIGHT, A. J., TREMAYNE, M. & BARRALET, J. E. 2006. Biologically mediated resorption of brushite cement in vitro. *Biomaterials,* 27**,** 2178-85.

GROVER, L. M., HOFMANN, M. P., GBURECK, U., KUMARASAMI, B. & BARRALET, J. E. 2008. Frozen delivery of brushite calcium phosphate cements. *Acta Biomater,* 4**,** 1916-23.

GROVER, L. M., KNOWLES, J. C., FLEMING, G. J. & BARRALET, J. E. 2003. In vitro ageing of brushite calcium phosphate cement. *Biomaterials,* 24**,** 4133-41.

GUO, F. & LI, B. [Effects of collagen on the properties of TTCP/MCPM bone cement]. 2010. *Sheng Wu Yi Xue Gong Cheng Xue Za Zhi,* 27**,** 328-31.

HABIB, M., BAROUD, G., GITZHOFER, F. & BOHNER, M. 2008. Mechanisms underlying the limited injectability of hydraulic calcium phosphate paste. *Acta Biomater,* 4**,** 1465-71.

HABIBOVIC, P., GBURECK, U., DOILLON, C. J., BASSETT, D. C., VAN BLITTERSWIJK, C. A. & BARRALET, J. E. 2008. Osteoconduction and osteoinduction of low-temperature 3D printed bioceramic implants. *Biomaterials,* 29**,** 944-53.

HAMANO, Y. 2011. Occurrence, biosynthesis, biodegradation, and industrial and medical applications of a naturally occurring epsilon-poly-L-lysine. *Biosci Biotechnol Biochem,* 75**,** 1226-33.

HAMANO, Y., NICCHU, I., SHIMIZU, T., ONJI, Y., HIRAKI, J. & TAKAGI, H. 2007. epsilon-Poly-L: -lysine producer, Streptomyces albulus, has feedback-inhibition resistant aspartokinase. *Appl Microbiol Biotechnol,* 76**,** 873-82.

HAN, B., MA, P. W., ZHANG, L. L., YIN, Y. J., YAO, K. D., ZHANG, F. J., ZHANG, Y. D., LI, X. L. & NIE, W. 2009. beta-TCP/MCPM-based premixed calcium phosphate cements. *Acta Biomater,* 5**,** 3165-77.

HASSAN, S. M., MOBARAK, E. H. & FAWZI, E. M. 2008. The efficacy of different regimens of chlorhexidine as an antimicrobial agent for a group of egyptians. *J Egypt Public Health Assoc,* 83**,** 435-50.

HEASMAN, P. A., HEASMAN, L., STACEY, F. & MCCRACKEN, G. I. 2001. Local delivery of chlorhexidine gluconate (PerioChip) in periodontal maintenance patients. *J Clin Periodontol,* 28**,** 90-5.

HEINI, P. F., BERLEMANN, U., KAUFMANN, M., LIPPUNER, K., FANKHAUSER, C. & VAN LANDUYT, P. 2001. Augmentation of mechanical properties in osteoporotic vertebral

bones--a biomechanical investigation of vertebroplasty efficacy with different bone cements. *Eur Spine J,* 10**,** 164-71.

HIGGS, W. A., LUCKSANASOMBOOL, P., HIGGS, R. J. & SWAIN, M. V. 2001. A simple method of determining the modulus of orthopedic bone cement. *J Biomed Mater Res,* 58**,** 188-95.

HIRAKI, J., ICHIKAWA, T., NINOMIYA, S., SEKI, H., UOHAMA, K., SEKI, H., KIMURA, S., YANAGIMOTO, Y. & BARNETT, J. W., JR. 2003. Use of ADME studies to confirm the safety of epsilon-polylysine as a preservative in food. *Regul Toxicol Pharmacol,* 37**,** 328-40.

HOFMANN, M. P., ANNE M. YOUNG, UWE GBURECK, NAZHA, S. N. & BARRALET, J. E. 2006a. FTIR-monitoring of a fast setting brushite bone cement: effect of intermediate phases. *Journal of Materials Chemistry***,** 3199-3206.

HOFMANN, M. P., MOHAMMED, A. R., PERRIE, Y., GBURECK, U. & BARRALET, J. E. 2009. High-strength resorbable brushite bone cement with controlled drug-releasing capabilities. *Acta Biomater,* 5**,** 43-9.

HOFMANN, M. P., NAZHAT, S. N., GBURECK, U. & BARRALET, J. E. 2006b. Real-time monitoring of the setting reaction of brushite-forming cement using isothermal differential scanning calorimetry. *J Biomed Mater Res B Appl Biomater,* 79**,** 360-4.

HOU, C. H., CHEN, C. W., HOU, S. M., LI, Y. T. & LIN, F. H. 2009. The fabrication and characterization of dicalcium phosphate dihydrate-modified magnetic nanoparticles and their performance in hyperthermia processes in vitro. *Biomaterials,* 30**,** 4700-7.

HOUMARD, M., FU, Q., GENET, M., SAIZ, E. & TOMSIA, A. P. 2013. On the structural, mechanical, and biodegradation properties of HA/beta-TCP robocast scaffolds. *J Biomed Mater Res B Appl Biomater,* 101**,** 1233-42.

HUAN, Z. & CHANG, J. 2009. Novel bioactive composite bone cements based on the beta-tricalcium phosphate-monocalcium phosphate monohydrate composite cement system. *Acta Biomater,* 5**,** 1253-64.

IKENAGA, M., HARDOUIN, P., LEMAITRE, J., ANDRIANJATOVO, H. & FLAUTRE, B. 1998. Biomechanical characterization of a biodegradable calcium phosphate hydraulic cement: a comparison with porous biphasic calcium phosphate ceramics. *J Biomed Mater Res,* 40**,** 139-44.

IMAI, Y. & ISHIKAWA, M. 1997. New initiator system for bonding to dentin using methylcyclohexanedione. *Dent Mater J,* 16**,** 31-9.

JEFFCOAT, M. K. 1993. Bone loss in the oral cavity. *J Bone Miner Res,* 8 Suppl 2**,** S467-73.

JIANG, P. J., PATEL, S., GBURECK, U., CALEY, R. & GROVER, L. M. 2009. Comparing the efficacy of three bioceramic matrices for the release of vancomycin hydrochloride. *J Biomed Mater Res B Appl Biomater,* 93**,** 51-8.

KAHAR, P., IWATA, T., HIRAKI, J., PARK, E. Y. & OKABE, M. 2001. Enhancement of epsilon-polylysine production by Streptomyces albulus strain 410 using pH control. *J Biosci Bioeng,* 91**,** 190-4.

KANIA, M. J., KEELING, S. D., MCGORRAY, S. P., WHEELER, T. T. & KING, G. J. 1996. Risk factors associated with incisor injury in elementary school children. *Angle Orthod,* 66**,** 423-32.

KAWAI, T., KUBOTA, T., HIRAKI, J. & IZUMI, Y. 2003. Biosynthesis of epsilon-poly-L-lysine in a cell-free system of Streptomyces albulus. *Biochem Biophys Res Commun,* 311**,** 635-40.

KHAIROUN, I., DRIESSENS, F. C., BOLTONG, M. G., PLANELL, J. A. & WENZ, R. 1999. Addition of cohesion promotors to calcium phosphate cements. *Biomaterials,* 20**,** 393-8.

KINNUNEN, I., AITASALO, K., POLLONEN, M. & VARPULA, M. 2000. Reconstruction of orbital floor fractures using bioactive glass. *J Craniomaxillofac Surg,* 28**,** 229-34.

KITO, M., ONJI, Y., YOSHIDA, T. & NAGASAWA, T. 2002. Occurrence of epsilon-poly-L-lysine-degrading enzyme in epsilon-poly-L-lysine-tolerant Sphingobacterium multivorum OJ10: purification and characterization. *FEMS Microbiol Lett,* 207**,** 147-51.

KLAMMERT, U., REUTHER, T., JAHN, C., KRASKI, B., KUBLER, A. C. & GBURECK, U. 2009. Cytocompatibility of brushite and monetite cell culture scaffolds made by three-dimensional powder printing. *Acta Biomater,* 5**,** 727-34.

KOLETSI-KOUNARI, H., MAMAI-HOMATA, E. & DIAMANTI, I. 2012. An in vitro study of the effect of aluminum and the combined effect of strontium, aluminum, and fluoride elements on early enamel carious lesions. *Biol Trace Elem Res,* 147**,** 418-27.

KUEMMERLE, J. M., OBERLE, A., OECHSLIN, C., BOHNER, M., FREI, C., BOECKEN, I. & VON RECHENBERG, B. 2005. Assessment of the suitability of a new brushite calcium phosphate cement for cranioplasty - an experimental study in sheep. *J Craniomaxillofac Surg,* 33**,** 37-44.

LEVIN, L., ZIGDON, H. & MAYER, Y. 2008. [Alveolar ridge preservation following tooth extraction]. *Refuat Hapeh Vehashinayim,* 25**,** 41-6, 83.

LILLEY, K. J., GBURECK, U., WRIGHT, A. J., FARRAR, D. F. & BARRALET, J. E. 2005. Cement from nanocrystalline hydroxyapatite: effect of calcium phosphate ratio. *J Mater Sci Mater Med,* 16**,** 1185-90.

LIN, S., WANG, Z., QI, J. C., WU, J. H., TIAN, T., HOU, L. L., HAO, L. M. & YANG, J. Q. 2011. One-pot fabrication and antimicrobial properties of novel PET nonwoven fabrics. *Biomed Mater,* 6**,** 045009.

LINDHE, J., LANG, P. N. & KARRING 2008. clinical periodontology and implant dentistry. Blackwell Munksgaard, Singapore.

LIPPERT, F. 2012. The effects of lesion baseline characteristics and different Sr:Ca ratios in plaque fluid-like solutions on caries lesion de- and remineralization. *Arch Oral Biol,* 57**,** 1299-306.

LOCHER, C. P., PUTNAM, D., LANGER, R., WITT, S. A., ASHLOCK, B. M. & LEVY, J. A. 2003. Enhancement of a human immunodeficiency virus env DNA vaccine using a novel polycationic nanoparticle formulation. *Immunol Lett,* 90**,** 67-70.

LOPEZ, M. S., MECERREYES, D., LOPEZ-CABARCOS, E. & LOPEZ-RUIZ, B. 2006. Amperometric glucose biosensor based on polymerized ionic liquid microparticles. *Biosens Bioelectron,* 21**,** 2320-8.

LU, J. X., ABOUT, I., STEPHAN, G., VAN LANDUYT, P., DEJOU, J., FIOCCHI, M., LEMAITRE, J. & PROUST, J. P. 1999. Histological and biomechanical studies of two bone colonizable cements in rabbits. *Bone,* 25**,** 41S-45S.

MA, D. D. & WEI, A. Q. 1996. Enhanced delivery of synthetic oligonucleotides to human leukaemic cells by liposomes and immunoliposomes. *Leuk Res,* 20**,** 925-30.

MA, J., SMIETANA, M. J., KOSTROMINOVA, T. Y., WOJTYS, E. M., LARKIN, L. M. & ARRUDA, E. M. 2012. Three-dimensional engineered bone-ligament-bone constructs for anterior cruciate ligament replacement. *Tissue Eng Part A,* 18**,** 103-16.

MALMGREN, B. 2000. Decoronation: how, why, and when? *J Calif Dent Assoc,* 28**,** 846-54.

MARINO, F. T., TORRES, J., HAMDAN, M., RODRIGUEZ, C. R. & CABARCOS, E. L. 2007. Advantages of using glycolic acid as a retardant in a brushite forming cement. *J Biomed Mater Res B Appl Biomater,* 83**,** 571-9.

MARTIN, I. G., DALY, C. G. & LIEW, V. P. 1990. After-hours treatment of anterior dental trauma in Newcastle and western Sydney: a four-year study. *Aust Dent J,* 35**,** 27-31.

MATEJICEK, P., CIGLER, P., PROCHAZKA, K. & KRAL, V. 2006. Molecular assembly of metallacarboranes in water: light scattering and microscopy study. *Langmuir,* 22**,** 575-81.

MATSUNAGA, K., MURATA, H. & SHITARA, K. 2010. Theoretical calculations of the thermodynamic stability of ionic substitutions in hydroxyapatite under an aqueous solution environment. *J Phys Condens Matter,* 22**,** 384210.

METZ, J., SARGENT, P. & CHU, T. M. 2006. Bovine albumin release and degradation analysis of dicalcium phosphate dihydrate cement. *Biomed Sci Instrum,* 42**,** 296-301.

MEYER, U., T, M. & J, H. (eds.) 2009. *Fundamentals of tissue engineering and regenerative medicine*.

MICHEL, M., IZQUIERDO, A., DECHER, G., VOEGEL, J. C., SCHAAF, P. & BALL, V. 2005. Layer by layer self-assembled polyelectrolyte multilayers with embedded phospholipid vesicles obtained by spraying: integrity of the vesicles. *Langmuir,* 21**,** 7854-9.

MICHEL, M., VAUTIER, D., VOEGEL, J. C., SCHAAF, P. & BALL, V. 2004. Layer by layer self-assembled polyelectrolyte multilayers with embedded phospholipid vesicles. *Langmuir,* 20**,** 4835-9.

MIRTCHI, A. A., LEMAITRE, J. & MUNTING, E. 1989. Calcium phosphate cements: action of setting regulators on the properties of the beta-tricalcium phosphate-monocalcium phosphate cements. *Biomaterials,* 10**,** 634-8.

MIRTCHI, A. A., LEMAITRE, J. & MUNTING, E. 1991. Calcium phosphate cements: effect of fluorides on the setting and hardening of beta-tricalcium phosphate-dicalcium phosphate-calcite cements. *Biomaterials,* 12**,** 505-10.

MOORE, W. R., GRAVES, S. E. & BAIN, G. I. 2001. Synthetic bone graft substitutes. *ANZ J Surg,* 71**,** 354-61.

NAJJAR, M. B., KASHTANOV, D. & CHIKINDAS, M. L. 2009. Natural Antimicrobials ε-Poly-l-lysine and Nisin A for Control of Oral Microflora. 143-147.

NORTON, M. R., ODELL, E. W., THOMPSON, I. D. & COOK, R. J. 2003. Efficacy of bovine bone mineral for alveolar augmentation: a human histologic study. *Clin Oral Implants Res,* 14**,** 775-83.

NURIT, J., MARGERIT, J., TEROL, A. & BOUDEVILLE, P. 2002. pH-metric study of the setting reaction of monocalcium phosphate monohydrate/calcium oxide-based cements. *J Mater Sci Mater Med,* 13**,** 1007-14.

O'BRIEN, M. 1994. Children's dental health in United Kingdom 1993. London: Office of Population Censuses and survey.

OSTLER, M. S. & KOKICH, V. G. 1994. Alveolar ridge changes in patients congenitally missing mandibular second premolars. *J Prosthet Dent,* 71**,** 144-9.

PASQUIER, G., FLAUTRE, B., LECLET, H. & HARDOUIN, P. 1998. Experimental evaluation of a percutaneous injectable biomaterial used in radio-interventional bone-filling procedures. *J Mater Sci Mater Med,* 9**,** 333-6.

PAXTON, J. Z., DONNELLY, K., KEATCH, R. P., BAAR, K. & GROVER, L. M. 2010. Factors affecting the longevity and strength in an in vitro model of the bone-ligament interface. *Ann Biomed Eng,* 38**,** 2155-66.

PELTOLA, M. J., SUONPAA, J. T., ANDERSSON, H., MAATTANEN, H. S., AITASALO, K. M., YLI-URPO, A. & LAIPPALA, P. J. 2000. In vitro model for frontal sinus obliteration with bioactive glass S53P4. *J Biomed Mater Res,* 53**,** 161-6.

PEREZ, R. A., KIM, H.-W. & MARIA-PAU 2012. Polymeric additives to enhance the functional properties of calcium phosphate cements. *J Tissue Eng*.

PIETROKOVSKI, J. & MASSLER, M. 1967. Alveolar ridge resorption following tooth extraction. *J Prosthet Dent,* 17**,** 21-7.

PINA, S., TORRES, P. M., GOETZ-NEUNHOEFFER, F., NEUBAUER, J. & FERREIRA, J. M. 2010. Newly developed Sr-substituted alpha-TCP bone cements. *Acta Biomater,* 6**,** 928-35.

PINA, S., VIEIRA, S. I., REGO, P., TORRES, P. M., DA CRUZ E SILVA, O. A., DA CRUZ E SILVA, E. F. & FERREIRA, J. M. Biological responses of brushite-forming Zn- and ZnSr- substituted beta-tricalcium phosphate bone cements. *Eur Cell Mater,* 20**,** 162-77.

PITTS, N. B., BOYLES, J., NUGENT, Z. J., THOMAS, N. & PINE, C. M. 2004. The dental caries experience of 14-year-old children in England and Wales. Surveys co-ordinated by the

British Association for the Study of Community Dentistry in 2002/2003. *Community Dent Health,* 21**,** 45-57.

ROBERTS, G. & LONGHURST, P. (eds.) 1996. *Oral and Dental Trauma in Children and Adolescents*: Oxford University Press.

RYF, C., MD, S. G., RADZIEJOWSKI, M., BLAUTH, M. & HANSON, B. 2009. A New Injectable Brushite Cement: First Results in Distal Radius and Proximal Tibia Fractures. 35**,** 389-396.

RYSER, H. J. & SHEN, W. C. 1980. Conjugation of methotrexate to poly (L-lysine) as a potential way to overcome drug resistance. *Cancer,* 45**,** 1207-11.

SANCHEZ-PANIAGUA LOPEZ, M., TAMIMI, F., LOPEZ-CABARCOS, E. & LOPEZ-RUIZ, B. 2009. Highly sensitive amperometric biosensor based on a biocompatible calcium phosphate cement. *Biosens Bioelectron,* 24**,** 2574-9.

SCHROEDER, H. E. 1986. [Healing and regeneration following periodontal treatment]. *Dtsch Zahnarztl Z,* 41**,** 536-8.

SHEN, W. C. & RYSER, H. J. 1981. Poly(L-lysine) has different membrane transport and drug-carrier properties when complexed with heparin. *Proc Natl Acad Sci U S A,* 78**,** 7589-93.

SHIMA, S., MATSUOKA, H., IWAMOTO, T. & SAKAI, H. 1984. Antimicrobial action of epsilon-poly-L-lysine. *J Antibiot (Tokyo),* 37**,** 1449-55.

TAMIMI-MARINO, F., MASTIO, J., RUEDA, C., BLANCO, L. & LOPEZ-CABARCOS, E. 2007. Increase of the final setting time of brushite cements by using chondroitin 4-sulfate and silica gel. *J Mater Sci Mater Med,* 18**,** 1195-201.

TAMIMI, F., SHEIKH, Z. & BARRALET, J. 2012. Dicalcium phosphate cements: brushite and monetite. *Acta Biomater,* 8**,** 474-87.

TAMIMI, F., TORRES, J., BETTINI, R., RUGGERA, F., RUEDA, C., LOPEZ-PONCE, M. & LOPEZ-CABARCOS, E. 2008. Doxycycline sustained release from brushite cements for the treatment of periodontal diseases. *J Biomed Mater Res A,* 85**,** 707-14.

TAMIMI, F., TORRES, J., LOPEZ-CABARCOS, E., BASSETT, D. C., HABIBOVIC, P., LUCERON, E. & BARRALET, J. E. 2009. Minimally invasive maxillofacial vertical bone augmentation using brushite based cements. *Biomaterials,* 30**,** 208-16.

TAMIMI, F. M., TORRES, J., TRESGUERRES, I., CLEMENTE, C., LOPEZ-CABARCOS, E. & BLANCO, L. J. 2006. Bone augmentation in rabbit calvariae: comparative study between Bio-Oss and a novel beta-TCP/DCPD granulate. *J Clin Periodontol,* 33**,** 922-8.

THEISS, F., APELT, D., BRAND, B., KUTTER, A., ZLINSZKY, K., BOHNER, M., MATTER, S., FREI, C., AUER, J. A. & VON RECHENBERG, B. 2005. Biocompatibility and resorption of a brushite calcium phosphate cement. *Biomaterials,* 26**,** 4383-94.

THIERRY, A. R., RAHMAN, A. & DRITSCHILO, A. 1993. Overcoming multidrug resistance in human tumor cells using free and liposomally encapsulated antisense oligodeoxynucleotides. *Biochem Biophys Res Commun,* 190**,** 952-60.

THOMAS, P., SCHUH, A., EBEN, R. & THOMSEN, M. 2008. [Allergy to bone cement components]. *Orthopade,* 37**,** 117-20.

THOMES, B., MURRAY, P. & BOUCHIER-HAYES, D. 2002. Development of resistant strains of Staphylococcus epidermidis on gentamicin-loaded bone cement in vivo. *J Bone Joint Surg Br,* 84**,** 758-60.

TIMONSHENKO, S. & K.S (eds.) 1964. *Theory of plates and shells*: MCGraw Hill Higher Education.

TSUJITA, T., TAKAICHI, H., TAKAKU, T., AOYAMA, S. & HIRAKI, J. 2006. Antiobesity action of epsilon-polylysine, a potent inhibitor of pancreatic lipase. *J Lipid Res,* 47**,** 1852-8.

TSUJITA, T., TAKAICHI, H., TAKAKU, T., SAWAI, T., YOSHIDA, N. & HIRAKI, J. 2007. Inhibition of lipase activities by basic polysaccharide. *J Lipid Res,* 48**,** 358-65.

TURNER, T. M., URBAN, R. M., SINGH, K., HALL, D. J., RENNER, S. M., LIM, T. H., TOMLINSON, M. J. & AN, H. S. 2008. Vertebroplasty comparing injectable calcium phosphate cement compared with polymethylmethacrylate in a unique canine vertebral body large defect model. *Spine J,* 8**,** 482-7.

VAN DE BELT, H., NEUT, D., SCHENK, W., VAN HORN, J. R., VAN DER MEI, H. C. & BUSSCHER, H. J. 2001. Staphylococcus aureus biofilm formation on different gentamicin-loaded polymethylmethacrylate bone cements. *Biomaterials,* 22**,** 1607-11.

VAN LANDUYT, P., PETER, B., BELUZE, L. & LEMAITRE, J. 1999. Reinforcement of osteosynthesis screws with brushite cement. *Bone,* 25**,** 95S-98S.

WAELTI, E. R. & GLUCK, R. 1998. Delivery to cancer cells of antisense L-myc oligonucleotides incorporated in fusogenic, cationic-lipid-reconstituted influenza-virus envelopes (cationic virosomes). *Int J Cancer,* 77**,** 728-33.

XIA, W., M. R. MOHD RAZI, P. ASHLEY, E. A. ABOU NEEL, AND, M. P. H. & YOUNG, A. M. 2014. Quantifying effects of interactions between polyacrylic acid and chlorhexidine in dicalcium phosphate – forming cements *J. Mater. Chem.* **,** 1673-1680.

XIE, D., BRANTLEY, W. A., CULBERTSON, B. M. & WANG, G. 2000. Mechanical properties and microstructures of glass-ionomer cements. *Dent Mater,* 16**,** 129-38.

YIN, Y., YE, F., CAI, S., YAO, K., CUI, J. & SONG, X. 2003. Gelatin manipulation of latent macropores formation in brushite cement. *J Mater Sci Mater Med,* 14**,** 255-61.

YOSHIDA, T. & NAGASAWA, T. 2003. epsilon-Poly-L-lysine: microbial production, biodegradation and application potential. *Appl Microbiol Biotechnol,* 62**,** 21-6.

YOUNG, A. M., NG, P. Y., GBURECK, U., NAZHAT, S. N., BARRALET, J. E. & HOFMANN, M. P. 2008. Characterization of chlorhexidine-releasing, fast-setting, brushite bone cements. *Acta Biomater,* 4**,** 1081-8.

YU, H., DENG, C., TIAN, H., LU, T., CHEN, X. & JING, X. 2011. Chemo-physical and biological evaluation of poly(L-lysine)-grafted chitosan copolymers used for highly efficient gene delivery. *Macromol Biosci,* 11**,** 352-61.

ZHANG, Y., PAJARES, A. & LAWN, B. R. 2004. Fatigue and damage tolerance of Y-TZP ceramics in layered biomechanical systems. *J Biomed Mater Res B Appl Biomater,* 71**,** 166-71.

APPENDICES

9 APPENDIX

Appendix 1:

1.1 : T-Test for different MCPM and β-TCP particle sizes for mechanical properties (MPa, GPa and toughness) at PLR 3.3:1 with CA 800 mM.

T-Test: Test_measure = 1 MPa

Group Statistics

	company	N	Mean	Std. Deviation	Std. Error Mean
powder_a4.32	1 SIGMA	6	22.300	2.0852	.8513
	2 HIMED	6	22.167	2.9582	1.2077
powder_b5.78	1 SIGMA	6	22.667	3.3446	1.3654
	2 HIMED	6	22.467	3.3548	1.3696
powder_c7.76	1 SIGMA	6	23.950	2.9878	1.2198
	2 HIMED	6	22.967	2.7645	1.1286
powder_d12.03	1 SIGMA	6	27.467	3.4407	1.4047
	2 HIMED	6	26.417	3.3973	1.3869
powder_e33.8	1 SIGMA	6	30.033	1.3545	.5530
	2 HIMED	6	28.500	2.2352	.9125

Independent Samples Test[a]

		Levene's Test for Equality of Variances		t-test for Equality of Means				
		F	Sig.	t	df	Sig. (2-tailed)	Mean Difference	Std. Error Difference
powder_a4.32	Equal variances assumed	.090	.770	.090	10	.930	.1333	1.4775
	Equal variances not assumed			.090	8.985	.930	.1333	1.4775
powder_b5.78	Equal variances assumed	.050	.827	.103	10	.920	.2000	1.9340
	Equal variances not assumed			.103	10.000	.920	.2000	1.9340
powder_c7.76	Equal variances assumed	.000	.990	.592	10	.567	.9833	1.6618
	Equal variances not assumed			.592	9.940	.567	.9833	1.6618
powder_d12.03	Equal variances assumed	.036	.854	.532	10	.606	1.0500	1.9740
	Equal variances not assumed			.532	9.998	.606	1.0500	1.9740
powder_e33.8	Equal variances assumed	.429	.527	1.437	10	.181	1.5333	1.0670
	Equal variances not assumed			1.437	8.236	.188	1.5333	1.0670

Test_measure = 2 GPa

Group Statistics[a]

	company	N	Mean	Std. Deviation	Std. Error Mean
powder_a4.32	1 SIGMA	6	1.817	.6494	.2651
	2 HIMED	6	2.567	.5279	.2155
powder_b5.78	1 SIGMA	6	2.083	.5076	.2072
	2 HIMED	6	1.867	.9309	.3801
powder_c7.76	1 SIGMA	6	2.400	1.1524	.4705
	2 HIMED	6	2.650	.9050	.3695
powder_d12.03	1 SIGMA	6	2.717	1.1161	.4556
	2 HIMED	6	2.850	.7007	.2861
powder_e33.8	1 SIGMA	6	3.517	1.3848	.5653
	2 HIMED	6	2.433	.6121	.2499

I

independent Samples Test[a]

		Levene's Test for Equality of Variances		t-test for Equality of Means				
		F	Sig.	t	df	Sig. (2-tailed)	Mean Difference	Std. Error Difference
powder_a4.32	Equal variances assumed	.321	.584	-2.195	10	.053	-.7500	.3416
	Equal variances not assumed			-2.195	9.600	.054	-.7500	.3416
powder_b5.78	Equal variances assumed	6.485	.029	.501	10	.628	.2167	.4329
	Equal variances not assumed			.501	7.732	.631	.2167	.4329
powder_c7.76	Equal variances assumed	.021	.887	-.418	10	.685	-.2500	.5982
	Equal variances not assumed			-.418	9.468	.685	-.2500	.5982
powder_d12.03	Equal variances assumed	2.738	.129	-.248	10	.809	-.1333	.5380
	Equal variances not assumed			-.248	8.412	.810	-.1333	.5380
powder_e33.8	Equal variances assumed	1.336	.275	1.753	10	.110	1.0833	.6181
	Equal variances not assumed			1.753	6.882	.124	1.0833	.6181

Test_measure = 3 toughness

Group Statistics[a]

	company	N	Mean	Std. Deviation	Std. Error Mean
powder_a4.32	1 SIGMA	6	1.200	.7348	.3000
	2 HIMED	6	.817	.3312	.1352
powder_b5.78	1 SIGMA	6	.683	.4792	.1956
	2 HIMED	6	.750	.3886	.1586
powder_c7.76	1 SIGMA	6	1.133	.6377	.2603
	2 HIMED	6	.550	.2258	.0922
powder_d12.03	1 SIGMA	6	.833	.3830	.1563
	2 HIMED	6	.867	.1966	.0803
powder_e33.8	1 SIGMA	6	.733	.3933	.1606
	2 HIMED	6	.667	.0816	.0333

Independent Samples Test[a]

		Levene's Test for Equality of Variances		t-test for Equality of Means				
		F	Sig.	t	df	Sig. (2-tailed)	Mean Difference	Std. Error Difference
powder_a4.32	Equal variances assumed	3.471	.092	1.165	10	.271	.3833	.3291
	Equal variances not assumed			1.165	6.950	.282	.3833	.3291
powder_b5.78	Equal variances assumed	.358	.563	-.265	10	.797	-.0667	.2519
	Equal variances not assumed			-.265	9.590	.797	-.0667	.2519
powder_c7.76	Equal variances assumed	5.362	.043	2.112	10	.061	.5833	.2762
	Equal variances not assumed			2.112	6.235	.077	.5833	.2762
powder_d12.03	Equal variances assumed	3.616	.086	-.190	10	.853	-.0333	.1758
	Equal variances not assumed			-.190	7.465	.855	-.0333	.1758
powder_e33.8	Equal variances assumed	8.996	.013	.407	10	.693	.0667	.1640
	Equal variances not assumed			.407	5.430	.700	.0667	.1640

1.2: UNIANOVA result for different MCPM and β-TCP particle sizes for mechanical properties (MPa, GPa and toughness)

company = 1 SIGMA, Test_measure = 1 MPa

Custom Hypothesis Tests

Contrast Results (K Matrix)[a]

powder Polynomial Contrast[b]			Dependent Variable result
Linear	Contrast Estimate		6.409
	Hypothesized Value		0
	Difference (Estimate - Hypothesized)		6.409
	Std. Error		1.127
	Sig.		.000
	95% Confidence Interval for Difference	Lower Bound	4.087
		Upper Bound	8.731

TCP powder	Mean	Std. Error	95% Confidence Interval	
			Lower Bound	Upper Bound
1	22.300	1.127	19.978	24.622
2	22.667	1.127	20.345	24.989
3	23.950	1.127	21.628	26.272
4	27.467	1.127	25.145	29.789
5	30.033	1.127	27.711	32.355

Profile Plots

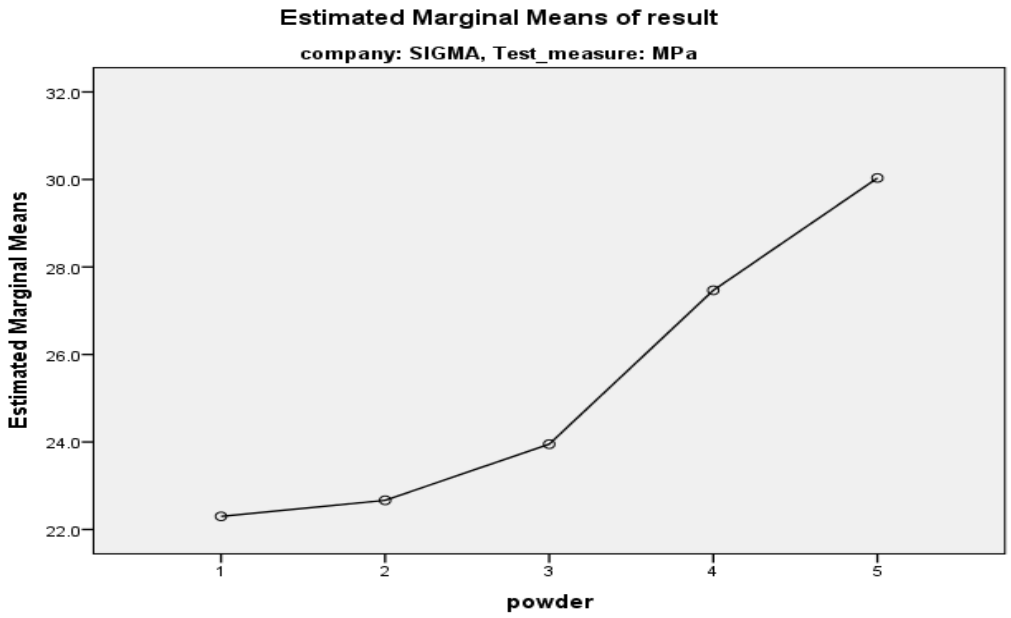

company = 1 SIGMA, Test_measure = 2 GPa

Custom Hypothesis Tests
Contrast Results (K Matrix)[a]

powder Polynomial Contrast[b]			Dependent Variable
			result
Linear	Contrast Estimate		1.275
	Hypothesized Value		0
	Difference (Estimate - Hypothesized)		1.275
	Std. Error		.415
	Sig.		.005
	95% Confidence Interval for Difference	Lower Bound	.420
		Upper Bound	2.130

powder	Mean	Std. Error	95% Confidence Interval	
			Lower Bound	Upper Bound
1	1.817	.415	.962	2.672
2	2.083	.415	1.228	2.938
3	2.400	.415	1.545	3.255
4	2.717	.415	1.862	3.572
5	3.517	.415	2.662	4.372

Profile Plots

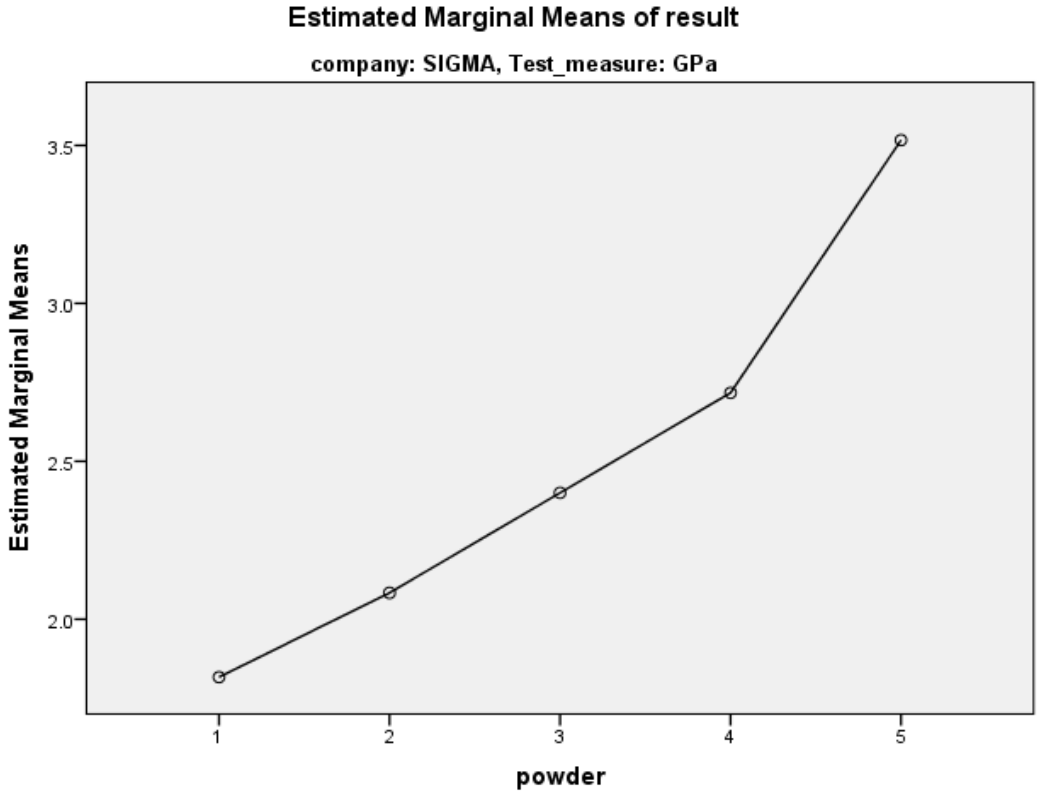

company = 1 SIGMA, Test_measure = 3 toughness

Custom Hypothesis Tests
Contrast Results (K Matrix)[a]

powder Polynomial Contrast[b]			Dependent Variable
			result
Linear	Contrast Estimate		-.248
	Hypothesized Value		0
	Difference (Estimate - Hypothesized)		-.248
	Std. Error		.222
	Sig.		.275
	95% Confidence Interval for Difference	Lower Bound	-.705
		Upper Bound	.209

powder	Mean	Std. Error	95% Confidence Interval	
			Lower Bound	Upper Bound
1	1.200	.222	.743	1.657
2	.683	.222	.226	1.140
3	1.133	.222	.676	1.590
4	.833	.222	.376	1.290
5	.733	.222	.276	1.190

Profile Plots

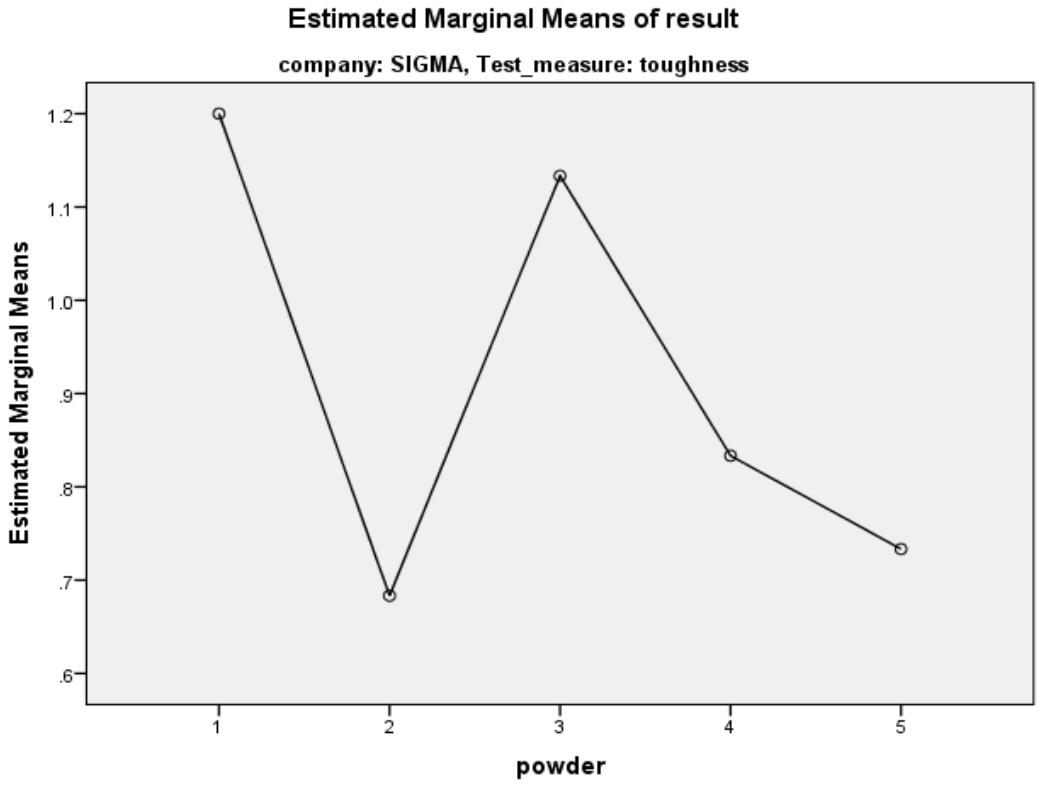

company = 2 HIMED, Test_measure = 1 MPa

Custom Hypothesis Tests
Contrast Results (K Matrix)[a]

powder Polynomial Contrast[b]			Dependent Variable
			result
Linear	Contrast Estimate		5.255
	Hypothesized Value		0
	Difference (Estimate - Hypothesized)		5.255
	Std. Error		1.214
	Sig.		.000
	95% Confidence Interval for Difference	Lower Bound	2.755
		Upper Bound	7.754

powder	Mean	Std. Error	95% Confidence Interval	
			Lower Bound	Upper Bound
1	22.167	1.214	19.667	24.666
2	22.467	1.214	19.967	24.966
3	22.967	1.214	20.467	25.466
4	26.417	1.214	23.917	28.916
5	28.500	1.214	26.001	30.999

Profile Plots

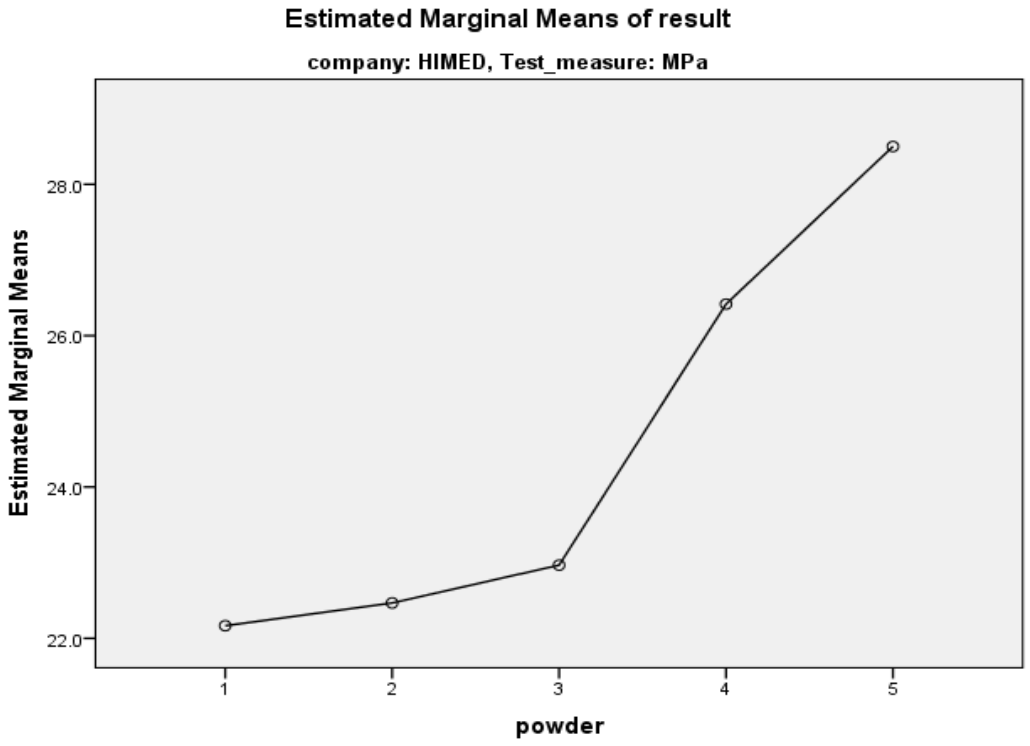

company = 2 HIMED, Test_measure = 2 GPa

Custom Hypothesis Tests
Contrast Results (K Matrix)[a]

powder Polynomial Contrast[b]			Dependent Variable result
Linear	Contrast Estimate		.227
	Hypothesized Value		0
	Difference (Estimate - Hypothesized)		.227
	Std. Error		.307
	Sig.		.467
	95% Confidence Interval for Difference	Lower Bound	-.406
		Upper Bound	.859

powder	Mean	Std. Error	95% Confidence Interval	
			Lower Bound	Upper Bound
1	2.567	.307	1.934	3.199
2	1.867	.307	1.234	2.499
3	2.650	.307	2.017	3.283
4	2.850	.307	2.217	3.483
5	2.433	.307	1.801	3.066

Profile Plots

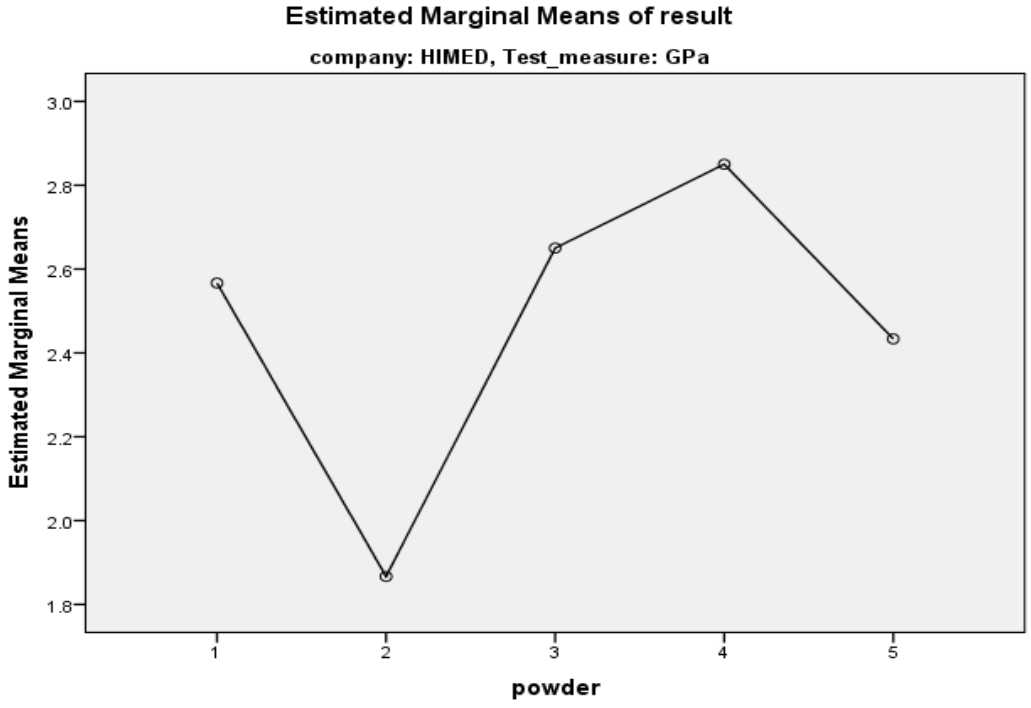

company = 2 HIMED, Test_measure = 3 toughness

Contrast Results (K Matrix)[a]

powder Polynomial Contrast[b]			Dependent Variable result
Linear	Contrast Estimate		-.058
	Hypothesized Value		0
	Difference (Estimate - Hypothesized)		-.058
	Std. Error		.109
	Sig.		.600
	95% Confidence Interval for Difference	Lower Bound	-.283
		Upper Bound	.167

powder	Mean	Std. Error	95% Confidence Interval	
			Lower Bound	Upper Bound
1	.817	.109	.592	1.041
2	.750	.109	.525	.975
3	.550	.109	.325	.775
4	.867	.109	.642	1.091
5	.667	.109	.442	.891

Profile Plots

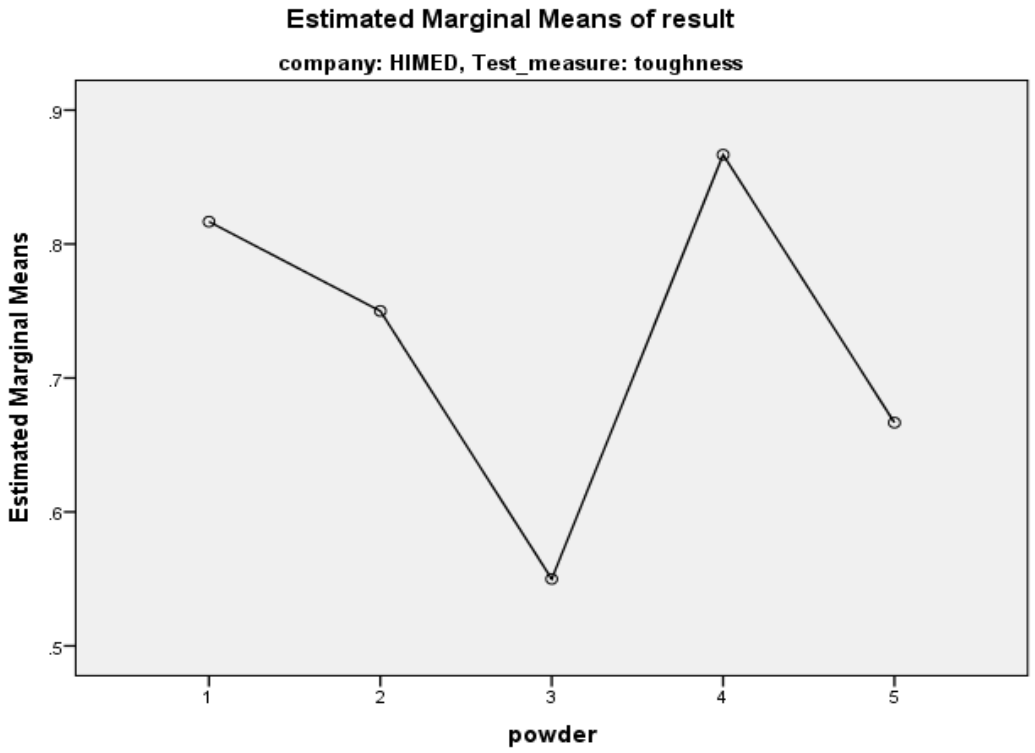

Appendix 2

2.1: Unianova for dry samples mechanical properties (MPa, GPA and toughness) with different PLR and increase wt % of PLS (MCPM 2, β-TCP 34 micron and CA 800 mM (n=6))

PLS_percentage = 1 PLS 0%, Test_measure = 1 MPa

Tests of Between-Subjects Effects[a]

Dependent Variable: score

Source	Type III Sum of Squares	df	Mean Square	F	Sig.
Corrected Model	17.763[b]	1	17.763	5.685	.038
Intercept	11718.750	1	11718.750	3750.400	.000
PLR	17.763	1	17.763	5.685	.038
Error	31.247	10	3.125		
Total	11767.760	12			
Corrected Total	49.010	11			

Dependent Variable: score

PLR	Mean	Std. Error	95% Confidence Interval	
			Lower Bound	Upper Bound
1 PLR 3.3:1	30.033	.722	28.425	31.641
2 PLR 4:1	32.467	.722	30.859	34.075

PLS_percentage = 1 PLS 0%, Test_measure = 2 GPa

Tests of Between-Subjects Effects[a]

Dependent Variable: score

Source	Type III Sum of Squares	df	Mean Square	F	Sig.
Corrected Model	.030[b]	1	.030	.024	.881
Intercept	144.213	1	144.213	113.943	.000
PLR	.030	1	.030	.024	.881
Error	12.657	10	1.266		
Total	156.900	12			
Corrected Total	12.687	11			

Dependent Variable:

PLR	Mean	Std. Error	95% Confidence Interval	
			Lower Bound	Upper Bound
1 PLR 3.3:1	3.517	.459	2.493	4.540
2 PLR 4:1	3.417	.459	2.393	4.440

PLS_percentage = 1 PLS 0%, Test_measure = 3 Toughness

Tests of Between-Subjects Effects[a]

Dependent Variable: score

Source	Type III Sum of Squares	df	Mean Square	F	Sig.
Corrected Model	3.741[b]	1	3.741	19.005	.001
Intercept	20.021	1	20.021	101.715	.000
PLR	3.741	1	3.741	19.005	.001
Error	1.968	10	.197		
Total	25.730	12			
Corrected Total	5.709	11			

Dependent Variable: score

PLR	Mean	Std. Error	95% Confidence Interval	
			Lower Bound	Upper Bound
1 PLR 3.3:1	.733	.181	.330	1.137
2 PLR 4:1	1.850	.181	1.446	2.254

PLS_percentage = 2 PLS 10%, Test_measure = 1 MPa

Tests of Between-Subjects Effects[a]

Dependent Variable: score

Source	Type III Sum of Squares	df	Mean Square	F	Sig.
Corrected Model	131.341[b]	1	131.341	34.411	.000
Intercept	11712.501	1	11712.501	3068.644	.000
PLR	131.341	1	131.341	34.411	.000
Error	38.168	10	3.817		
Total	11882.010	12			
Corrected Total	169.509	11			

Dependent Variable: score

PLR	Mean	Std. Error	95% Confidence Interval	
			Lower Bound	Upper Bound
1 PLR 3.3:1	27.933	.798	26.156	29.710
2 PLR 4:1	34.550	.798	32.773	36.327

PLS_percentage = 2 PLS 10%, Test_measure = 2 GPa

Tests of Between-Subjects Effects[a]

Dependent Variable: score

Source	Type III Sum of Squares	df	Mean Square	F	Sig.
Corrected Model	2.001[b]	1	2.001	2.738	.129
Intercept	103.841	1	103.841	142.086	.000
PLR	2.001	1	2.001	2.738	.129
Error	7.308	10	.731		
Total	113.150	12			
Corrected Total	9.309	11			

Dependent Variable: score

PLR	Mean	Std. Error	95% Confidence Interval	
			Lower Bound	Upper Bound
1 PLR 3.3:1	2.533	.349	1.756	3.311
2 PLR 4:1	3.350	.349	2.572	4.128

PLS_percentage = 2 PLS 10%, Test_measure = 3 Toughness

Tests of Between-Subjects Effects[a]

Dependent Variable: score

Source	Type III Sum of Squares	df	Mean Square	F	Sig.
Corrected Model	.030[b]	1	.030	.307	.592
Intercept	15.413	1	15.413	157.816	.000
PLR	.030	1	.030	.307	.592
Error	.977	10	.098		
Total	16.420	12			
Corrected Total	1.007	11			

Dependent Variable: score

PLR	Mean	Std. Error	95% Confidence Interval	
			Lower Bound	Upper Bound
1 PLR 3.3:1	1.083	.128	.799	1.368
2 PLR 4:1	1.183	.128	.899	1.468

PLS_percentage = 3 PLS 20%, Test_measure = 1 MPa

Tests of Between-Subjects Effects[a]

Dependent Variable: score

Source	Type III Sum of Squares	df	Mean Square	F	Sig.
Corrected Model	129.363[b]	1	129.363	11.064	.008
Intercept	10138.453	1	10138.453	867.103	.000
PLR	129.363	1	129.363	11.064	.008
Error	116.923	10	11.692		
Total	10384.740	12			
Corrected Total	246.287	11			

Dependent Variable: score

PLR	Mean	Std. Error	95% Confidence Interval	
			Lower Bound	Upper Bound
1 PLR 3.3:1	25.783	1.396	22.673	28.894
2 PLR 4:1	32.350	1.396	29.240	35.460

PLS_percentage = 3 PLS 20%, Test_measure = 2 GPa

Tests of Between-Subjects Effects[a]

Dependent Variable: score

Source	Type III Sum of Squares	df	Mean Square	F	Sig.
Corrected Model	7.841[b]	1	7.841	11.974	.006
Intercept	101.501	1	101.501	155.003	.000
PLR	7.841	1	7.841	11.974	.006
Error	6.548	10	.655		
Total	115.890	12			
Corrected Total	14.389	11			

Dependent Variable: score

PLR	Mean	Std. Error	95% Confidence Interval	
			Lower Bound	Upper Bound
1 PLR 3.3:1	2.100	.330	1.364	2.836
2 PLR 4:1	3.717	.330	2.981	4.453

PLS_percentage = 3 PLS 20%, Test_measure = 3 Toughness

Tests of Between-Subjects Effects[a]

Dependent Variable: score

Source	Type III Sum of Squares	df	Mean Square	F	Sig.
Corrected Model	1.763[b]	1	1.763	2.718	.130
Intercept	28.830	1	28.830	44.445	.000
PLR	1.763	1	1.763	2.718	.130
Error	6.487	10	.649		
Total	37.080	12			
Corrected Total	8.250	11			

Dependent Variable: score

PLR	Mean	Std. Error	95% Confidence Interval	
			Lower Bound	Upper Bound
1 PLR 3.3:1	1.933	.329	1.201	2.666
2 PLR 4:1	1.167	.329	.434	1.899

PLS_percentage = 4 PLS 30%, Test_measure = 1 MPa

Tests of Between-Subjects Effects[a]

Dependent Variable: score

Source	Type III Sum of Squares	df	Mean Square	F	Sig.
Corrected Model	124.163[b]	1	124.163	32.663	.000
Intercept	9086.003	1	9086.003	2390.215	.000
PLR	124.163	1	124.163	32.663	.000
Error	38.013	10	3.801		
Total	9248.180	12			
Corrected Total	162.177	11			

Dependent Variable: score

PLR	Mean	Std. Error	95% Confidence Interval	
			Lower Bound	Upper Bound
1 PLR 3.3:1	24.300	.796	22.526	26.074
2 PLR 4:1	30.733	.796	28.960	32.507

PLS_percentage = 4 PLS 30%, Test_measure = 2 GPa

Tests of Between-Subjects Effects[a]

Dependent Variable: score

Source	Type III Sum of Squares	df	Mean Square	F	Sig.
Corrected Model	.607[b]	1	.607	1.344	.273
Intercept	118.441	1	118.441	261.941	.000
PLR	.607	1	.607	1.344	.273
Error	4.522	10	.452		
Total	123.570	12			
Corrected Total	5.129	11			

Dependent Variable: score

PLR	Mean	Std. Error	95% Confidence Interval	
			Lower Bound	Upper Bound
1 PLR 3.3:1	2.917	.275	2.305	3.528
2 PLR 4:1	3.367	.275	2.755	3.978

PLS_percentage = 4 PLS 30%, Test_measure = 3 Toughness

Tests of Between-Subjects Effects[a]

Dependent Variable: score

Source	Type III Sum of Squares	df	Mean Square	F	Sig.
Corrected Model	.853[b]	1	.853	2.498	.145
Intercept	28.830	1	28.830	84.380	.000
PLR	.853	1	.853	2.498	.145
Error	3.417	10	.342		
Total	33.100	12			
Corrected Total	4.270	11			

Dependent Variable: score

PLR	Mean	Std. Error	95% Confidence Interval	
			Lower Bound	Upper Bound
1 PLR 3.3:1	1.283	.239	.752	1.815
2 PLR 4:1	1.817	.239	1.285	2.348

PLS_percentage = 5 PLS 40%, Test_measure = 1 MPa

Tests of Between-Subjects Effects[a]

Dependent Variable: score

Source	Type III Sum of Squares	df	Mean Square	F	Sig.
Corrected Model	118.441[b]	1	118.441	12.307	.006
Intercept	8634.968	1	8634.968	897.217	.000
PLR	118.441	1	118.441	12.307	.006
Error	96.242	10	9.624		
Total	8849.650	12			
Corrected Total	214.683	11			

Dependent Variable: score

PLR	Mean	Std. Error	95% Confidence Interval	
			Lower Bound	Upper Bound
1 PLR 3.3:1	23.683	1.267	20.861	26.505
2 PLR 4:1	29.967	1.267	27.145	32.789

PLS_percentage = 5 PLS 40%, Test_measure = 2 GPa

Tests of Between-Subjects Effects[a]

Dependent Variable: score

Source	Type III Sum of Squares	df	Mean Square	F	Sig.
Corrected Model	1.080[b]	1	1.080	3.133	.107
Intercept	103.253	1	103.253	299.574	.000
PLR	1.080	1	1.080	3.133	.107
Error	3.447	10	.345		
Total	107.780	12			
Corrected Total	4.527	11			

Dependent Variable: score

PLR	Mean	Std. Error	95% Confidence Interval	
			Lower Bound	Upper Bound
1 PLR 3.3:1	2.633	.240	2.099	3.167
2 PLR 4:1	3.233	.240	2.699	3.767

PLS_percentage = 5 PLS 40%, Test_measure = 3 Toughness

Tests of Between-Subjects Effects[a]

Dependent Variable: score

Source	Type III Sum of Squares	df	Mean Square	F	Sig.
Corrected Model	.141[b]	1	.141	.443	.521
Intercept	21.068	1	21.068	66.215	.000
PLR	.141	1	.141	.443	.521
Error	3.182	10	.318		
Total	24.390	12			
Corrected Total	3.322	11			

Dependent Variable: score

PLR	Mean	Std. Error	95% Confidence Interval	
			Lower Bound	Upper Bound
1 PLR 3.3:1	1.433	.230	.920	1.946
2 PLR 4:1	1.217	.230	.704	1.730

PLS_percentage = 6 PLS 50%, Test_measure = 1 MPa

Tests of Between-Subjects Effects[a]

Dependent Variable: score

Source	Type III Sum of Squares	df	Mean Square	F	Sig.
Corrected Model	35.021[b]	1	35.021	3.379	.096
Intercept	7345.801	1	7345.801	708.723	.000
PLR	35.021	1	35.021	3.379	.096
Error	103.648	10	10.365		
Total	7484.470	12			
Corrected Total	138.669	11			

Dependent Variable: score

PLR	Mean	Std. Error	95% Confidence Interval	
			Lower Bound	Upper Bound
1 PLR 3.3:1	23.033	1.314	20.105	25.962
2 PLR 4:1	26.450	1.314	23.521	29.379

PLS_percentage = 6 PLS 50%, Test_measure = 2 GPa

Tests of Between-Subjects Effects[a]

Dependent Variable: score

Source	Type III Sum of Squares	df	Mean Square	F	Sig.
Corrected Model	1.333[b]	1	1.333	3.127	.107
Intercept	68.163	1	68.163	159.883	.000
PLR	1.333	1	1.333	3.127	.107
Error	4.263	10	.426		
Total	73.760	12			
Corrected Total	5.597	11			

Dependent Variable: score

PLR	Mean	Std. Error	95% Confidence Interval	
			Lower Bound	Upper Bound
1 PLR 3.3:1	2.050	.267	1.456	2.644
2 PLR 4:1	2.717	.267	2.123	3.311

PLS_percentage = 6 PLS 50%, Test_measure = 3 Toughness

Tests of Between-Subjects Effects[a]

Dependent Variable: score

Source	Type III Sum of Squares	df	Mean Square	F	Sig.
Corrected Model	.003[b]	1	.003	.022	.886
Intercept	32.670	1	32.670	211.228	.000
PLR	.003	1	.003	.022	.886
Error	1.547	10	.155		
Total	34.220	12			
Corrected Total	1.550	11			

Dependent Variable: score

PLR	Mean	Std. Error	95% Confidence Interval	
			Lower Bound	Upper Bound
1 PLR 3.3:1	1.667	.161	1.309	2.024
2 PLR 4:1	1.633	.161	1.276	1.991

Appendix 3

3.1: Unianova for dry vs wet samples at PLR 4:1 and increase wt % of PLS on mechanical properties (MPa, GPA and toughness) (MCPM 2, β-TCP 34 micron and CA 800 mM (n=6))

PLS_percentage = 1 PLS 0%, Test_measure = 1 MPa

Tests of Between-Subjects Effects[a]

Dependent Variable: score

Source	Type III Sum of Squares	df	Mean Square	F	Sig.
Corrected Model	604.920[b]	1	604.920	61.484	.000
Intercept	7721.613	1	7721.613	784.823	.000
Sample_condition	604.920	1	604.920	61.484	.000
Error	98.387	10	9.839		
Total	8424.920	12			
Corrected Total	703.307	11			

Dependent Variable: score

Sample_condition	Mean	Std. Error	95% Confidence Interval	
			Lower Bound	Upper Bound
1 Dry samples	32.467	1.281	29.613	35.320
2 Wet samples	18.267	1.281	15.413	21.120

PLS_percentage = 1 PLS 0%, Test_measure = 2 GPa

Tests of Between-Subjects Effects[a]

Dependent Variable: score

Source	Type III Sum of Squares	df	Mean Square	F	Sig.
Corrected Model	6.021[b]	1	6.021	9.636	.011
Intercept	88.021	1	88.021	140.871	.000
Sample_condition	6.021	1	6.021	9.636	.011
Error	6.248	10	.625		
Total	100.290	12			
Corrected Total	12.269	11			

Dependent Variable: score

Sample_condition	Mean	Std. Error	95% Confidence Interval	
			Lower Bound	Upper Bound
1 Dry samples	3.417	.323	2.698	4.136
2 Wet samples	2.000	.323	1.281	2.719

PLS_percentage = 1 PLS 0%, Test_measure = 3 Toughness

Tests of Between-Subjects Effects[a]

Dependent Variable: score

Source	Type III Sum of Squares	df	Mean Square	F	Sig.
Corrected Model	3.308[b]	1	3.308	21.832	.001
Intercept	21.068	1	21.068	139.059	.000
Sample_condition	3.308	1	3.308	21.832	.001
Error	1.515	10	.152		
Total	25.890	12			
Corrected Total	4.823	11			

Dependent Variable: score

Sample_condition	Mean	Std. Error	95% Confidence Interval	
			Lower Bound	Upper Bound
1 Dry samples	1.850	.159	1.496	2.204
2 Wet samples	.800	.159	.446	1.154

PLS_percentage = 2 PLS 10%, Test_measure = 1 MPa

Tests of Between-Subjects Effects[a]

Dependent Variable: score

Source	Type III Sum of Squares	df	Mean Square	F	Sig.
Corrected Model	597.841[b]	1	597.841	101.971	.000
Intercept	9069.501	1	9069.501	1546.948	.000
Sample_condition	597.841	1	597.841	101.971	.000
Error	58.628	10	5.863		
Total	9725.970	12			
Corrected Total	656.469	11			

Dependent Variable: score

Sample_condition	Mean	Std. Error	95% Confidence Interval	
			Lower Bound	Upper Bound
1 Dry samples	34.550	.989	32.347	36.753
2 Wet samples	20.433	.989	18.231	22.636

PLS_percentage = 2 PLS 10%, Test_measure = 2 GPa

Tests of Between-Subjects Effects[a]

Dependent Variable: score

Source	Type III Sum of Squares	df	Mean Square	F	Sig.
Corrected Model	.241[b]	1	.241	.413	.535
Intercept	123.521	1	123.521	211.932	.000
Sample_condition	.241	1	.241	.413	.535
Error	5.828	10	.583		
Total	129.590	12			
Corrected Total	6.069	11			

Dependent Variable: score

Sample_condition	Mean	Std. Error	95% Confidence Interval	
			Lower Bound	Upper Bound
1 Dry samples	3.350	.312	2.656	4.044
2 Wet samples	3.067	.312	2.372	3.761

PLS_percentage = 2 PLS 10%, Test_measure = 3 Toughness

Tests of Between-Subjects Effects[a]

Dependent Variable: score

Source	Type III Sum of Squares	df	Mean Square	F	Sig.
Corrected Model	.083[b]	1	.083	.454	.516
Intercept	14.520	1	14.520	79.056	.000
Sample_condition	.083	1	.083	.454	.516
Error	1.837	10	.184		
Total	16.440	12			
Corrected Total	1.920	11			

Dependent Variable: score

Sample_condition	Mean	Std. Error	95% Confidence Interval	
			Lower Bound	Upper Bound
1 Dry samples	1.183	.175	.793	1.573
2 Wet samples	1.017	.175	.627	1.407

PLS_percentage = 3 PLS 20%, Test_measure = 1 MPa

Tests of Between-Subjects Effects[a]

Dependent Variable: score

Source	Type III Sum of Squares	df	Mean Square	F	Sig.
Corrected Model	465.007[b]	1	465.007	56.698	.000
Intercept	8190.188	1	8190.188	998.621	.000
Sample_condition	465.007	1	465.007	56.698	.000
Error	82.015	10	8.202		
Total	8737.210	12			
Corrected Total	547.022	11			

Dependent Variable: score

Sample_condition	Mean	Std. Error	95% Confidence Interval	
			Lower Bound	Upper Bound
1 Dry samples	32.350	1.169	29.745	34.955
2 Wet samples	19.900	1.169	17.295	22.505

PLS_percentage = 3 PLS 20%, Test_measure = 2 GPa

Tests of Between-Subjects Effects[a]

Dependent Variable: score

Source	Type III Sum of Squares	df	Mean Square	F	Sig.
Corrected Model	2.803[b]	1	2.803	2.639	.135
Intercept	125.453	1	125.453	118.092	.000
Sample_condition	2.803	1	2.803	2.639	.135
Error	10.623	10	1.062		
Total	138.880	12			
Corrected Total	13.427	11			

Dependent Variable: score

Sample_condition	Mean	Std. Error	95% Confidence Interval	
			Lower Bound	Upper Bound
1 Dry samples	3.717	.421	2.779	4.654
2 Wet samples	2.750	.421	1.812	3.688

PLS_percentage = 3 PLS 20%, Test_measure = 3 Toughness

Tests of Between-Subjects Effects[a]

Dependent Variable: score

Source	Type III Sum of Squares	df	Mean Square	F	Sig.
Corrected Model	.403[b]	1	.403	6.798	.026
Intercept	11.603	1	11.603	195.562	.000
Sample_condition	.403	1	.403	6.798	.026
Error	.593	10	.059		
Total	12.600	12			
Corrected Total	.997	11			

Dependent Variable: score

Sample_condition	Mean	Std. Error	95% Confidence Interval	
			Lower Bound	Upper Bound
1 Dry samples	1.167	.099	.945	1.388
2 Wet samples	.800	.099	.578	1.022

PLS_percentage = 4 PLS 30%, Test_measure = 1 MPa

Tests of Between-Subjects Effects[a]

Dependent Variable: score

Source	Type III Sum of Squares	df	Mean Square	F	Sig.
Corrected Model	492.801[b]	1	492.801	126.874	.000
Intercept	7100.468	1	7100.468	1828.054	.000
Sample_condition	492.801	1	492.801	126.874	.000
Error	38.842	10	3.884		
Total	7632.110	12			
Corrected Total	531.643	11			

Dependent Variable: score

Sample_condition	Mean	Std. Error	95% Confidence Interval	
			Lower Bound	Upper Bound
1 Dry samples	30.733	.805	28.941	32.526
2 Wet samples	17.917	.805	16.124	19.709

PLS_percentage = 4 PLS 30%, Test_measure = 2 GPa

Tests of Between-Subjects Effects[a]

Dependent Variable: score

Source	Type III Sum of Squares	df	Mean Square	F	Sig.
Corrected Model	1.080[b]	1	1.080	1.582	.237
Intercept	112.853	1	112.853	165.313	.000
Sample_condition	1.080	1	1.080	1.582	.237
Error	6.827	10	.683		
Total	120.760	12			
Corrected Total	7.907	11			

Dependent Variable: score

Sample_condition	Mean	Std. Error	95% Confidence Interval	
			Lower Bound	Upper Bound
1 Dry samples	3.367	.337	2.615	4.118
2 Wet samples	2.767	.337	2.015	3.518

PLS_percentage = 4 PLS 30%, Test_measure = 3 Toughness

Tests of Between-Subjects Effects[a]

Dependent Variable: score

Source	Type III Sum of Squares	df	Mean Square	F	Sig.
Corrected Model	3.101[b]	1	3.101	15.595	.003
Intercept	20.541	1	20.541	103.307	.000
Sample_condition	3.101	1	3.101	15.595	.003
Error	1.988	10	.199		
Total	25.630	12			
Corrected Total	5.089	11			

Dependent Variable: score

Sample_condition	Mean	Std. Error	95% Confidence Interval	
			Lower Bound	Upper Bound
1 Dry samples	1.817	.182	1.411	2.222
2 Wet samples	.800	.182	.394	1.206

PLS_percentage = 5 PLS 40%, Test_measure = 1 MPa

Tests of Between-Subjects Effects[a]

Dependent Variable: score

Source	Type III Sum of Squares	df	Mean Square	F	Sig.
Corrected Model	453.870[b]	1	453.870	86.638	.000
Intercept	6806.803	1	6806.803	1299.339	.000
Sample_condition	453.870	1	453.870	86.638	.000
Error	52.387	10	5.239		
Total	7313.060	12			
Corrected Total	506.257	11			

Dependent Variable: score

Sample_condition	Mean	Std. Error	95% Confidence Interval	
			Lower Bound	Upper Bound
1 Dry samples	29.967	.934	27.885	32.049
2 Wet samples	17.667	.934	15.585	19.749

PLS_percentage = 5 PLS 40%, Test_measure = 2 GPa

Tests of Between-Subjects Effects[a]

Dependent Variable: score

Source	Type III Sum of Squares	df	Mean Square	F	Sig.
Corrected Model	1.841[b]	1	1.841	3.861	.078
Intercept	96.901	1	96.901	203.217	.000
Sample_condition	1.841	1	1.841	3.861	.078
Error	4.768	10	.477		
Total	103.510	12			
Corrected Total	6.609	11			

Dependent Variable: score

Sample_condition	Mean	Std. Error	95% Confidence Interval	
			Lower Bound	Upper Bound
1 Dry samples	3.233	.282	2.605	3.861
2 Wet samples	2.450	.282	1.822	3.078

PLS_percentage = 5 PLS 40%, Test_measure = 3 Toughness

Tests of Between-Subjects Effects[a]

Dependent Variable: score

Source	Type III Sum of Squares	df	Mean Square	F	Sig.
Corrected Model	.801[b]	1	.801	21.742	.001
Intercept	11.021	1	11.021	299.208	.000
Sample_condition	.801	1	.801	21.742	.001
Error	.368	10	.037		
Total	12.190	12			
Corrected Total	1.169	11			

Dependent Variable: score

Sample_condition	Mean	Std. Error	95% Confidence Interval	
			Lower Bound	Upper Bound
1 Dry samples	1.217	.078	1.042	1.391
2 Wet samples	.700	.078	.525	.875

PLS_percentage = 6 PLS 50%, Test_measure = 1 MPa

Tests of Between-Subjects Effects[a]

Dependent Variable: score

Source	Type III Sum of Squares	df	Mean Square	F	Sig.
Corrected Model	491.520[b]	1	491.520	81.042	.000
Intercept	4824.030	1	4824.030	795.388	.000
Sample_condition	491.520	1	491.520	81.042	.000
Error	60.650	10	6.065		
Total	5376.200	12			
Corrected Total	552.170	11			

Dependent Variable: score

Sample_condition	Mean	Std. Error	95% Confidence Interval	
			Lower Bound	Upper Bound
1 Dry samples	26.450	1.005	24.210	28.690
2 Wet samples	13.650	1.005	11.410	15.890

PLS_percentage = 6 PLS 50%, Test_measure = 2 GPa

Tests of Between-Subjects Effects[a]

Dependent Variable: score

Source	Type III Sum of Squares	df	Mean Square	F	Sig.
Corrected Model	3.308[b]	1	3.308	6.946	.025
Intercept	57.641	1	57.641	121.052	.000
Sample_condition	3.308	1	3.308	6.946	.025
Error	4.762	10	.476		
Total	65.710	12			
Corrected Total	8.069	11			

Dependent Variable: score

Sample_condition	Mean	Std. Error	95% Confidence Interval	
			Lower Bound	Upper Bound
1 Dry samples	2.717	.282	2.089	3.344
2 Wet samples	1.667	.282	1.039	2.294

PLS_percentage = 6 PLS 50%, Test_measure = 3 Toughness

Tests of Between-Subjects Effects[a]

Dependent Variable: score

Source	Type III Sum of Squares	df	Mean Square	F	Sig.
Corrected Model	3.000[b]	1	3.000	73.770	.000
Intercept	15.413	1	15.413	379.016	.000
Sample_condition	3.000	1	3.000	73.770	.000
Error	.407	10	.041		
Total	18.820	12			
Corrected Total	3.407	11			

Dependent Variable: score

Sample_condition	Mean	Std. Error	95% Confidence Interval	
			Lower Bound	Upper Bound
1 Dry samples	1.633	.082	1.450	1.817
2 Wet samples	.633	.082	.450	.817

ABSTRACT FOR IADR CONFERENCE

N.A. ISMAIL[1], P. ASHLEY[1], and A. YOUNG[2], [1]Eastman Dental Institute, University College London, London, England, [2]University College London, London, England

Development of novel remineralising antimicrobial brushite cements

Abstract:

Background: Brushite cements have potential as drug carriers and bone filling materials. They can also act as a reservoir for calcium and phosphate ions in remineralisation of hard tissues.

Objective: To optimize brushite cement properties and assess the effect of incorporation of a novel polymeric antimicrobial (PAM).

Method: Cement powders were mixed with aqueous solutions at a powder to liquid ratio (PLR) of 3.3:1 or 4:1 to produce cement pastes and start the setting reaction. The powder consisted of 1g of monocalcium phosphate monohydrate (MCPM) and 1.23g of β - tricalcium phosphate (β-TCP). MCPM from two sources was employed (particles sizes of 53 and 65 micron). Additionally β-TCP particle size ranged from 4 to 34 micron. The liquid phase was prepared by dissolving PAM powder (0, 10, 20, 30, 40 or 50 wt%) in 800 mM aqueous citric acid. Biaxial Flexural strength was determined with a ball on ring jig and Instron frame. Setting kinetics and microstructure were examined using FTIR and SEM.

Results: The viscosity of the brushite cements was advantageously lowered with MCPM of larger particle size. The largest particle size of β-TCP (34 micron) also gave cements of higher flexural strength (up to 30 MPa). Higher PLR increased strength by 5 – 7MPa. High levels of PAM could be added with only a minor reduction in the strength however setting time was delayed and less brushite formed. Adding PAM resulted in a more homogenous and less porous structure.

Conclusion: Brushite cement strength can be raised by optimising component particle size and raising powder content. High levels of PAM can be added without significant reduction in strength but the setting time is delayed and final brushite crystal microstructure altered.